



UNESP - Universidade Estadual Paulista
“Júlio de Mesquita Filho”
Faculdade de Odontologia de Araraquara



HÉRCULES BEZERRA DIAS

**PROPRIEDADES ANTIBACTERIANAS, FÍSICAS E MECÂNICAS DE
UMA RESINA COMPOSTA MODIFICADA COM NANOPARTÍCULAS DE
ZnO E TiO₂, PURAS E DECORADAS COM PRATA, OBTIDAS POR
DIFERENTES SÍNTESES.**

Araraquara
2017



UNESP - Universidade Estadual Paulista
“Júlio de Mesquita Filho”
Faculdade de Odontologia de Araraquara



HÉRCULES BEZERRA DIAS

**PROPRIEDADES ANTIBACTERIANAS, FÍSICAS E MECÂNICAS DE
UMA RESINA COMPOSTA MODIFICADA COM NANOPARTÍCULAS DE
ZnO E TiO₂, PURAS E DECORADAS COM PRATA, OBTIDAS POR
DIFERENTES SÍNTESES.**

Tese apresentada ao Programa de Pós-graduação em Ciências Odontológicas – Área de Concentração em Dentística Restauradora, da Faculdade de Odontologia de Araraquara, da Universidade Estadual Paulista “Júlio de Mesquita Filho” – UNESP, como parte dos requisitos para obtenção do título de Doutor em Ciências Odontológicas.

Orientadora: Prof^ª. Dr^ª. Alessandra Nara de Souza Rastelli

Araraquara
2017

Dias, Hércules Bezerra

Propriedades antibacterianas, físicas e mecânicas de uma resina composta modificada com nanopartículas de ZnO e TiO₂, puras e decoradas com prata, obtidas por diferentes sínteses / Hércules Bezerra
Dias.-- Araraquara: [s.n.], 2017

108 f. ; 30 cm.

Tese (Doutorado em Dentística Restauradora) – Universidade Estadual Paulista, Faculdade de Odontologia

Orientadora: Profa. Dra. Alessandra Nara de Souza Rastelli

Co-Orientador: Prof. Dr. Antônio Carlos Hernandes

1. Nanotecnologia 2. Nanoestruturas 3. Resinas compostas
4. Produtos com ação antimicrobiana I. Título

HÉRCULES BEZERRA DIAS

PROPRIEDADES ANTIBACTERIANAS, FÍSICAS E MECÂNICAS DE
UMA RESINA COMPOSTA MODIFICADA COM NANOPARTÍCULAS DE
ZnO E TiO₂, PURAS E DECORADAS COM PRATA, OBTIDAS POR
DIFERENTES SÍNTESES.

COMISSÃO JULGADORA

Tese para obtenção do grau de Doutor

Presidente e Orientadora: Prof^a. Dr^a. Alessandra Nara de Souza Rastelli

2º Examinador: Profa. Dra. Ângela Cristina Cilense Zuanon

3º Examinador: Profa. Dra. Patrícia Petromilli Nordi Sasso Garcia

4º Examinador: Profa. Dra. Taís Maria Bauab

5º Examinador: Dra. Maria Inês Basso Bernardi

Araraquara, 24 de Agosto de 2017.

Dados Curriculares

HÉRCULES BEZERRA DIAS

NASCIMENTO:	16/05/1983 – Manaus, Amazonas
FILIAÇÃO:	Maria Bezerra Dias José Ferreira Dias
2001-2005:	Curso de Graduação em Química pela Universidade Federal do Amazonas – UFAM.
2004-2009:	Curso de Graduação em Odontologia pela Universidade do Estado do Amazonas – UEA.
2011-2014:	Curso de Especialização em Ortodontia pelo Instituto de Ensino Superior Pinelli Henriques, Bauru, SP.
2012-2014:	Curso de Pós-Graduação em Ciência e Engenharia de Materiais, Área de Concentração em Desenvolvimento e Caracterização de Materiais, nível Mestrado, pela Universidade de São Paulo – USP de São Carlos.
2014-2015:	Curso de Atualização em Dentística Estética na Fundação Araraquarense de Ensino e Pesquisa em Odontologia- UNESP de Araraquara.
2014-Atual:	Curso de Pós-Graduação em Ciências Odontológicas, Área de Concentração em Dentística Restauradora, nível Doutorado, pela Universidade Estadual Paulista “Júlio de Mesquita Filho” – UNESP de Araraquara.
2017-Atual:	Professor de ensino superior no Centro Universitário do Norte, Manaus, AM.

DEDICATÓRIA

Dedico este trabalho primeiramente A **Deus**, minha rocha e fortaleza contra as intempéries do destino.

Aos meus pais, **José Ferreira Dias e Maria Bezerra Dias**, por me permitirem o acesso ao conhecimento, pelo caráter em mim forjado e pelo incentivo em cada dia dessa jornada.

AGRADECIMENTOS

À Universidade Estadual Paulista “Júlio de Mesquita Filho” – UNESP, na presença de seu Magnífico Reitor, **Prof. Dr. Sandro Roberto Valentini**.

À Faculdade de Odontologia de Araraquara – UNESP, representada pela **Prof^a. Dr^a. Elaine Maria Sgavioli Massucato** (Diretora) e **Prof. Dr. Edson Alves de Campos** (Vice-Diretor).

Ao Programa de Pós-Graduação em Ciências Odontológicas, da Faculdade de Odontologia de Araraquara, coordenado pelo **Profa. Dra. Fernanda Lourenção Brighenti**.

Aos docentes da disciplina de Dentística Restauradora: **Prof^a. Dr^a. Alessandra Nara de Souza Rastelli**, **Prof^a. Dr^a. Andréa Abi Rached Dantas**, **Prof. Dr. Edson Alves de Campos**, **Prof. Dr. José Roberto Cury Saad**, **Prof. Dr. Marcelo Ferrarezi Andrade**, **Prof. Dr. Osmir Batista de Oliveira Júnior** e **Prof. Dr. Sizenando de Toledo Porto Neto** pelo suporte e ensinamentos ao longo desse curso.

À **Prof^a. Dr^a. Alessandra Nara de Souza Rastelli**, minha orientadora, pela amizade e ensinamentos ao longo do doutorado.

Aos colegas de pós-graduação, em especial à **Tamara Trevisan**, **Maria Tereza Tavares**, **Ricardo Tangari**, **Keren Jordão**, **Daniele Wajngarten**, **Thaís Piragibe**, **Cristiina Presoto**, **Camila de Foggi**, **Luís Carlos Santana**, **Jonleno Pitombo**, **Tiago Fonseca**, **Mariana Mena**, **Lauriê Garcia** e **Vinícius de Paiva** pela amizade e agradável convivência na FOAr.

À **Prof^a. Dr^a. Taís Maria Bauab**, Docente do Departamento de Ciências Biológicas da Faculdade de Ciências Farmacêuticas da UNESP de Araraquara,

por disponibilizar seu laboratório para realização de parte da pesquisa, amizade e ensinamentos.

Aos alunos de pós-graduação e pós-doutorado do laboratório de Microbiologia do Departamento de Ciências Biológicas da Faculdade de Ciências Farmacêuticas da UNESP de Araraquara, **Matheus Ramos, Bruna Bonifácio, Larissa Spósito, Luciani Toledo, Anderson Noronha e Patrícia Bento** pela amizade e ajuda no laboratório.

Ao meu querido **Fábio Regis**, pelo apoio, por tornar os meus dias mais felizes e esta caminhada mais agradável.

Aos funcionários da Seção de Pós-Graduação da Faculdade de Odontologia de Araraquara – UNESP, **José Alexandre Garcia e Cristiano Lamounier**, pela atenção e prestatividade.

Aos funcionários do Departamento de Odontologia Restauradora da Faculdade de Odontologia de Araraquara – UNESP, **Creuza, Dona Cida, Alessandra (*in memorian*), Marinho e Vanderlei**, pela disponibilidade e ajuda.

À **Fundação de Amparo à Pesquisa do Estado do Amazonas**, pela bolsa de estudos concedida para realização do doutorado.

Ao Grupo de Crescimentos de Cristais e Materiais Cerâmicos (IFSC-USP), especialmente ao **Prof Dr. Antônio Carlos Hernandez e Dra. Maria Inês Bernardi**, pela amizade e disponibilização da estrutura física para a realização de parte da pesquisa.

Aos amigos do Grupo de Crescimentos de Cristais e Materiais Cerâmicos (IFSC-USP), especialmente **Lílian Menezes, Ariadne Cato e Luís Fernando da Silva**, pela amizade, ensinamentos e agradável convivência em São Carlos.

Aos amigos **Paula Daniele Corrêa, Dayane Portilho, Rodrigo de Castro e Bruno Batista**, ainda que distantes, sempre se fazendo presentes com palavras de carinho e incentivo, meus sinceros agradecimentos.

Ao **Dr. Sebastião Pratavieira**, do Grupo de Óptica do Instituto de Física de São Carlos, pela ajuda para obtenção das imagens da Microscopia Confocal a Laser.

E a todos que de alguma forma colaboraram com este trabalho.

Dias HB. Propriedades antibacterianas, físicas e mecânicas de uma resina composta modificada com nanopartículas de ZnO e TiO₂ puras e decoradas com prata, obtidas por diferentes sínteses [Tese de Doutorado]. Araraquara: Faculdade de Odontologia da UNESP; 2017.

RESUMO

Estudos recentes relatam que resinas compostas contendo nanopartículas (NPs) de óxidos metálicos, tais como óxido de zinco (ZnO) e dióxido de titânio (TiO₂) têm potencial antibacteriano e podem controlar a formação do biofilme oral cariogênico. O objetivo desse estudo foi avaliar a capacidade antibacteriana de uma resina composta modificada por NPs de óxido de zinco e dióxido de titânio puras e decoradas com prata (ZnO, ZnO/Ag, TiO₂ e TiO₂/Ag), bem como, avaliar as propriedades de resistência à compressão e à tensão diametral, estabilidade de cor, rugosidade superficial e grau de conversão após modificação da resina composta com as NPs. As NPs foram sintetizadas pelos métodos dos precursores poliméricos e hidrotermal assistido por micro-ondas, e caracterizadas por DRX, área de superfície BET, FTIR e MET. A resina Filtek™ Z350XT modificada com 0,5; 1 e 2% (em massa) foi testada sobre *Streptococcus mutans* por meio do teste do contato direto (UFC/mL) para determinação da menor concentração inibitória e então avaliada em biofilme de 7 dias por meio decontagem das unidades formadoras de colônias (UFC/mL). As resistências à compressão e à tração diametral da resina composta modificada (n=40) foram avaliadas utilizando-se máquina de ensaio universal (EMIC). O grau de conversão (n=25) foi realizado por análise em FTIR e a leitura da rugosidade superficial (n=50) foi realizada utilizando-se rugosímetro portátil. A estabilidade de cor (n=180) foi avaliada por leitura espectrofotométrica após imersão dos espécimes em solução de café e saliva artificial. Os dados foram analisados utilizando-se o software IBM SPSS Statistics 20.0 (SPSS Inc. Chicago, EUA) por ANOVA a um fator para a atividade antibacteriana e testes mecânicos; ANOVA a dois fatores e teste de Tukey para o grau de conversão; ANOVA de medidas repetidas e pós teste com ajuste de Bonferroni para estabilidade de cor e teste de rugosidade superficial, com nível de significância de 5%. A

inclusão de 2% (em massa) de NPs de ZnO e TiO₂ puros e decorados com Ag na resina composta inibiu o crescimento do biofilme de *S. mutans*, sem drásticas alterações nas propriedades mecânicas e físicas. Melhora nas propriedades mecânicas foi alcançada após a inclusão de TiO₂/Ag. O grau de conversão permaneceu inalterado após a modificação da resina com todas os NPs testadas e a rugosidade superficial não foi significativamente alterada após a inclusão de TiO₂/Ag (PREC POL). A estabilidade de cor da resina foi afetada após a inclusão das nanopartículas, especialmente quando armazenada em solução de café e após 90 dias. O desenvolvimento de um material restaurador dental antibacteriano que iniba a formação do biofilme de *S. mutans* sobre sua superfície sem sacrificar suas propriedades mecânicas e físicas poderia evitar a progressão de cáries secundárias.

PALAVRAS-CHAVE: *Nanotecnologia. Nanoestruturas. Resinas compostas. Produtos com ação antimicrobiana.*

Dias HB. Antibacterial, physical and mechanical properties of a composite resin modified with pure and silver-decorated ZnO and TiO₂ nanoparticles, obtained by different synthesis [Tese de Doutorado]. Araraquara: Faculdade de Odontologia da UNESP; 2017.

ABSTRACT

Different methods to inhibit biofilm formation on dental restorative materials have been studied for decades and recent studies report that composite resins containing metal oxide nanoparticles (NPs), such as zinc oxide (ZnO) and titanium dioxide (TiO₂), have antibacterial potential and can control the formation of cariogenic oral biofilm. In this way, the purpose of this study was to evaluate the antibacterial capacity of a resin modified by pure and silver decorated ZnO and TiO₂ (ZnO, ZnO/Ag, TiO₂ and TiO₂/Ag) NPs and to evaluate the compressive and diametral tensile strength, color stability, surface roughness and degree of conversion after modification of the composite resin with the NPs. The NPs were synthesized by polymeric precursor and microwave-assisted hydrothermal methods, characterized by XRD, BET surface area, FTIR and MET. The direct contact test with Filtek™ Z350XT modified with 0.5; 1 and 2% (by mass) of NPs against *Streptococcus mutans* was performed in order to choose the minor concentration to perform the other tests. The modified resin was tested against the 7-days *S. mutans* biofilm.

The compressive strength and diametral tensile strength of the modified composite resin (n = 40) was tested using a universal test machine (EMIC). The degree of conversion (n = 25) was performed by FTIR analysis and the surface roughness reading (n = 50) was performed using a portable surface roughness tester. The color stability (n=180) was evaluated by spectrophotometric readings after storage in coffee solution and artificial saliva. The data was analyzed using the software IBM SPSS Statistics 20.0 (SPSS Inc. Chicago, USA). One-way ANOVA were performed to antibacterial and mechanical tests data, two-way ANOVA for degree of conversion and a mixed model repeated measurements ANOVA and a post hoc test for repeated measures with adjustment of Bonferroni were performed for surface roughness and

color stability test. All tests were performed at 5% significance level. The inclusion of 2% (wt%) of ZnO and ZnO/Ag NPs from different synthesis provide *S. mutans* biofilm formation control without sacrificing of mechanical and physical properties of the composite resin, when the inclusion of pure and Ag decorated TiO₂ into the composite resin can decrease *S. mutans* biofilm formation over the resin surface. An enhancement of mechanical properties was achieved after inclusion of TiO₂/Ag. The degree of conversion remains unchanging after resin modification with all tested NPs and the surface roughness was not significantly increased after inclusion of TiO₂/Ag (PREC POL). Regarding the color stability, after inclusion of nanoparticles, the color stability was affected, especially when stored in coffee solution after 90 days. The development of an antibacterial dental restorative material that hind *S. mutans* biofilm without sacrificing mechanical and physical properties could decrease the progression of secondary caries.

KEYWORDS: *Nanotechnology. Nanostructures. Composite resins. Products with antimicrobial action.*

SUMÁRIO

1 INTRODUÇÃO	13
2 PROPOSIÇÃO	17
3 ARTIGOS.....	18
3.1 Artigo 1: The use of TiO₂ and TiO₂/Ag nanoparticles as an anti <i>Streptococcus mutans</i> filler content for composite resins.	18
3.2 Artigo 2: Antibacterial, physical and mechanical properties of a composite resin modified by ZnO and ZnO/Ag nanoparticles.	48
3.3 Artigo 3: Color stability of a composite resin modified by metal oxides antibacterial nanoparticles.	77
4 CONCLUSÃO.....	100
REFERÊNCIAS	101
APÊNDICE	103

1 INTRODUÇÃO

Materiais compósitos podem ser definidos como um composto de dois ou mais materiais diferentes com propriedades que são superiores ou intermediárias àquelas dos constituintes individualmente (Anusavice³, 2013). Resinas compostas são compósitos que contém como constituintes principais matriz polimérica e partículas inorgânicas de carga, além de um agente de ligação que promove a ligação entre as partículas de carga e a matriz resinosa, um agente iniciador necessário para a polimerização e inibidor da mesma reação. As resinas compostas podem ser distinguidas, dentre outros fatores, pelas características de suas partículas de carga e em particular pelo seu tamanho (Ferracane⁹, 2001).

Sua formulação evoluiu significativamente desde que foram introduzidas na Odontologia há mais de 50 anos. Até recentemente, as mudanças mais importantes envolveram as partículas de carga do material (Anusavice³, 2013; Ferracane⁹, 2001), com o desenvolvimento de compósitos nanoparticulados, contendo apenas partículas em nanoescala, além de compósitos nanohíbridos que incluem nanopartículas em sua composição. O desenvolvimento de novas formulações de resinas compostas evoluiu constantemente nos últimos anos. Dessa forma, resinas compostas nanoparticuladas e nanohíbridas representam o estágio mais avançado em termos de composição de partículas desses materiais (Ferracane⁹, 2001).

Nanopartículas são unidades moleculares tipicamente definidas como tendo diâmetros compreendidos entre 0,1 e 100 nm, tendo seu uso disseminado na formulação de resinas compostas, por propiciarem melhor resistência flexural e microdureza superficial, além de melhor estética após confecção de restaurações, quando comparadas às resinas híbridas e microparticuladas (Ferracane⁹, 2001; Saunders²², 2009). Resinas compostas nanoparticuladas são compostas por partículas de carga entre 20 e 75 nanômetros (Ferracane⁹, 2001). Nessas, as partículas se distribuem adequadamente dentro do compósito dental, permitindo assim melhora na viscosidade do material. Além disso, essas resinas mostram melhor dureza e resistência à abrasão (Conceição⁶, 2007; Saunders²², 2009). As propriedades reológicas favoráveis desses materiais facilitam a manipulação e inserção no preparo cavitário a ser restaurado. Resinas compostas nanoparticuladas se mostram mais resistentes e com menor contração de polimerização, mantendo a baixa viscosidade. Proporcionam maior lisura superficial após acabamento e polimento, quando comparadas às antecessoras e esse aspecto aliado à sua elevada resistência mecânica, tem influenciado na

sua utilização clínica, tanto em dentes posteriores quanto anteriores (Conceição⁶, 2007; Klapdohr, Moszner¹³, 2005; Saunders²², 2009; Schneider et al.²³, 2006).

Apesar das excelentes propriedades e vantagens em utilizar resinas compostas nanoparticuladas, seus componentes têm pouco ou nenhum efeito antibacteriano (Hojati et al.¹¹, 2013). Pesquisas laboratoriais e clínicas demonstraram que, comparando-se com outros materiais restauradores e tecidos dentários duros, a resina composta proporciona maior acúmulo de biofilme, o que resulta em maior prevalência de cáries secundárias nas margens de restaurações confeccionadas com esse material (Chen et al.⁵, 2012; Fermaniam⁸, 1984; Hojati et al.¹¹, 2013). Um dos métodos para prevenir lesões cáries nas margens das restaurações é o uso de materiais resistentes ao acúmulo bacteriano. Dessa forma, estudos recentes têm focado na atividade antibacteriana desses materiais, a fim de minimizar o risco do aparecimento de lesões cáries secundárias (Chen et al.⁵, 2012; Hojati et al.¹¹, 2013).

Dentre os agentes utilizados para promover ação antibacteriana em resinas compostas, nanopartículas de metais (como prata e zinco) e polímeros antimicrobianos ganharam interesse significativo ao longo dos anos, devido às notáveis propriedades antimicrobianas (Sahu et al.²¹, 2013). O excelente efeito antibacteriano destes agentes contendo nanopartículas é atribuído, principalmente, à grande área de superfície que possuem em relação ao volume, permitindo maior presença de átomos na superfície, o que proporciona o máximo contato das partículas com o meio. Além disso, o pequeno tamanho dessas partículas torna a penetração através das membranas celulares mais fácil, afetando processos intracelulares, resultando em maiores reatividade e atividade antimicrobiana (Sahu et al.²¹, 2013).

Nos últimos anos, pesquisas têm sido focadas na modificação de partículas de carga para se obter resinas compostas com propriedades antibacterianas (Allaker¹, 2010; Hojati et al.¹¹, 2013; Liang et al.¹⁵, 2012). Dentre os métodos usados para a síntese de nanopartículas, destaca-se o método dos precursores poliméricos, uma modificação da síntese de Pechini (Pechini¹⁹, 1967; Walton²⁴, 2002). Partículas inorgânicas, como a prata (por exemplo, íon prata e nanopartículas de prata) são agentes antibacterianos de amplo espectro e seu mecanismo antibacteriano está associado com a sua interação com o grupo tiol de compostos de células bacterianas. A ligação da prata com a parede celular inibe o processo de respiração. Pura ou como dopante de outros agentes, têm mostrado resultados particularmente encorajadores como antibacterianos. Um estudo que avaliou a adição de nanopartículas de prata (Ag), de benzoato de prata, sílica dopada com prata, materiais

híbridos zinco-prata, e óxido de zinco mostraram que todos forneceram compósitos odontológicos com atividade antibacteriana (Chen et al.⁵, 2012).

Com potencial antibacteriano, o ZnO além de possuir excelentes propriedades físicas e químicas, exhibe, provavelmente, a maior variedade de diferentes nanoestruturas, tais como: *nanowires*, *nanorods*, *nanobelts*, *nanopencils*, *nanosprings*, *nanocombs*, *nanoboxes*, *nanorings* entre outros. A atividade antibacteriana de nanopartículas de ZnO é dependente do tamanho das mesmas mostrando efeito antibacteriano em bactérias gram-positivas e negativas (Raghupathi et al.²⁰, 2011; Sahu et al.²¹, 2013). O estudo das propriedades antibacteriana, física e mecânica de resinas compostas do tipo *flow* contendo nanopartículas de ZnO, realizado por Hojati et al.¹¹ (2013), revelou significativa inibição do crescimento de *Streptococcus mutans* pela resina modificada, além de observarem insignificantes alterações nas propriedades mecânicas com a inclusão de pequenas quantidades (cerca de 1%) de nanopartículas (Sahu et al.²¹, 2013).

O TiO₂ é um material fotocatalítico que ocorre como dois importantes polimorfos: a fase rutilo estável e a anatase metaestável. Estes polimorfos exibem propriedades diferentes e, conseqüentemente, diferentes performances fotocatalíticas (Cui et al.⁷, 2012). Nanopartículas de TiO₂ têm demonstrado eficácia multifuncional. Com a diminuição do tamanho das partículas, especialmente menores que 50 nm, elas apresentam atividades fotoinduzidas, liberando energia que pode ser expressa quimicamente na forma de radicais livres e que pode ser aplicada em atividades fotocatalíticas incluindo inibição de bactérias e vírus (Fu et al.¹⁰, 2005). No estudo de Cai et al.⁴ (2014), foi avaliado in vitro a inativação fotocatalítica de biofilme de *Streptococcus mutans* em adesivo dental contendo nanopartículas de TiO₂. Utilizando 8,43 J/cm² de dose de radiação UV-A, observaram que o novo adesivo foi capaz de reduzir o número de células bacterianas viáveis em ordem de magnitude correspondente a 90% dessas células. Além disso, a resistência a adesão do adesivo não foi afetada com a inclusão de até 30% em peso de nanopartículas de TiO₂ (Cai et al.⁴, 2014)

Nanotubos de TiO₂ sintetizados por oxidação eletroquímica sobre bloco de titânio puro exibiram atividade anti *Streptococcus mutans* (Cui et al.⁷, 2012). Híbridos de titânio-prata (TiO₂.Ag) testados em bactérias altamente patogênicas como *Escherichia coli* mostraram significativa atividade antimicrobiana, que deve estar ligada à mesoporosidade, alta área superficial e energia de *band gap* do TiO₂, aliando-se à capacidade antimicrobiana da Ag (Liu et al.¹⁶, 2008).

Embora a incorporação de nanopartículas de metais e óxidos metálicos em compósitos dentais proporcionem atividade antibacteriana como demonstrado por alguns estudos, podem afetar adversamente diferentes propriedades desses materiais (Allaker¹, 2010; Lepri, Palma-Dibb¹⁴, 2012; Liang et al.¹⁵, 2012; Lizenboim et al.¹⁷, 2008; Melo et al.¹⁸, 2013). Outra desvantagem pode ser a pobre estabilidade de cor obtida em materiais contendo nanopartículas metálicas tornando essa propriedade provavelmente clinicamente inaceitável em se tratando de materiais estéticos (Chen et al.⁵, 2012).

Observa-se que, apesar dos estudos atuais abordarem a capacidade antibacteriana de resinas compostas e outros materiais dentários contendo nanopartículas, suas propriedades físicas e mecânicas não foram amplamente estudadas, bem como a inserção de híbridos como ZnO.Ag e TiO₂.Ag, uma vez que as propriedades como efeitos fotocatalítico e antibacteriano de híbridos, devem ser diferente daquelas exibidas por cada material isoladamente (Allaker¹, 2010; Hojati et al.¹¹, 2013; Liang et al.¹⁵, 2012; Lizenboim et al.¹⁷, 2008; Melo et al.¹⁸, 2013)..

Dessa forma, o domínio das técnicas de síntese, caracterização e conhecimento das propriedades físico-químicas dos nanomateriais usados como partículas de carga em resinas compostas, pode levar a obtenção de um compósito que demonstre atividade antibacteriana sem alteração nas propriedades mecânicas e ópticas originais. O desenvolvimento de um material restaurador dental antibacteriano que iniba a formação do biofilme de *S. mutans* sobre sua superfície, poderia evitar a progressão de cáries secundárias.

2 PROPOSIÇÃO

2.1 Objetivo Geral

Modificar uma resina composta comercial com nanopartículas de óxidos de metais puras e decoradas com prata para desenvolvimento de um material restaurador com potencial antibacteriano, sem que altere negativamente suas propriedades físicas e mecânicas.

2.2 Objetivos Específicos

O objetivo do estudo relatado nos artigos 1 e 2 foi avaliar a atividade anti *Streptococcus mutans* de uma resina composta modificada com nanopartículas de TiO₂, TiO₂/Ag, ZnO e ZnO/Ag e suas possíveis alterações nas propriedades de resistência à compressão e tração diametral, rugosidade superficial e grau de conversão. O objetivo do estudo relatado no artigo 3 foi avaliar a estabilidade de cor de uma resina composta modificada com ZnO e TiO₂ (puros e decorados com prata) sintetizados por diferentes sínteses.

Artigo 1 – Preparado para ser submetido à Dental Materials.

Título: The use of TiO₂ and TiO₂/Ag nanoparticles as an anti *Streptococcus mutans* filler content for composite resins.

Artigo 2 – Preparado para ser submetido à Brazilian Dental Journal

Título: Antibacterial, physical and mechanical properties of a composite resin modified by ZnO and ZnO/Ag nanoparticles.

Artigo 3- Preparado para ser submetido à Brazilian Oral Research

Título: Color stability of a composite resin modified by metal oxides antibacterial nanoparticles.

3 ARTIGOS

3.1 Artigo 1

Title page

Title: The use of TiO₂ and TiO₂/Ag nanoparticles as an anti *Streptococcus mutans* filler content for composite resins.*

Short Title: Application of TiO₂ nanoparticles in composite resins.

Authors: Hércules Bezerra Dias¹, Maria Inês Basso Bernardi², Taís Maria Bauab³, Antônio Carlos Hernandes², *Alessandra Nara de Souza Rastelli¹

¹Department of Restorative Dentistry, Araraquara School of Dentistry, Sao Paulo State University – UNESP, Araraquara, SP 14801-903, Brazil.

²Department of Physics and Materials Science, Physics Institute of São Carlos, University of São Paulo, São Carlos, SP 13566-590, Brazil.

³Department of Biological Sciences, School of Pharmaceutical Sciences, Sao Paulo State University – UNESP, Araraquara, SP 14801-902, Brazil.

*Corresponding author: Prof. Dr. Alessandra Nara de Souza Rastelli, Sao Paulo State University – UNESP, Araraquara School of Dentistry, Department of Restorative Dentistry, Araraquara, SP, Brazil. 1680 Humaitá St., Araraquara, Sao Paulo, Brazil. MailBox: 331. ZipeCode: 14.801-903. Telephone: +55 (016) 3301-6524 Fax: +55 (016) 3301-6393. e-mail address: alrastelli@foar.unesp.br

Abstract

Objectives: The aim of this study was to evaluate the antibacterial activity of a composite resin modified by TiO₂ and TiO₂/Ag nanoparticles and the possible changes over physical and mechanical properties.

Methods: TiO₂ and TiO₂/Ag NPs were synthesized by polymeric precursor and microwave-assisted hydrothermal methods, characterized by XRD, BET surface area, FTIR and MET. Direct contact test was performed using Filtek™ Z350XT blended with 0.5; 1 and 2% (wt.) of NPs against *Streptococcus mutans* in order to screening the best concentration to perform the following tests. After that, the modified composite resin (G1: Control - unmodified composite resin; G2 – Composite resin + TiO₂ and G3: Composite resin + TiO₂/Ag for both synthesis) was tested against *S. mutans* 7-day biofilm (CFU/mL) and by confocal laser scanning microscopy. The TiO₂ and TiO₂/Ag nanoparticles were treated with an organosilane agent and then the composite resin was modified with NPs to perform compressive and diametral tensile strength (n=40) using a universal test machine (EMIC). The degree of conversion (n=25) was performed by FTIR analysis. The reading of the surface roughness (n=50) was performed using a portable surface roughness tester. The data were analyzed using the software IBM SPSS Statistics 20.0 (SPSS Inc. Chicago, USA) by one-way ANOVA for the antibacterial activity over the biofilm and mechanical tests; two-way ANOVA for degree of conversion and Tukey test for multiple comparison; repeated measurements ANOVA and a post hoc test with adjustment of Bonferroni for color stability and surface roughness test, at 5% significance level.

Results: The inclusion of 2% of TiO₂/Ag NPs significantly decreased (p <0.05) the biofilm accumulation of *S. mutans* on the composite resin surface compared to the control Group. The TiO₂ NPs treated with an organosilane increased compressive strength of

composite resin. Degree of conversion remained unchanged, when the surface roughness increase after resin modification, except for the TiO₂ by polymeric precursor Group.

Significance: The development of an antibacterial dental restorative material that hind *Streptococcus mutans* biofilm without sacrificing the mechanical and physical properties could decrease biofilm accumulation and avoid the progression of secondary caries.

Key-words: titanium; composite resins; products with antimicrobial action; *Streptococcus mutans*; biofilms.

1. Introduction

A broad-spectrum antimicrobial composite resin materials is desired for dentistry, especially because composite resin materials accumulate more biofilm than other restorative materials and the current dental restorative materials did not have antimicrobial materials in the composition [1,2]. The high biofilm accumulation by composite resin restoration can contributes to the progress of secondary caries [3]. Because of that, researchers have focused their studies on nanostructured materials with antimicrobial potential, such as silver [4,5], zinc oxide [6,7], titanium dioxide [8,9], hydroxyapatite and chlorhexidine, in order to fabricate a novel resin based restorative material.

Metal oxides and silver doped metal oxides have been reported to show high antimicrobial activity and these metal oxides can be obtained by several chemical methods, which can provide different sizes and shapes [6]. The excellent antibacterial effect of these nanoparticles is mainly attributed to their large surface area, allowing a great presence of atoms on the surface, which provides the maximum contact of the particles with the external enviroment [10,11]. In addition, the small size of these particles facilitates the penetration through cell membranes, changing the intracellular processes that result in increased reactivity and antimicrobial activity [11,12].

Titanium dioxide (TiO₂) is one of the most studied metal oxide considered as an antibacterial, is a photocatalyst material that occurs mainly as two important polymorphs: the stable rutile phase and the metastable anatase [13]. These structures exhibit different properties and, consequently, different photocatalytic performances [13,14]. With the decrease of particle size, especially smaller than 50 nm, they have photoinduced activities, releasing energy that can be expressed chemically as free radicals and that can be applied in photocatalytic activities including the killing of bacteria and viruses [13,15,16].

In order to improve the antibacterial activity of Ag NPs and meanwhile to cut down the expense, a bunch of Ag containing complex materials have been developed and have been used as another approach to dental materials modification [17]. Ghosh et al. [18] synthesized ZnO/Ag nanohybrid employing chitosan as mediator by purely electrostatic interaction and verified that the synergistic antibacterial effect of ZnO/Ag nanohybrid on Gram-positive and Gram-negative bacteria is found to be more effective, compared to the individual components (ZnO and Ag). Zhang et al. [17] synthesized Ag islands on ZnO, by a two-step preparation using a self-catalytic reaction and verified that the antibacterial activity of Ag/ZnO NPs, especially with 5.0 wt.% of Ag, against *Escherichia coli* and *Staphylococcus aureus* was greatly enhanced in contrast with the simple mixture of Ag and ZnO NPs. The authors attributed this enhancement to the obvious increase in the reactive oxidative species (especially superoxide) and the increased damage to plasmid DNA induced by Ag/ZnO NPs [17]. Zamperini et al. [5] synthesized and characterized hydroxyapatite nanoparticles decorated with silver and evaluated the antifungal effect of these nanoparticles in distilled water solution against *Candida albicans*. These authors found an interaction between the structure and the defect density variation in the interfacial Ag decorated NPs and intrafacial pure NPs region with the fungal medium resulted in fungistatic and fungicidal activity.

Although the incorporation of metal nanoparticles and metal oxides into dental composites provides antimicrobial activity, they might adversely affect the physical and mechanical properties of these materials [4–7]. Another disadvantage could be the poor color stability obtained in materials containing metal nanoparticles, making this property probably clinically unacceptable in the case of aesthetic materials [19].

In this way, the purpose of this study was to modify a commercial composite resin with TiO₂ and Ag decorated TiO₂ NPs in order to provide antibacterial capacity without sacrificing the mechanical and physical properties. The null hypothesis tested in the study is that the addition of small amounts of TiO₂ and Ag decorated TiO₂ NPs into a commercial composite resin do not affect the antimicrobial activity, compressive and diametral tensile strength, surface roughness and degree of conversion.

2. Material and Methods:

2.1 Experimental design:

This is an experimental study, which has dependent variables (4 levels) [compressive strength, diametral tensile strength, degree of conversion, surface roughness and antibacterial capacity (UFC/mL)] and independent variables [NPs concentrations (wt.%) and synthesis method].

2.2 Synthesis of TiO₂ NPs by polymeric precursor method (PREC POL):

For synthesizing TiO₂ NPs by polymeric precursor method [20], titanium isopropoxide (Ti(OC₃H₇)₄) (Sigma Aldrich P.A.) and citric acid (C₆H₈O₇·H₂O, 99.5%) (Synth) were used as precursors. The ethylene glycol (HOCH₂CH₂OH, P.A. >99.5%) (Synth) was added to polymerize the citrate by a polyesterification reaction. The citric acid:metal molar ratio was 3:1, while the citric acid:ethylene glycol (CA:EG) molar ratio was 60:40. The resulting resin was calcined at 300°C for 4h at 10°C/min, leading to the formation of the precursors powder. The data of synthesized NPs are shown in Table 1.

2.3 Synthesis of TiO₂ NPs by microwave-assisted hydrothermal method (HYDROT):

For the preparation of TiO₂ nanoparticles by this method, 54 mL of the previously prepared titanium citrate precursor solution was taken into the reaction cup and 33.3 mL of NaOH was added to the precursor solution. The final solution filled out at least 90% of the total volume of the reaction cup in order to obtain maximum efficiency in relation to the self-generated pressure [21]. The reaction cup was inserted inside the reaction cell, it was closed and transferred to the microwave assisted hydrothermal system, where the reaction occurred at a heating rate of 140°C min⁻¹ and held at 140°C for 10 minutes.

2.4 Silver decoration of the nanoparticles:

The Ag decorated NPs were prepared using the previously prepared and TiO₂ powder dispersed in distilled water, and the pH was adjusted to 5 with HNO₃ [5]. The solution was stirred at 60°C, and then 5 mL of AgNO₃ solution (1.4×10^{-2} M) was added in order to obtain a concentration of 1 mol NP: 1 mol Ag. The precipitate was washed with distilled water until pH 7 and then dried in an oven.

2.5 Characterization of the nanoparticles:

The X-Ray diffraction (XRD) patterns of the NPs powder were recorded on a Rigaku, Rotaflex RU200B diffraction system with high intensity Cu K α radiation ($\lambda = 1.5406 \text{ \AA}$), at 25°C with 2θ values ranging from 20-80°C and scanning rate of 0.02°C per min. The crystallite size was determined by the following Scherrer equation where λ is the wavelength of the X-ray radiation, K is a constant taken as 0.89, θ is the diffraction angle and β is the full width at half maximum (FWHM)).

$$D = \frac{K\lambda}{(\beta \cos \theta)} \quad [1]$$

The FTIR measurements of NPs were carried out in the Nexus 670 FTIR spectrophotometer (Thermo Scientific, Madison, WI). A total of 64 scans were collected

from 4000cm^{-1} to 650cm^{-1} at 4cm^{-1} resolution. Nitrogen adsorption–desorption measurements for the products were performed using a Micromeritics ASAP 2020 M + C instrument using Barrett–Emmett–Teller calculations for surface area determination. The isotherms and hysteresis curves were classified according to IUPAC (*International Union of Pure and Applied Chemistry*). The particle size (D_{BET}) was calculated using the following equation:

$$D_{\text{BET}} = \frac{6}{A_s \cdot \rho} \quad [2]$$

Where A is the superficial area (m^2/g) and ρ is the density of material ($\text{TiO}_2 = 4,23 \text{ g/cm}^3$ JCPDF 73-1764).

The samples were structurally characterized using an automatic X-ray diffractometer (Rigaku, Ultima IV) with $\text{CuK}\alpha$ radiation (40 kV, 46 mA, $\theta = 1.5405 \text{ \AA}$) and in a θ - 2θ configuration using a graphite monochromator. The scanning range was between 20 and 80° (2θ), with a step size of 0.02° and a step time of 1.0 s .

The thermal decomposition processes were studied by thermogravimetry (TG, Netzsch STA 409C), in an oxygen atmosphere at a heating rate of $10^\circ\text{C min}^{-1}$. Al_2O_3 was used as reference material during the thermal analysis.

The morphology and size of Ag decorated NPs were performed by transmission electron microscopy (TEM, Tecnai G2TF20, FEI).

The specific surface area (BET) and the diameter of NPs were estimated from the N_2 desorption/adsorption isotherms at liquid nitrogen temperature, using a Micromeritics ASAP 2020.

2.6 Composite resin used in this study:

The nanofilled composite resin Filtek™ Z350XT (3M Brazil) at color A2B (Body) employed as a control Group and modified by TiO₂ and TiO₂/Ag nanoparticles for experimental Groups.

2.6.1 Composite resin modification:

The NPs were added into the composite resin Filtek™ Z350XT (3M Brazil) using a standardized protocol based on the inclusion of weight percentage of particles into the composite resin [22]. The NPs were incorporated into the resin by manual mixing during 1 min, using a metal spatula and a glass plate. For direct contact test, the NPs were weighed corresponding to 0.5 and 1 and 2% (wt.%). After the antibacterial screening, the specimens for the following tests were prepared with 2% (wt.%) of NPs.

2.7 Antibacterial assay for composite resin modified by TiO₂ nanoparticles:

2.7.1 Bacterial strain and growing conditions:

The *Streptococcus mutans* strain ATCC 25175 provided by Fio Cruz Foundation (Department of Microbiology, Reference Materials Laboratory, Sector Reference Bacteria located in the Oswaldo Cruz Foundation, National Institute of Health Quality Control - INCQS, Av Brazil , 4365 - Manguinhos, Cep: 21045-900, Rio de Janeiro, RJ, Brazil) was used in this study. Initially, 3 to 5 colonies were collected from the Petri dish containing BHI agar (Brain Heart Infusion, Difco Laboratories, Becton Dickinson and Company, USA) + 1% sucrose, placed in a 15 mL falcon tube containing 5mL Bacto™ BHI broth + 1% sucrose and incubated at 37°C (± 1°C) for 18 hours. After growing, the bacterial culture was centrifuged (Excelsa® II Centrifuge, FANEM, Mod. 206 BL, serial number: HV 9462) at 3000 rpm for 15 minutes to obtain the pellet. The supernatant was discarded and the pellet resuspended in PBS (phosphate buffered saline) until reaching the absorbance of 0.08 read at 600nm, with amount of cells in the order of 10⁸ CFU/mL using a spectrophotometer

(Eppendorf AG, Hamburg, Germany). This suspension was used for the direct contact test and 7-days biofilm.

2.7.2 Direct contact test:

The antibacterial activity of modified composite resin was tested by direct contact test [23]. The specimens were prepared immediately after composite resin modification as previously described. Specimens for antibacterial test were prepared using a stainless steel mold (4 mm in diameter and 2 mm in height). The splits mold were placed on a glass slide and overfilled with the composite resin containing TiO₂ and TiO₂/Ag NPs (0.2; 0.5 e 1% in weight). The holes of the mold were pressed with polyester strips and the top surface with another glass slide and specimens were light cured (LED Raddi Plus - SDI, Australia) under 1500 mW/cm² of power density for 40s.

A suspension of *Streptococcus mutans* was prepared and standardized as previously described in the Section 2.7.1. For direct contact test, specimens were light-cured for 40s on the top and sterilized in an autoclave (121°C/15 min) prior to the beginning of the antibacterial tests. The sterilized composite resin specimens were placed in a 24-well plate (Nunclon™, Nunc), the wells were filled with 100µL of *Streptococcus mutans* BHI suspension. They were incubated in an incubator at 37°C in 10% of CO₂ for 1 hour. After that, the wells were filled with 900 µL of BHI broth plus 1% sucrose and incubated at 37°C for 18h. The resultant suspensions of each well were submitted to ten-fold several dilutions until 1:100000. A micropipette was used to retrieve 25µL from each tube to spread on brain-heart infusion agar (BHI Agar, HiMedia Laboratories Pvt. Ltd, India) plates, which was incubated at 37°C in 10% of CO₂ for 48h, and then the colony forming units (CFU's) were counted.

The better concentration found in direct contact test against *Streptococcus mutans* was used to perform the antibacterial activity against *S. mutans* 7-days biofilm, physical and mechanical tests of modified composite resin in this study.

2.7.3 Biofilm formation and bacterial counting:

The composite resin specimens (4 mm in height and 2 mm in diameter; n=15) were placed in a 24-wells microculture plates (Nunclon™, Nunc) and the wells were filled with 100µL of *Streptococcus mutans* BHI suspension plus 900µL of BHI broth with 1% sucrose. Then, the plates were incubated at 37°C (±1°C) for 7 days. The BHI broth solution containing 1% of sucrose was replaced every 48 hours. After 7 days, the BHI broth solution was removed, and the specimens were washed with sterile phosphate-buffered saline (PBS) for three times to remove non-adherent cells. The specimens were placed into sterile test tubes containing 5mL of PBS (Phosphate-buffered saline) solution, stirring using a vortex for 1 min and immersed in an ultrasonic bath (Cristófoli Equipamentos de Biossegurança Ltda, Campo Mourão, Paraná, Brasil) during 5 min (room temperature; 42kHz; 160W). Serial dilution was performed using a micropipette to transfer 100µL of this resultant solution to an Eppendorff® tube containing 900µL of PBS, and then mix to obtain the first ten-fold solution. A new sterile tip was used to carry out each ten-fold solution, and the dilutions were made until the last tube (1:100000). A micropipette was used to retrieve 25µL from each tube to spread on brain-heart infusion agar (BHI Agar, HiMedia Laboratories Pvt. Ltd, India) plates, which was incubated at 37°C (±1°C) for 48 h, and then the colony forming units (CFU/mL) were counted.

2.8 Compressive strength and diametral tensile strength tests

According to ANSI ADA specification number 27 (American National Standard, 1993), the composite resin specimens for compressive strength (n=40) (8 specimens for each Group) and diametral tensile strength (n=40) (8 specimens for each Group) were prepared

using a stainless steel split molds (4 mm in diameter and 8 mm in height). The specimens were light cured (LED Radian Plus - SDI, Australia) under 1500 mW/cm^2 of power density on the top and bottom for 40s and after removal from the mold, the photo-activation was also performed over the different sides of the specimens for the same time (total irradiation time of 1min and 40s). These specimens were stored in artificial saliva (Arte & Ciência, Araraquara, SP, Brazil, pH 7.0) and incubated (SPLabor, SP-200) at 37°C for 24 h prior to the test.

The compressive strength was performed employing a mechanical test machine (DL2000, EMIC - Equipamentos e Sistemas de Ensaio Ltda., São José dos Pinhais, Paraná - Brazil) with a load cell of 5 KN at a cross-speed of 0.5 mm.min^{-1} . For compressive assessment, the composite resin specimens were placed with their flat ends between the plates of the testing machine and the compressive load was applied along the long axis of the specimens. For diametral tensile assessment, the specimens were compressed diametrically introducing tensile stress in the material.

2.9. Surface roughness test:

The reading of the surface roughness was obtained by the use of one $5\mu\text{m}$ radius diamond tip of the portable surface roughness tester (Surftest Mitutoyo SJ-401, Mitutoyo Corporation, Japan) of 1 mm length, at a speed of 1 mm/s, with accuracy of $0.01\mu\text{m}$ over the composite resin specimens ($n=50$) (10 specimens for each group). This procedure was performed in three different places, creating three values that resulted in an average final R_a , which was calculated for each specimen. For the standardization of the readings, three equidistant lines were marked in the specimens in order to guiding the positioning of the diamond tip of the surface roughness tester to obtain the three reading points. The composite resin specimens were stored in artificial saliva (Arte & Ciência, Araraquara, SP, Brazil, pH 7.0) and incubated (SPLabor, SP-200) at 37°C for 24 h prior the test, and then reading of the

initial roughness was performed (baseline reading) and final roughness reading was performed after 28 days of the immersion procedures.

2.10. Degree of conversion measurements:

Fourier transform infrared (FTIR) spectroscopy was used to evaluate the degree of conversion (DC). The composite resin specimens were made and analyzed 24 h after the photo-activation. The light-cured composite resin specimens (n=25), 5 specimens for each Group) were pulverized into a fine powder. To prepare the pellet, 5 mg of the powder was mixed with 100 mg of potassium bromide powder (Merck, EMSURE[®], ACS, Reag. Ph Eur; Lot K45884805) and then pressed to produce a thin pellet. The pellet was placed into a holder attachment into the spectrometer (Espectrum 2000, Perkin Elmer, USA). Uncured specimens (n=25), 5 specimens for each Group) were also mixed with potassium bromide powder (Merck, EMSURE[®], ACS, Reag. Ph Eur; Lot K45884805) and pressed to obtain the pellets, as previously described. The measurements were recorded in the absorbance mode under the following conditions: 32 scans, a 4cm⁻¹ resolution and from 300 to 4000cm⁻¹ wavelength.

The degree of conversion was determined by the ratio of the absorbance intensities of aliphatic C=C peak at 1638 cm⁻¹ against an internal standard peak of aromatic C=C at 1608 cm⁻¹ before and after photoactivation. The DC (%) was determined by the following equation:

$$DC (\%) = \left\{ 1 - \frac{(1638\text{cm}^{-1}/1608\text{cm}^{-1})^{\text{cured}}}{(1638\text{cm}^{-1}/1608\text{cm}^{-1})^{\text{uncured}}} \right\} \times 100 \quad [3]$$

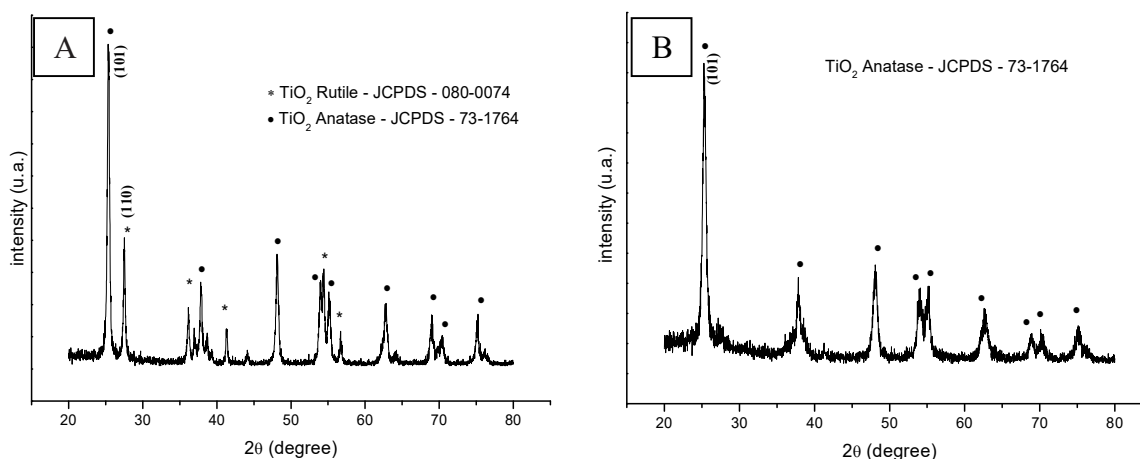
2.11 Statistical analysis

The data was analyzed using the software IBM SPSS Statistics 20.0 (SPSS Inc. Chicago, USA). The normal distribution of the data was determined by Shapiro-Wilk test. Two-way ANOVA and Tukey's test for multiple comparison were performed to direct

contact tests and degree of conversion data. One-way ANOVA and Tukey's test for multiple comparison were performed for the antibacterial activity over the biofilm and mechanical tests. The Mauchly's sphericity test, a mixed model repeated measurements ANOVA and a post hoc test for repeated measures with adjustment of Bonferroni were performed for surface roughness test. All tests were performed at 5% significance level.

3. Results

The crystal structure and phase composition of TiO_2 was revealed by XRD analysis (Figure 1). The typical pattern showed is corresponding to crystalline TiO_2 powder (polymeric precursor) and the diffraction peaks could be indexed to anatase phase (JCPDS – 73-1764) as the main peak of the diffraction plane (101), in addition to rutile phase (JCPDS - 080-0074) with the main peak of the diffraction plane (110). The NPs obtained by microwave-assisted hydrothermal synthesis the pattern is consistent with pure anatase phase. Figure 1. XRD pattern of TiO_2 synthesized by (A) polymeric precursor method and (B) and



hydrothermal synthesis.

The Figure 2 shows the N_2 adsorption–desorption isotherms of the crystalline TiO_2 powder. The adsorption/desorption curve (hysteresis loop), in Figure 2, for TiO_2 NPs obtained by both synthesis methods presents typical of characteristic mesopores adsorbed

with strong and weak affinity and with average pore diameter between 2-50 nm, considered H2 type according to the classification of IUPAC [24]. The TiO₂ and TiO₂/Ag NPs synthesized by hydrothermal synthesis presented the highest values of surface area and consequently the lowest values of average particle size, as can be seen in Table 1.

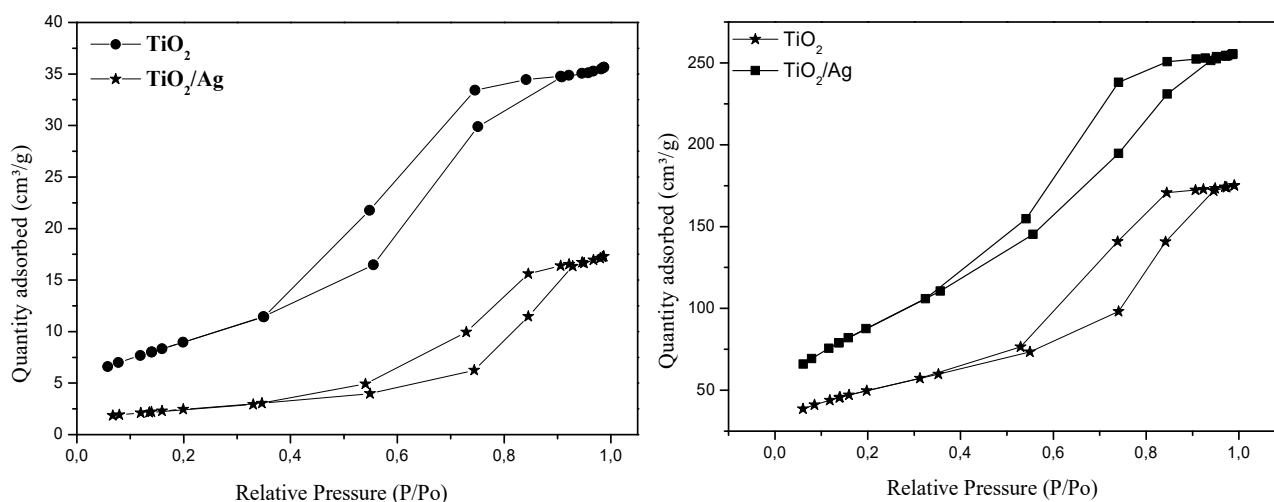


Figure 2. N₂ adsorption–desorption isotherms of TiO₂ powder synthesized by (A) polymeric precursor method and (B) hydrothermal approach.

Table 1. Particle surface area and diameter calculated by BET data

Material	Surface area BET (m ² /g)	Diameter by BET (nm)
TiO ₂ PREC POL	58,02	24,44
TiO ₂ /Ag PREC POL	56,26	25,21
TiO ₂ HYDROT	322,58	4,40
TiO ₂ /Ag HYDROT	447,60	3,17

Note: PREC POL = Polymeric precursor method; HYDROT = microwave assisted hydrothermal method.

The Figure 3 shows the transmission electron microscopy of TiO₂/Ag synthesized by polymeric precursor and hydrothermal approach. Typical agglomerates of spherical

nanoparticles with size ranging 5-10 nm were found to the NPs powder obtained by polymeric precursor and microwave-assisted hydrothermal synthesis.

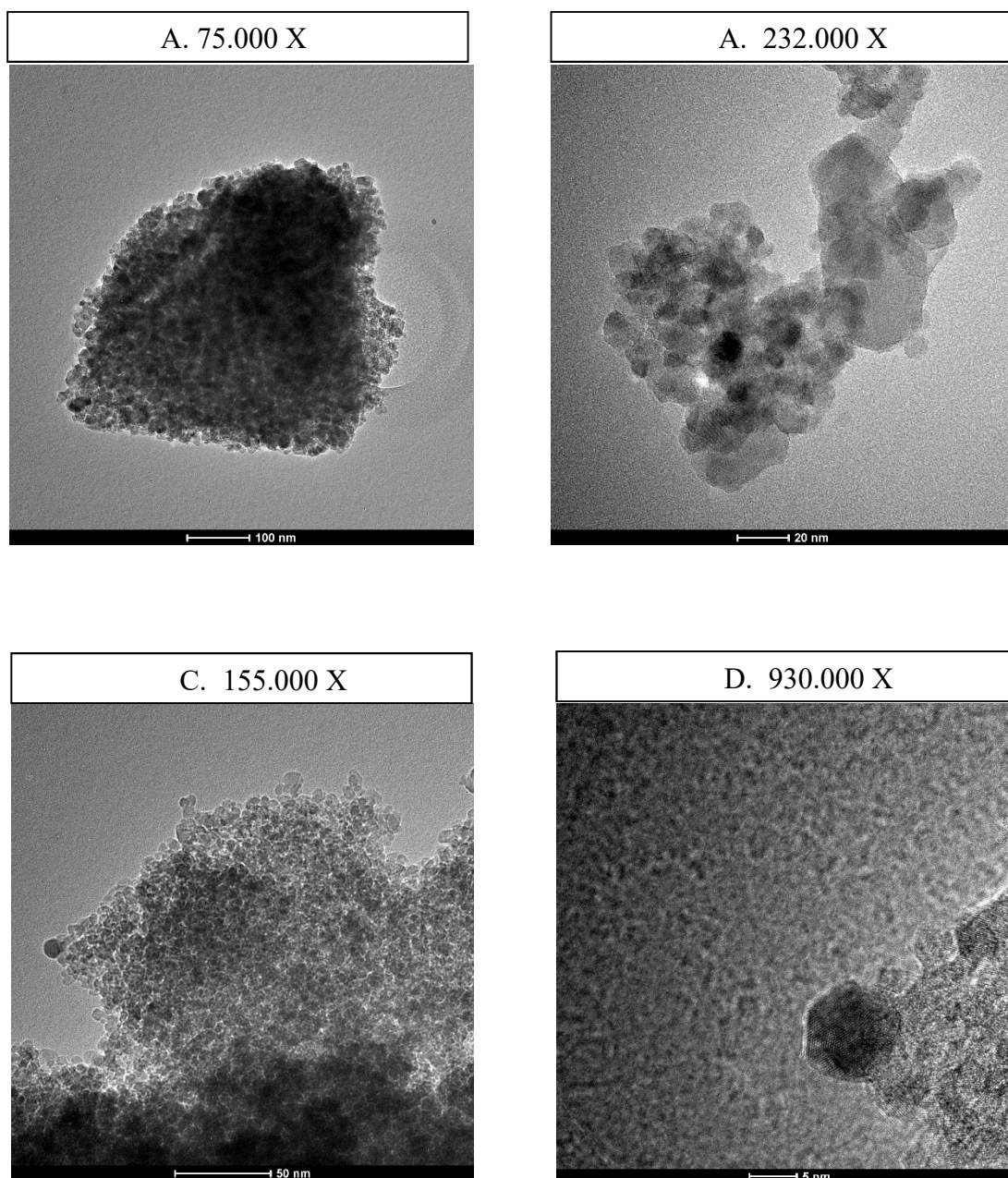


Figure 3. Transmission electron microscopy of Ag decorated TiO_2 synthesized by polymeric precursor (A-B) and hydrothermal approach (C-D).

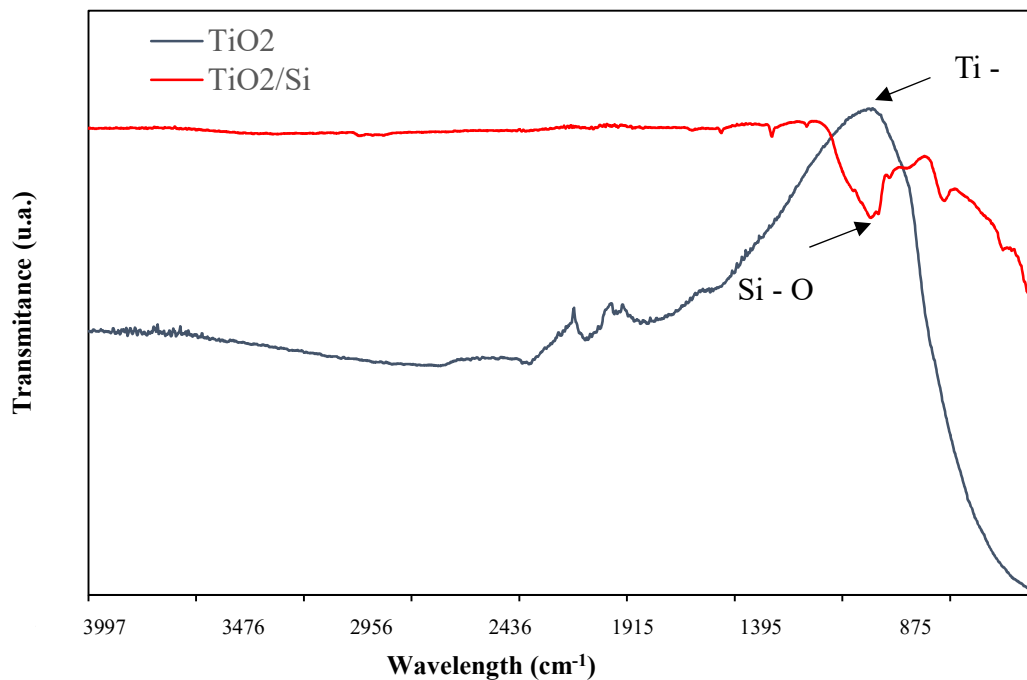


Figure 4. The FTIR spectrum of the pure TiO₂ and TiO₂ modified by TEVS (Triethoxyvinylsilane) (TiO₂/Si).

The FTIR spectrum representing the silanization pattern for the TiO₂ and TiO₂/Ag samples are showed in Figure 4. After treatment of these NPs with TEVS, the absorption bands at 1007 and 1409 cm⁻¹ indicating vibrational modes of SiO₂ bonds suggest that TiO₂ was successfully modified. The broad band with peak at 1012 cm⁻¹ is relative to the Ti-O stretch.

The colony forming unit per mL (CFU/mL) for unmodified and modified composite resin by TiO₂ and TiO₂/Ag NPs (polymeric precursors technique) are shown in Figure 5. The inclusion of 0.5; 1 and 2% by weight of TiO₂; 1 and 2% of TiO₂/Ag NPs (polymeric precursor) significantly inhibited ($p < 0.05$) the growth of *S. mutans* on the composite resin surface compared to the unmodified control Group. For the composite resin modified by TiO₂ and TiO₂/Ag NPs (hydrothermal technique), the results of CFU/mL are shown in

Figure 6. The inclusion of 2% by mass of TiO₂/Ag NPs significantly decreased ($p < 0.05$) *S. mutans* growth on the composite resin surface compared to the control Group. Based on the great antibacterial capacity of composite resin modified by 2% (weight), the following tests were performed using this concentration.

The colony forming unit per mL (CFU/mL) following 7-days *S. mutans* biofilm formation over unmodified and modified composite resin by 2% in weight of TiO₂ and TiO₂/Ag NPs are shown in Figure 7.

The images of confocal laser microscopy for unmodified and modified composite resin by TiO₂ and TiO₂/Ag NPs are showed in Figure 8. These images showed yellow stained which can be attributed to no viable bacterial cells. The control Group, with live bacterial cells, was stained only by green dye.

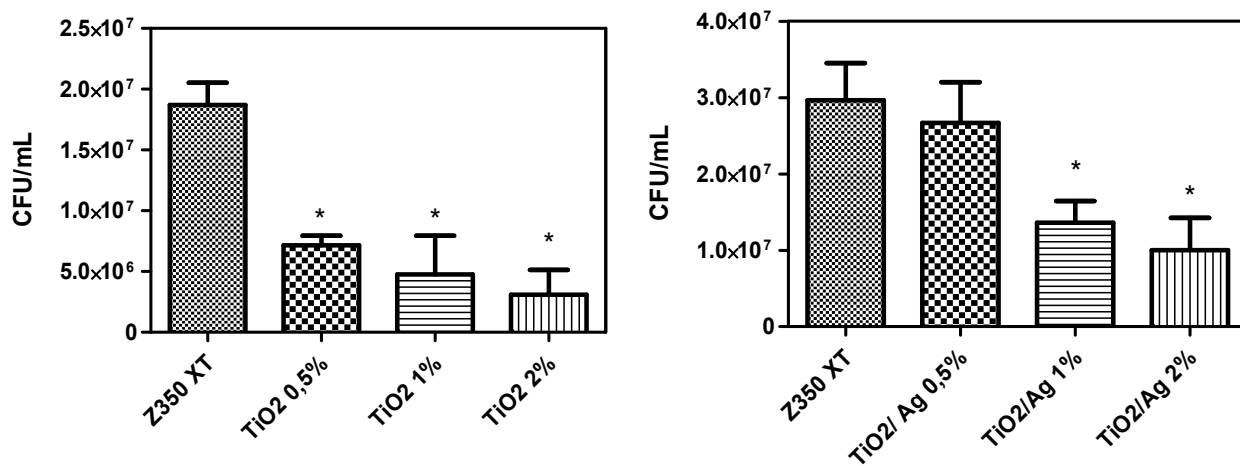


Figure 5. Colony forming unit per mL (CFU/mL) following direct contact between *S. mutans* biofilm and unmodified and modified composite resin by TiO₂ and TiO₂/Ag NPs (PREC POL) (% weight). *Indicate significant statistical differences in comparison to unmodified resin composite.

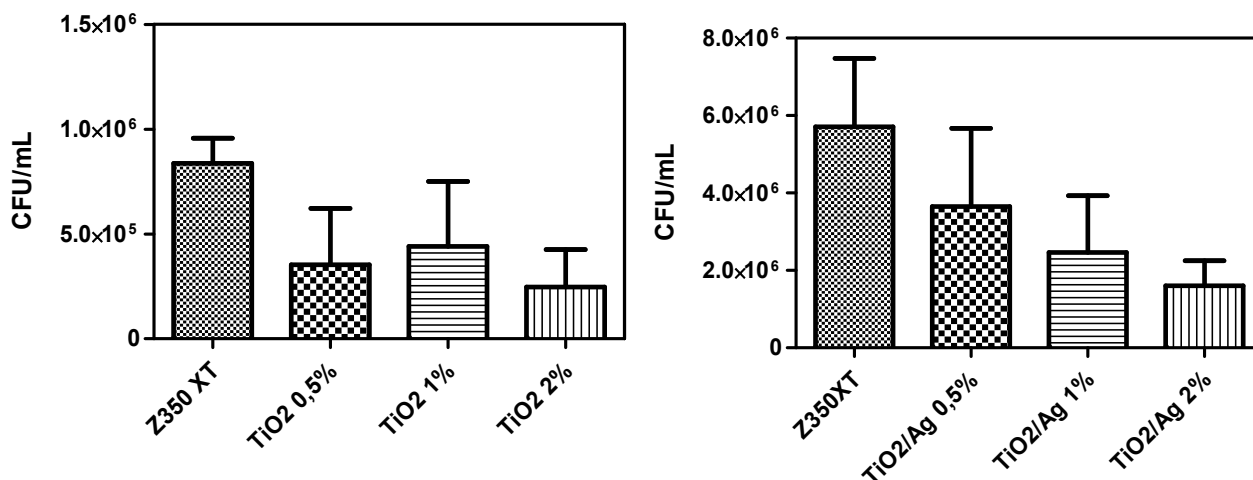


Figure 6. Colony forming unit per mL (CFU/mL) following direct contact between *S. mutans* biofilm unmodified and modified composite resin by TiO₂ and TiO₂/Ag NPs (HYDROT) (% weight). *Indicate significant statistical differences in comparison to unmodified composite resin.

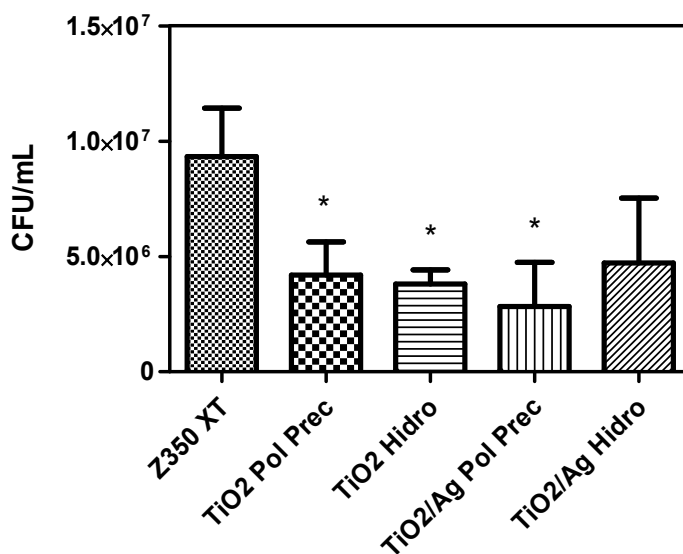


Figure 7. Colony forming unit per mL (CFU/mL) following 7-days *S. mutans* biofilm formation over unmodified and modified composite resin by TiO₂ and TiO₂/Ag NPs (2% in weight). *Indicate significant statistical differences in comparison to unmodified composite resin. Note: PREC POL: polymeric precursor; HYDROT: hydrothermal.

The mean and standard deviation values (MPa) for compressive strength and diametral tensile strength of unmodified and modified composite resin by TiO₂ and TiO₂/Ag NPs (wt.%) are showed in Figure 8. The inclusion of 2% (wt.) of TiO₂ NPs (PREC POL) into the composite resin significantly increased ($p < 0,05$) the compressive strength of the composite resin compared to the unmodified Group.

The degree of conversion (DC%) of unmodified and modified composite resin by 2% (weighth) of TiO₂ and TiO₂/Ag NPs are presented in Table 2. Although the DC% value of composite resin modified by TiO₂ and TiO₂/Ag NPs are lower than unmodified resin, no significant differences were showed ($p > 0.05$) compared to control Group.

Table 2. Degree of conversion (%) of unmodified and modified composite resin by 2% (weighth) TiO₂ and TiO₂/Ag NPs. *Same superscript letters indicates no significant statistical differences

Material	Degree of conversion (%) and standard deviation (SD)
Z350 XT	59.2 ± 1.0 ^a
TiO ₂ PREC POL 2% (wt.)	49.6 ± 3.2 ^a
TiO ₂ HYDROT 2% (wt.)	51.8 ± 2.7 ^a
TiO ₂ /Ag PREC POL 2% (wt.)	48.9 ± 2.6 ^a
TiO ₂ /Ag HYDROT 2% (wt.)	57.3 ± 1.9 ^a

Note: PREC POL = Polymeric precursor method; HYDROT = microwave assisted hydrothermal method.

The mean values of the surface roughness (SR) over time of the composite resin Filtek™ Z350 XT modified by TiO₂ and TiO₂/Ag NPs are showed in the Table 3. A mixed-

model repeated measures ANOVA analysis for SR showed that the sphericity assumption was not met (after Mauchly test) for the Group in artificial saliva (Mauchly $W=0,584$; $p<0,001$). Adjustments for degrees of freedom were performed in order to correct this values. The general analysis showed no significant effect of repeated measures interaction with the tested Groups of modified composite resin ($p=0,820$) on SR values over time (a within-subjects effect), indicating that the surface roughness of Filtek™ Z350 XT modified by the NPs was not significantly affected over time. However, when the pairwise comparison based on estimated marginal means with adjust of Bonferroni showed that only the Group containing TiO₂ NPs (PREC POL) provide no significant changes ($p=1.00$) on composite resin SR compared to unmodified Group.

Table 3. Surface roughness and standard deviation of unmodified and modified composite resin with TiO₂ and TiO₂/Ag NPs (2% in weight) over time. *Different superscript letters at the same line indicates significant statistical differences overtime

Group	Baseline	7 days	14 days	28 days
Unmodified Z350XT	0.18 ± 0.22 ^a	0.16 ± 0.08 ^a	0.35 ± 0.34 ^a	0.31 ± 0.21 ^a
TiO ₂ PREC POL	0.22 ± 0.17 ^a	0.20 ± 0.12 ^a	0.36 ± 0.26 ^a	0.35 ± 0.21 ^a
TiO ₂ /Ag PREC POL	0.55 ± 0.26 ^a	0.55 ± 0.27 ^a	0.80 ± 0.72 ^a	0.70 ± 0.55 ^a
TiO ₂ Hydro	0.60 ± 0.36 ^{ab}	0.27 ± 0.16 ^a	0.66 ± 0.37 ^{ab}	0.68 ± 0.35 ^b
TiO ₂ /Ag Hydro	0.59 ± 0.25 ^a	0.33 ± 0.10 ^a	0.47 ± 0.35 ^a	0.64 ± 0.61 ^a

Note: PREC POL = Polymeric precursor method; HYDROT = microwave assisted hydrothermal method

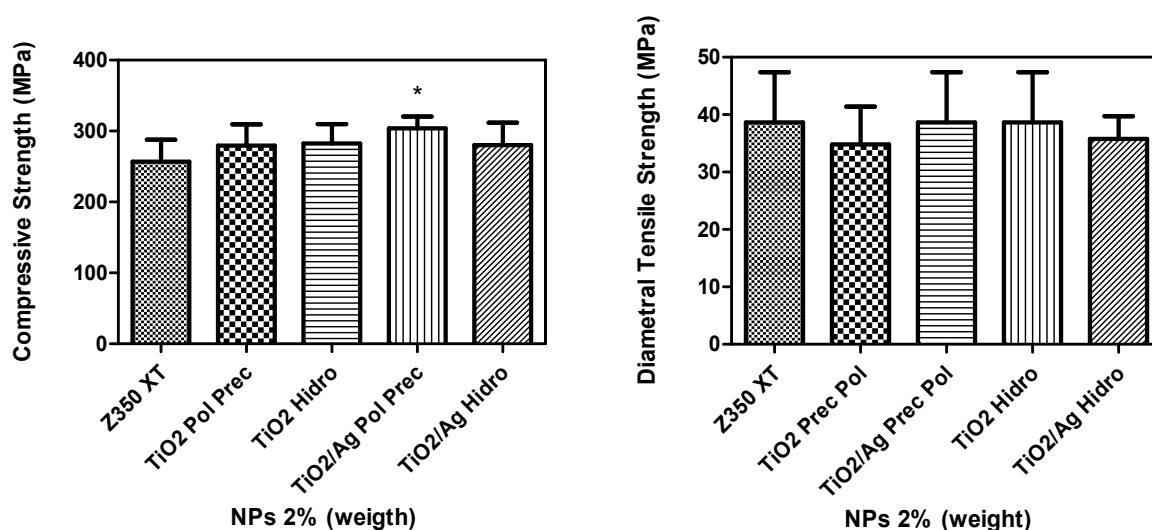


Figure 8. Compressive strength and diametral tensile strength of modified composite resin by TiO_2 and TiO_2/Ag nanoparticles (wt.%). Note: PREC POL: polymeric precursor; Hidro: hydrothermal.

4. Discussion

The synthesis obtained in this current study successfully provided nanosized materials, with high surface area, which is an important characteristic in terms of antibacterial activity, since it could enhance the contact of nanoparticles with cell membrane, contributing to the cell damage process [10]. The results of our study demonstrated a significant antibacterial activity against *S. mutans* biofilm, both in direct contact test and against a mature 7-days biofilm. The hydrothermal samples with high surface area did not demonstrated a great antibacterial capacity in the first test, but could significantly hinder the mature biofilm over 7 days. These findings could be related to the physical-chemical characteristics of the nanoparticles, such as synthesis route, size, shape and surface area. In the case of polymeric precursor method, it is based on polymerization of metal and the crystallinity of their products can be improved with increasing of EG:CA mole ratio, because

the frequency of collisions of that reactant success allows an increase of the reaction towards the formation of the products [25]. On the other hand, the use of microwave irradiations for the synthesis have some advantages, which includes efficient internal heating, increasing the temperature of the whole volume simultaneously and uniformly [26,27]. The ability to absorb microwave energy can vary by orders of magnitude among different compounds and materials, and metal oxides can be successfully synthesized in different sizes and shapes by microwave synthesis [26]. The size and shape control of nanoparticles using microwaves rely on changing “classical” synthesis parameters like precursor concentration or precursor-to-additive ratio [28–30].

Antibacterial activity of TiO₂ nanoparticles has been described in the literature against several microorganisms [31,32,2], contributing besides the antibacterial activity to the improvement of physical and mechanical properties [8,9,33]. According to our results, the literature shows that nanofillers can reduce enamel demineralization without compromising physical properties of the composite, by adding titanium oxide nanoparticles [8]. Ahn et al. [34] also related similar results, showing that composite adhesives containing silver nanoparticles could prevent enamel demineralization around bracket surfaces without compromising physical properties.

The NPs used in this current study significantly decrease biofilm formation over the composite resin, however no differences were found between pure and Ag decorated NPs. However, previous studies reported the enhancement of antibacterial effect by synergetic effect between Ag and metal oxides, which could be mainly due to the obvious increase in the reactive oxidative species (especially superoxide) and the increased damage to plasmid DNA induced by Ag doped NPs [17,18]. Bahadur et al. [15] also analyzed the effect of silver for effective improvement in antibacterial properties of TiO₂. They studied the antibacterial, micro-structural, and fluorescence properties of silver Ag doped TiO₂ and

demonstrated that an excellent antibacterial performance was achieved using TiO₂ with an increasing concentration of Ag, as compared to the pure TiO₂, suggesting that antibacterial activity of nanoparticles remarkably enhances with increasing the Ag concentration in TiO₂. Obviously, the antibacterial effect of hybrids of metal oxides and Ag depends on the concentration of silver. For dental applications, various forms of Ag or Ag-ion containing fillers have been used such as Ag ion-implanted SiO₂, Ag-containing silica glass, Ag-zeolite, Ag-apatite, Ag-supported zirconium phosphate and Ag decorated metal oxides [4]. However, with the increasing of Ag concentration into dental restorative materials some physical properties could be affected, such as color instability and the difficulty in dispersing and homogeneous incorporation into the composite resin. Because of that, in our study we choose to create an Ag decoration of the previously synthesized NPs, using an aqueous silver solution. The use of silver decorated NPs synthesized for several chemical methods have been described, and the products were found to show high antimicrobial effect [5,35,36]. A study reported that the Ag decorated hydroxyapatite nanospheres obtained by microwave-assisted hydrothermal synthesis showed fungistatic and fungicidal effects against *C. albicans* planktonic cells and also exhibited antibiofilm activity, affecting mainly the extra-cellular matrix production [5]. The high antimicrobial capacity of Ag doped and decorated nanomaterials is mainly due the enhancement of oxidative stress and the increased DNA damage induced by Ag containing NPs [17].

It is well known that a dental composite resin should have satisfactory mechanical properties besides the antibacterial activity, especially in positions with heavily occlusal stress [8,37], and because of that an improvement or at least no significant changes on mechanical properties is desired, for the acceptance as a successful dental restorative material. Our findings demonstrated a significant improvement of compressive strength of composite resin after inclusion of TiO₂ NPs, due probably to surface treatment with

organosilane agent. These results are similar to others studies, that modified a resin based restorative material with TiO₂ and improved some properties such as the microhardness and flexural strength [38,39]. Organosilanes, as the TEVS used in this current study, encourages further combination of the nanoparticles with the resin matrix, besides the improvement of the homogeneity of the particles with a resin monomer [38,40].

The resin based restorative materials modified by antibacterial nanoparticles has been reported with smoother surface roughness when compared with the materials containing a hybrid of nano and microsized fillers [41]. As previous reported in the literature, our findings also demonstrated that almost all groups of nanoparticles drastically increased the SR after inclusion of the NPs. An increase of surface roughness could contribute to increase *S. mutans* biofilm accumulation over the dental restorations, which can contribute to progress of secondary caries [41,3]. Otherwise, Ahn et al. [34] reported a significant lower bacterial adhesion of cariogenic streptococci than conventional adhesives.

The degree of conversion of modified composite resin remains unchanged after the inclusion of NPs into the composite resin, as demonstrated in Table 2. These data are in agreement with the others works, which report no significant differences between the degree of conversion after inclusion of small amounts of NPs into the dental resin [37]. In agreement with our results, Sun et al. [39] reported an improving by 3-7% on DC% of a composite resin after inclusion of TiO₂ NPs. An increase of DC% is an important factor for a modified composite resin, since it could make a huge difference in terms of the number of crosslinks and polymer chain mobility, increasing the mechanical properties of the formed polymer.

In summary, this study demonstrate that the inclusion of pure and Ag decorated TiO₂ into the composite resin can decrease *S. mutans* biofilm formation over the composite resin surface. An enhancement of mechanical properties was achieved after inclusion of TiO₂/Ag (PREC POL). The DC% remains unchanging after resin modification with all tested

NPs and the surface roughness was not significantly increased after inclusion of TiO₂/Ag (PREC POL). The TiO₂/Ag nanospheres obtained by polymeric precursor synthesis seems to be, between the tested NPs, the best nanomaterial to fill an antibacterial dental restorative composite resin

REFERENCES

- [1] Ferracane JL. Resin composite—State of the art. *Dent Mater* 2011;27:29–38. doi:10.1016/j.dental.2010.10.020.
- [2] Chen L, Shen H, Suh BI. Antibacterial dental restorative materials: a state-of-the-art review. *Am J Dent* 2012;25:337–46.
- [3] Nedeljkovic I, Teughels W, De Munck J, Van Meerbeek B, Van Landuyt KL. Is secondary caries with composites a material-based problem? *Dent Mater* 2015;31:e247–77. doi:10.1016/j.dental.2015.09.001.
- [4] Fan C, Chu L, Rawls HR, Norling BK, Cardenas HL, Whang K. Development of an antimicrobial resin - A pilot study. *Dent Mater* 2011;27:322–8. doi:10.1016/j.dental.2010.11.008.
- [5] Zamperini CA, André RS, Longo VM, Mima EG, Vergani CE, Machado AL, et al. Antifungal applications of Ag-decorated hydroxyapatite nanoparticles. *J Nanomater* 2013;2013. doi:10.1155/2013/174398.
- [6] Dias HB, Bernardi MIB, Ramos MA dos S, Trevisan TC, Bauab TM, Hernandez AC, et al. Zinc oxide 3D microstructures as an antimicrobial filler content for composite resins. *Microsc Res Tech* 2017:1–10. doi:10.1002/jemt.22840.
- [7] Tavassoli Hojati S, Alaghemand H, Hamze F, Ahmadian Babaki F, Rajab-Nia R, Rezvani MB, et al. Antibacterial, physical and mechanical properties of flowable resin composites containing zinc oxide nanoparticles. *Dent Mater* 2013;29:495–505. doi:10.1016/j.dental.2013.03.011.

- [8] Poosti M, Ramazanzadeh B, Zebarjad M, Javadzadeh P, Naderinasab M, Shakeri MT. Shear bond strength and antibacterial effects of orthodontic composite containing TiO₂ nanoparticles. *Eur J Orthod* 2013;35:676–9. doi:10.1093/ejo/cjs073.
- [9] Cai Y, Strømme M, Welch K. Photocatalytic Antibacterial Effects Are Maintained on Resin-Based TiO₂ Nanocomposites after Cessation of UV Irradiation. *PLoS One* 2013;8. doi:10.1371/journal.pone.0075929.
- [10] Allaker RP. The Use of Nanoparticles to Control Oral Biofilm Formation. *J Dent Res* 2010;89:1175–86. doi:10.1177/0022034510377794.
- [11] Nel AE, Mädler L, Velegol D, Xia T, Hoek EM V, Somasundaran P, et al. Understanding biophysicochemical interactions at the nano-bio interface. *Nat Mater* 2009;8:543–57. doi:10.1038/nmat2442.
- [12] Sahu DR, Liu CP, Wang RC, Kuo CL, Huang JL. Growth and application of ZnO nanostructures. *Int J Appl Ceram Technol* 2013;10:814–38. doi:10.1111/j.1744-7402.2012.02795.x.
- [13] Hanaor DAH, Sorrell CC. Review of the anatase to rutile phase transformation. *J Mater Sci* 2011;46:855–74. doi:10.1007/s10853-010-5113-0.
- [14] Dwivedi C, Dutta V. Size controlled synthesis and photocatalytic activity of anatase TiO₂ hollow microspheres. *Appl Surf Sci* 2012;258:9584–8. doi:10.1016/j.apsusc.2012.05.151.
- [15] Bahadur J, Agrawal S, Panwar V, Parveen A, Pal K. Antibacterial properties of silver doped TiO₂ nanoparticles synthesized via sol-gel technique. *Macromol Res* 2016;24:488–93. doi:10.1007/s13233-016-4066-9.
- [16] Cai Y, Strømme M, Melhus A, Engqvist H, Welch K. Photocatalytic inactivation of biofilms on bioactive dental adhesives. *J Biomed Mater Res - Part B Appl Biomater* 2014;102:62–7. doi:10.1002/jbm.b.32980.

- [17] Zhang Y, Gao X, Zhi L, Liu X, Jiang W, Sun Y, et al. The synergetic antibacterial activity of Ag islands on ZnO (Ag/ZnO) heterostructure nanoparticles and its mode of action. *J Inorg Biochem* 2014;130:74–83. doi:10.1016/j.jinorgbio.2013.10.004.
- [18] Ghosh S, Goudar VS, Padmalekha KG, Bhat S V., Indi SS, Vasani HN. ZnO/Ag nanohybrid: synthesis, characterization, synergistic antibacterial activity and its mechanism. *RSC Adv* 2012;2:930. doi:10.1039/c1ra00815c.
- [19] Chen YC, Chen LH, Min YL, Zhang YG. Simple method to synthesize novel mesoporous zinc oxide. *J Mater Sci Mater Electron* 2012;23:1759–63. doi:10.1007/s10854-012-0658-0.
- [20] Leite ER, Bernardi MIB, Longo E, Varela JA, Paskocimas CA. Enhanced electrical property of nanostructured Sb-doped SnO₂ thin film processed by soft chemical method. *Thin Solid Films* 2004;449:67–72. doi:10.1016/j.tsf.2003.10.101.
- [21] Walton RI. Subcritical solvothermal synthesis of condensed inorganic materials. *Chem Soc Rev* 2002;31:230–8. doi:10.1039/b105762f.
- [22] das Neves PBA, Agnelli JAM, Kurachi C, de Souza CWO. Addition of silver nanoparticles to composite resin: Effect on physical and bactericidal properties in vitro. *Braz Dent J* 2014;25:141–5. doi:10.1590/0103-6440201302398.
- [23] Kasraei S, Sami L, Hendi S, Alikhani M-Y, Rezaei-Soufi L, Khamverdi Z. Antibacterial properties of composite resins incorporating silver and zinc oxide nanoparticles on *Streptococcus mutans* and *Lactobacillus*. *Restor Dent Endod* 2014;39:109–14. doi:10.5395/rde.2014.39.2.109.
- [24] Thommes M, Kaneko K, Neimark A V., Olivier JP, Rodriguez-Reinoso F, Rouquerol J, et al. Physisorption of gases, with special reference to the evaluation of surface area and pore size distribution (IUPAC Technical Report). *Pure Appl Chem* 2015;87:1051–69. doi:10.1515/pac-2014-1117.

- [25] Razavi RS, Loghman-estarki MR, Farhadi-khouzani M. Synthesis and Characterization of ZnO Nanostructures by Polymeric Precursor Route 2012;121:98–100.
- [26] Bilecka I, Niederberger M. Microwave chemistry for inorganic nanomaterials synthesis. *Nanoscale* 2010;2:1358–74. doi:10.1039/b9nr00377k.
- [27] Jhung SH, Jin T, Hwang YK, Chang JS. Microwave effect in the fast synthesis of microporous materials: Which stage between nucleation and crystal growth is accelerated by microwave irradiation? *Chem - A Eur J* 2007;13:4410–7. doi:10.1002/chem.200700098.
- [28] He M, Jiu H, Liu Y, Tian Y, Li D, Sun Y, et al. Controllable synthesis of ZnO microstructures with morphologies from rods to disks. *Mater Lett* 2013;92:154–6. doi:10.1016/j.matlet.2012.10.049.
- [29] Aneesh PM, Vanaja K a., Jayaraj MK. Synthesis of ZnO nanoparticles by hydrothermal method. *Nanosci Eng* 2007;6639:66390J–66390J. doi:10.1117/12.730364.
- [30] Moura KF, Maul J, Albuquerque AR, Casali GP, Longo E, Keyson D, et al. TiO₂ synthesized by microwave assisted solvothermal method: Experimental and theoretical evaluation. *J Solid State Chem* 2014;210:171–7. doi:10.1016/j.jssc.2013.11.023.
- [31] Özyildiz F, Güden M, Uzel A, Karaboz I, Akil O, Bulut H. Antimicrobial activity of TiO₂-coated orthodontic ceramic brackets against *Streptococcus mutans* and *Candida albicans*. *Biotechnol Bioprocess Eng* 2010;15:680–5. doi:10.1007/s12257-009-3005-4.
- [32] Catauro M, Raucci M, Convertito C, Melisi D, Rimoli M. Characterization, bioactivity and ampicillin release kinetics of TiO₂ and TiO₂4SiO₂ synthesized by

- sol-gel processing. *J Mater Sci Mater Med* 2006;17:413–20. doi:10.1007/s10856-006-8468-7.
- [33] Yu B, Ahn JS, Lim JI, Lee YK. Influence of TiO₂ nanoparticles on the optical properties of resin composites. *Dent Mater* 2009;25:1142–7. doi:10.1016/j.dental.2009.03.012.
- [34] Ahn SJ, Lee SJ, Kook JK, Lim BS. Experimental antimicrobial orthodontic adhesives using nanofillers and silver nanoparticles. *Dent Mater* 2009;25:206–13. doi:10.1016/j.dental.2008.06.002.
- [35] Peng J min, Lin J cheng, Chen Z yu, Wei M chao, Fu Y xiang, Lu S shen, et al. Enhanced antimicrobial activities of silver-nanoparticle-decorated reduced graphene nanocomposites against oral pathogens. *Mater Sci Eng C* 2017;71:10–6. doi:10.1016/j.msec.2016.09.070.
- [36] Takahashi C, Matsubara N, Akachi Y, Ogawa N, Kalita G, Asaka T, et al. Visualization of silver-decorated poly (DL-lactide-co-glycolide) nanoparticles and their efficacy against *Staphylococcus epidermidis*. *Mater Sci Eng C Mater Biol Appl* 2017;72:143–9. doi:10.1016/j.msec.2016.11.051.
- [37] Tavassoli Hojati S, Alaghemand H, Hamze F, Ahmadian Babaki F, Rajab-Nia R, Rezvani MB, et al. Antibacterial, physical and mechanical properties of flowable resin composites containing zinc oxide nanoparticles. *Dent Mater* 2013;29:495–505. doi:10.1016/j.dental.2013.03.011.
- [38] Xia Y, Zhang F, Xie H, Gu N. Nanoparticle-reinforced resin-based dental composites. *J Dent* 2008;36:450–5. doi:10.1016/j.jdent.2008.03.001.
- [39] Sun J, Forster AM, Johnson PM, Eidelman N, Quinn G, Schumacher G, et al. Improving performance of dental resins by adding titanium dioxide nanoparticles. *Dent Mater* 2011;27:972–82. doi:10.1016/j.dental.2011.06.003.

- [40] Yang C, Yang C. Preparation of TiO₂ particles and surface silanization modification for electronic ink. *J Mater Sci Mater Electron* 2014;25:3285–9. doi:10.1007/s10854-014-2015-y.
- [41] Park JW, Song CW, Jung JH, Ahn SJ, Ferracane JL. The effects of surface roughness of composite resin on biofilm formation of *Streptococcus mutans* in the presence of saliva. *Oper Dent* 2012;37:532–9. doi:10.2341/11-371-L.

3.2 Artigo 2

Title page

Title: Antibacterial, physical and mechanical properties of a composite resin modified by ZnO and ZnO/Ag nanoparticles.*

Short Title: Application of ZnO and ZnO/Ag in Dental Resins.

Authors: Hércules Bezerra Dias¹, Maria Inês Basso Bernardi², Taís Maria Bauab³, Antônio Carlos Hernandes², Alessandra Nara de Souza Rastelli^{1*}

¹Department of Restorative Dentistry, Araraquara School of Dentistry, Sao Paulo State University – UNESP, Araraquara, SP 14801-903, Brazil.

² Department of Physics and Materials Science, Physics Institute of São Carlos - IFSC, University of São Paulo, São Carlos, São Paulo, 13566-590, Brazil.

³Department of Biological Sciences, School of Pharmaceutical Sciences, Univ. Estadual Paulista - UNESP, Araraquara, SP 14801-902, Brazil.

*Corresponding author: Prof. Dr. Alessandra Nara de Souza Rastelli, São Paulo State University - UNESP, Araraquara School of Dentistry, Department of Restorative Dentistry, Araraquara, SP, Brazil. 1680 Humaita St., Araraquara, São Paulo, Brazil. MailBox: 331. ZipCode: 14.801-903. Telephone: +55 (016) 3301-6524 Fax: +55 (016) 3301-6393. e-mail address: alrastelli@foar.unesp.br

Manuscript

Title: Antibacterial, physical and mechanical properties of a composite resin modified by ZnO and ZnO/Ag nanoparticles.

Short Title: Application of ZnO and ZnO/Ag in Dental Resins.

Summary

The goal of this study was to modify a composite resin with zinc oxide (ZnO) and silver decorated zinc oxide (ZnO/Ag) nanoparticles (NPs) and evaluate the antibacterial, mechanical and physical properties of the modified composite resin. The NPs were synthesized by polymeric precursor and microwave-assisted hydrothermal methods and treated with an organosilane agent. The Filtek™Z350 XT composite resin was modified with 0.5, 1 and 2% (in weight) of NPs to perform an antibacterial screening by contact direct test with *Streptococcus mutans* biofilm. The following tests were performed with 2% of NPs. The modified composite resin was tested against *S. mutans* 7-day biofilm by CFU/mL and confocal laser scanning microscopy. The compressive and diametral tensile strength of modified composite resin (n=40), 8 specimens for each Group, was tested using a universal test machine (EMIC). The degree of conversion (n=25), 5 specimens for each Group, was performed by FTIR analysis. The reading of the surface roughness (n=50), 10 specimens for each Group, was performed using a portable surface roughness tester. The data were analyzed using the software IBM SPSS Statistics 20.0 (SPSS Inc. Chicago, USA) by one-way ANOVA for the antibacterial activity over the biofilm and mechanical tests; two-way ANOVA for degree of conversion and Tukey test for multiple comparison; repeated measurements ANOVA and a post hoc test with adjustment of Bonferroni for color stability and surface roughness test, at 5% significance level. The modified composite resin significantly decreased the biofilm formation ($p < 0.05$) by CFU/mL test confirmed by the confocal microscopy images, regardless of the nanoparticles used. The mechanical properties, surface roughness and degree of conversion did not change drastically by incorporation of NPs compared to unmodified resin. Although no statistical differences were found for the mechanical and physical tests, the maintenance of these properties is important to development of a new antibacterial composite resin without sacrificing of others original properties.

Key-words: Zinc oxide, Silver, Anti-bacterial agent, Biofilm, *Streptococcus mutans*.

Introduction

The composite resin evolution is mainly related to the filler contents. The inorganic particles used in the production and their physicochemical properties are directly related to this composition (1,2). Regarding nanofilled composite resins, although they presented excellent mechanical and physical properties, the lack of antibiofilm properties still remains (1,3). Currently, it is not known whether secondary caries with composites is only a material-based problem, but it is well defined that the resin-based restorative materials might influence the development of secondary caries in different ways (4). Among the approaches to promote antibacterial action in composite resins, the incorporation of metal (such as silver and zinc), metal oxides (such as zinc oxide) and antimicrobial polymers have been used to modify resin based restorative materials (5–7). The use of metal nanoparticles have gained significant interest over years, due to the remarkable antimicrobial properties (6,8).

The physicochemical characteristics of particles in nanoscale allows greater presence of atoms over the surface, providing the maximum contact of the particles with the environment (9,10). Once cariogenic bacterial acids can degrade restorative materials and allows secondary caries formation, dental composites containing zinc and silver-doped zinc materials have been developed in order to inhibit growth of bacteria over the restorations (3,9–14).

ZnO (zinc oxide) nanoparticles exhibit excellent physical and chemical properties and a great variety of different shapes, which have been described as an important role in the reactive oxygen species production and antibacterial activity (15–17). Since the antibacterial activity of ZnO nanoparticles is dependent on its size, this variety of ZnO micro and nanostructures has showing a great antibacterial effect on gram-positive and negative bacteria (18,19). ZnO nanoparticles in different shapes have been demonstrated a broad antimicrobial spectrum (19–22), and the inclusion on resin based restorative materials demonstrated a great control of bacterial biofilms on the surface of this materials (6,7,23).

Although the antibacterial activity of ZnO nano and microparticles has been demonstrated in the literature, the use as a filler content in a composite resin should be investigated in order to formulate a composite resin with the ability to inhibit bacterial biofilm formation without affect the mechanical and physical properties. In this way, the aim of this study was to synthesize and characterize ZnO nanoparticles by different chemical routes, incorporate into a composite resin and evaluate the antibacterial, mechanical and physical properties in order to obtain a novel restorative material with antibacterial capacity,

providing longevity of dental restorations. The null hypotheses tested were: 1. There is no difference on antibacterial capacity of a composite resin after modification with ZnO nanoparticles. 2. There is no difference on the tested mechanical and physical properties of a composite resin after modification with ZnO microstructures.

Materials e Methods

Experimental design

This is an in vitro experimental study, which have dependent variables (antibacterial capacity (CFU/mL), compressive strength, diametral tensile strength, surface roughness and degree of conversion) and independent variables [ZnO and ZnO/Ag synthesized by different chemical routes].

Synthesis of ZnO NPs by polymeric precursor method (PREC POL)

For synthesise ZnO NPs by polymeric precursor method (24), zinc nitrate ($\text{Zn}(\text{NO}_3)_2 \cdot 6\text{H}_2\text{O}$) (Sigma- Aldrich) and citric acid ($\text{C}_6\text{H}_8\text{O}_7 \cdot \text{H}_2\text{O}$, 99.5%) (Synth) were used as precursors. The zinc nitrate, citric acid, and dopants were dissolved in water and then mixed into an aqueous citric acid solution (100°C) under constant stirring. Then, ethylene glycol ($\text{HOCH}_2\text{CH}_2\text{OH}$, P.A. >99,5%) (Synth) was added to polymerize the citrate by a polyesterification reaction. The citric acid:metal molar ratio was 3:1, while the citric acid:ethylene glycol (CA:EG) molar ratio was 60:40. The resulting resin was calcined at 300°C for 4h at $10^\circ\text{C}/\text{min}$, leading to the formation of the precursors powder. The data sample (ZPS – Ag doped ZnO NPs) was showed in Table 1.

Synthesis of ZnO NPs by microwave-assisted hydrothermal method (HYDROT)

The synthesis of ZnO by the microwave assisted hydrothermal method was prepared from the mass ratio of ZnCl_2 . In a typical procedure, 2.726 g of ZnCl_2 (2% molar) were diluted in 10 mL of water in a teflon[®] vessel (called a reaction vessel) under constant stirring using magnetic stirrer. Then, 10 mL of NaOH was added to the precursor solution and the final solution filled out at least 90% of the total volume of the reaction vessel in order to obtain maximum efficiency in relation to the self-generated pressure (25). The reaction cup was inserted inside the reaction cell, it was closed and transferred to the microwave assisted hydrothermal system, where the reaction occurred at a heating rate of $140^\circ\text{C min}^{-1}$ and held at 140°C for 10 minutes.

Silver decoration of nanoparticles

The Ag decorated NPs were synthesized (26) using the previously prepared ZnO powder dispersed in distilled water, and the pH was adjusted to 5 with HNO₃. The solution was stirred at 60°C, and then 5 mL of AgNO₃ solution (1.4×10^{-2} M) was added in order to obtain a concentration of 1 mol NP : 1 mol Ag. The precipitate was washed with distilled water until pH 7 and then dried in an oven.

Characterization of nanoparticles

The X-Ray diffraction (XRD) patterns of the ZnO powder were recorded on a Rigaku, Rotaflex RU200B diffraction system with high intensity Cu K α radiation ($\lambda = 1.5406 \text{ \AA}$), at 25°C with 2θ values ranging from 20–80°C and scanning rate of 0.02°C per min. The crystallite size was determined by Scherrer equation above (where λ is the wavelength of the X-ray radiation, K is a constant taken as 0.89, θ is the diffraction angle and β is the full width at half maximum (FWHM)).

$$D = \frac{K\lambda}{(\beta \cos \theta)} \quad [1]$$

The FTIR measurements of ZnO particles were carried out in the Nexus 670 FTIR spectrophotometer (Thermo Scientific, Madison, WI). A total of 64 scans were collected from 4000 cm⁻¹ to 650 cm⁻¹ at 4cm⁻¹ resolution. Nitrogen adsorption–desorption measurements for the products were performed using a Micromeritics ASAP 2020 M + C instrument using Barrett–Emmett–Teller calculations for surface area determination. The isotherms and hysteresis curves were classified according to IUPAC (*International Union of Pure and Applied Chemistry*). The particle size (D_{BET}) was calculated using the following equation:

$$D_{BET} = \frac{6}{A_s \cdot \rho} \quad [2]$$

Where A_s is the superficial area (m²/g) and ρ is the density of material (ZnO = 5.675 JCPDF 36-1451).

The samples were structurally characterized using an automatic X-ray diffractometer (Rigaku, Ultima IV) with CuK α radiation (40 kV, 46 mA, $\theta = 1.5405 \text{ \AA}$) and in a θ - 2θ configuration using a graphite monochromator. The scanning range was between 20 and 80° (2θ), with a step size of 0.02° and a step time of 1.0 s.

The thermal decomposition processes were studied by thermogravimetry (TG, Netzsch STA 409C), in an oxygen atmosphere at a heating rate of $10^{\circ}\text{C min}^{-1}$. Al_2O_3 was used as reference material during the thermal analysis.

The morphology and size of Ag decorated nanoparticles were performed by transmission electron microscopy (TEM, Tecnai G2TF20, FEI).

The specific surface area (BET) and the diameter of nanoparticles was estimated from the N_2 desorption/adsorption isotherms at liquid nitrogen temperature, using a Micrometrics ASAP 2020.

Composite resin used in this study

The nanofilled composite resin Filtek™ Z350XT (3M Brazil) at color A₂B (Body), employed as a control Group and modified by ZnO and ZnO/Ag nanoparticles for experimental Groups was used.

Composite resin modification:

ZnO nanoparticles were added into the composite resin Filtek™ Z350XT (3M Brazil) using a standardized protocol based on the inclusion of weight percentage of particles into the composite resin (8). The NPs were incorporated into the composite resin by manual mixing for 1 min, using a metal spatula and a glass plate. For direct contact test, the NPs were weighed corresponding to 0.5 and 1 and 2% (wt.%). After the antibacterial screening, the specimens for the following tests were prepared with 2% (wt.%) of NPs.

Antibacterial assay for composite resin modified by ZnO microstructures

Bacterial strain and growing conditions:

The *Streptococcus mutans* strain ATCC 25175 provided by Fio Cruz Foundation (Department of Microbiology, Reference Materials Laboratory, Sector Reference Bacteria located in the Oswaldo Cruz Foundation, National Institute of Health Quality Control -. INCQS, Av Brazil , 4365 - Manguinhos, Cep: 21045-900, Rio de Janeiro, RJ, Brazil) was used in this study. Initially, 3 to 5 colonies were collected from the Petri dish containing BHI agar (Brain Heart Infusion, Difco Laboratories, Becton Dickinson and Company, USA) + 1% sucrose, placed in a 15 mL falcon tube containing 5mL Bacto™ BHI broth + 1% sucrose and incubated at 37°C ($\pm 1^{\circ}\text{C}$) for 18 hours. After growing, the bacterial culture was centrifuged (Excelsa® II Centrifuge, FANEM, Mod. 206 BL, serial number: HV 9462) at 3000 rpm for 15 minutes to obtain the pellet. The supernatant was discarded and the pellet

resuspended in PBS (phosphate buffered saline) until reaching the absorbance of 0.08 read at 600nm, with amount of cells in the order of 10^8 CFU/mL using a spectrophotometer (Eppendorf AG, Hamburg, Germany). This suspension was used for the direct contact test and 7-days biofilm.

Direct contact test

For direct contact test, nanoparticles were weighed corresponding to 0.5 and 1 and 2% (wt.%), these amounts were incorporated into the resin by manual mixing for 1 min, using a metal spatula and a glass plate. The specimens were prepared immediately after resin modification. Specimens for antibacterial test were prepared using a stainless steel mold (4 mm in diameter and 2 mm in height). The splits mold were placed on a glass slide and overfilled with the composite resin containing ZnO microstructures (0.2; 0.5 e 1% in weight). The holes of the mold were pressed with polyester strips and the top surface with another glass slide and specimens were light cured (LED Raddi Plus - SDI, Australia) under 1500 mW/cm^2 of power density for 40s.

Since *Streptococcus mutans* is the leading cause of dental caries worldwide and is considered the most cariogenic of all of the oral streptococci (27), this bacteria was the first choice to be used in this antibacterial assay. The composite resin modified by ZnO microstructures was tested by direct contact test (7). A suspension of *S. mutans* was prepared and standardized as described in the section Bacterial Strain and Growing Conditions. For direct contact test, specimens were light-cured for 40s on the top and sterilized in an autoclave ($121^\circ\text{C}/15 \text{ min}$) prior the test. The sterilized composite resins specimens were placed in a 24-well plate (Nunclon™, Nunc), the wells were filled with 100μL of *Streptococcus mutans* BHI suspension. They were incubated in an incubator at 37°C in 10% of CO_2 for 1 hour. After that, the wells were filled with 900 μL of BHI broth plus 1% sucrose and incubated at 37°C for 18h. The resultant suspensions of each well were submitted to ten-fold several dilutions until 1:100000. A micropipette was used to retrieve 25μL from each tube to spread on brain-heart infusion agar (BHI Agar, HiMedia Laboratories Pvt. Ltd, India) plates, which was incubated at 37°C in 10% of CO_2 for 48h, and then the colony forming units (CFU's) were counted.

The better concentration found in direct contact test against *Streptococcus mutans* was used to perform the antibacterial activity against *S. mutans* 7-days biofilm, physical and mechanical tests of modified composite resin in this study.

Biofilm formation and bacterial counting

The composite resin specimens (4 mm in height and 2 mm in diameter; n=15) were placed in a 24-wells microculture plates (Nunclon™, Nunc) and the wells were filled with 100µL of *Streptococcus mutans* BHI suspension plus 900µL of BHI broth with 1% sucrose. Then, the plates were incubated at 37°C (±1°C) for 7 days. The BHI broth solution containing 1% of sucrose was replaced every 48 hours. After 7 days, the BHI broth solution was removed, and the specimens were washed with sterile phosphate-buffered saline (PBS) for three times to remove non-adherent cells. The specimens were placed into sterile test tubes containing 5mL of PBS (Phosphate-buffered saline) solution, stirring using a vortex for 1 min and immersed in an ultrasonic bath (Cristófoli Equipamentos de Biossegurança Ltda, Campo Mourão, Paraná, Brasil) during 5 min (room temperature; 42kHz; 160W). Serial dilution was performed using a micropipette to transfer 100µL of this resultant solution to an Eppendorff® tube containing 900µL of PBS, and then mix to obtain the first ten-fold solution. A new sterile tip was used to carry out each ten-fold solution, and the dilutions were made until the last tube (1:100000). A micropipette was used to retrieve 25µL from each tube to spread on brain-heart infusion agar (BHI Agar, HiMedia Laboratories Pvt. Ltd, India) plates, which was incubated at 37°C (±1°C) for 48 h, and then the colony forming units (CFU/mL) were counted.

Compressive strength and diametral tensile strength tests

According to ANSI ADA specification number 27 (American National Standard, 1993), the composite resin specimens for compressive strength (n=40), (8 specimens for each Group) and diametral tensile strength (n=40) (8 specimens for each Group) were prepared using a stainless steel split molds (4 mm in diameter and 8 mm in height). The specimens were light cured (LED Raddi Plus - SDI, Australia) under 1500 mW/cm² of power density on the top and bottom for 40s and after the removal from the mold, the photo-activation was also performed over the different sides of the specimens for the same time (total irradiation time of 1min and 40s). These specimens were stored in artificial saliva (Arte & Ciência, Araraquara, SP, Brazil, pH 7.0) and incubated (SPLabor, SP-200) at 37°C for 24 h prior to test. For direct contact test, specimens were light-cured for 40s on the top and sterilized in an autoclave (120°C/15 min) prior the test.

The compressive strength was performed employing a mechanical test machine (DL2000, EMIC - Equipamentos e Sistemas de Ensaio Ltda., São José dos Pinhais, Paraná - Brazil) with a load cell of 5 KN at a cross-speed of $0.5 \text{ mm}\cdot\text{min}^{-1}$. For compressive assessment, the composite resin specimens were placed with their flat ends between the plates of the testing machine and the compressive load was applied along the long axis of the specimens. For diametral tensile assessment, the specimens were compressed diametrically introducing tensile stress in the material.

Surface roughness test

The reading of the surface roughness was obtained by the use of one the $5 \mu\text{m}$ radius diamond tip of the portable surface roughness tester (Surftest Mitutoyo SJ-401, Mitutoyo Corporation, Japan) of 1 mm length, at a speed of 1 mm/s, with accuracy of $0.01 \mu\text{m}$ over the composite resin specimens ($n=50$) (10 specimens for each group). This procedure was performed in three different places, creating three values that resulted in an average final Ra, which was calculated for each test specimen. For the standardization of the readings, three equidistant lines were marked in the specimens in order to guiding the positioning of the diamond tip of the surface roughness tester to obtain the three reading points. The composite resin specimens were stored in artificial saliva (Arte & Ciência, Araraquara, SP, Brazil, pH 7.0) and incubated (SPLabor, SP-200) at 37°C for 24h prior the test, and then reading of the initial roughness was performed (baseline reading) and final roughness reading was performed after 28 days of the immersion procedures.

Degree of conversion measurements

Fourier transform infrared (FTIR) spectroscopy was used to evaluate the degree of conversion (DC). The composite resin specimens were made and analyzed 24 h after the photo-activation. The cured composite resin specimens ($n=25$) (5 specimens for each group) were pulverized into a fine powder. To prepare the pellet, 5 mg of the powder was mixed with 100 mg of potassium bromide powder (Merck, EMSURE[®], ACS, Reag. Ph Eur; Lot K45884805) and then pressed to produce a pellet. The pellet was placed into a holder attachment into the spectrometer (Espectrum 2000, Perkin Elmer, Brazil). Uncured specimens ($n=25$) (5 specimens for each group) of each composite resin group were mixed with potassium bromide powder (Merck, EMSURE[®], ACS, Reag. Ph Eur; Lot K45884805)

and pressed to obtain the pellets, as previously described. The measurements were recorded in the absorbance mode operating under the following conditions: 32 scans, a 4 cm⁻¹ resolution, and from 300 to 4000 cm⁻¹ wavelength.

The degree of conversion was determined by the ratio of the absorbance intensities of aliphatic C—C peak at 1638 cm⁻¹ against an internal standard peak of aromatic C—C at 1608 cm⁻¹ before and after light-curing. The DC (%) was determined by the following equation:

$$DC (\%) = \left\{ 1 - \frac{\left(\frac{1638\text{cm}^{-1}}{1608\text{cm}^{-1}} \right)_{\text{cured}}}{\left(\frac{1638\text{cm}^{-1}}{1608\text{cm}^{-1}} \right)_{\text{uncured}}} \right\} \times 100 \quad [3]$$

Statistical analysis

The data was analyzed using the software IBM SPSS Statistics 20.0 (SPSS Inc. Chicago, USA). The normal distribution of the data was determined by Shapiro-Wilk test. Two-way ANOVA and Tukey's test for multiple comparison were performed to direct contact tests and degree of conversion data. One-way ANOVA and Tukey's test for multiple comparison were performed for the antibacterial activity over the biofilm and mechanical tests. The Mauchly's sphericity test, a mixed model repeated measurements ANOVA and a post hoc test for repeated measures with adjustment of Bonferroni were performed for surface roughness test. All tests were performed at 5% significance level.

Results

The crystal structure and phase composition of ZnO was revealed by XRD analysis. The typical pattern showed in Figure 1 is corresponding to crystalline ZnO powder and the diffraction peaks could be indexed to ZnO hexagonal structure (JCPDF file n°. 36-1451).

The Figure 2 shows the N₂ adsorption–desorption isotherms of the crystalline ZnO powder. The isotherms shown are type IV with H1 hysteresis loops, characteristic of mesoporous materials with a narrow pore size distribution. According to IUPAC classification, it can be classified as a microporous, mesoporous or macroporous.

Transmission electron microscopy of Ag decorated ZnO (ZnO/Ag) synthesized by polymeric precursor and hydrothermal approach are presented in Figure 3. Typical agglomerates of spherical nanoparticles with average size of 5 nm were found to powder

obtained by polymeric precursor synthesis, when self-assembled nanowires were found to the NPs obtained by hydrothermal synthesis.

The Table 1 shows the specific surface area values of the ZnO and ZnO/Ag and the average particle diameter calculated from surface area data.

The Figure 4 shows the FTIR spectrum representing the silanization pattern for the ZnO and ZnO/Ag samples. After treatment of these NPs with TEVS, some new absorption peaks were observed, suggesting silanization success. The peak at 720 cm^{-1} represents the mode of vibrational stretching of Si-C, while peaks at 1440 and 1468 cm^{-1} , represent modes of binding for the Si-O-C and Si-O-Si groups, respectively. The broadband peak between 350 and 550 cm^{-1} is relative to the Zn-O stretch mode.

The colony forming unit per mL (CFU/mL) following direct contact between *S. mutans* biofilm and unmodified and modified composite resin by ZnO and ZnO/Ag NPs (polymeric precursors) are shown in Figure 5. The groups containing 0.5; 1 and 2% by weight of ZnO and 2% ZnO/Ag NPs (PREC POL) significantly decreased ($p < 0.05$) the accumulation of *S. mutans* biofilm on the surface of the composite resin compared to the unmodified control Group.

The colony forming unit per mL (CFU/mL) following direct contact between *S. mutans* biofilm and resin composite unmodified and modified by ZnO and ZnO/Ag NPs (hydrothermal synthesis) are shown in Figure 6. The inclusion of 1 and 2% by mass of ZnO and ZnO/Ag NPs (Hidro) significantly decreased ($p < 0.05$) the biofilm accumulation of *S. mutans* on the resin surface compared to the control group.

Because the great antibacterial capacity of the composite resin modified by 2% (weight) of NPs in the direct contact test, the following biological, mechanical and physical tests were performed with the composite resin modified by that concentration.

The colony forming unit per mL (CFU/mL) following 7-days *S. mutans* biofilm formation over resin composite unmodified and modified by 2% in weight of ZnO and ZnO/Ag NPs are shown in Figure 7.

The mean and standard deviation values (MPa) for compressive strength and diametral tensile strength of unmodified and modified composite resin composite by ZnO NPs (wt.%) are shown in Figure 8. Compressive strength (Figure 8a) and diametral tensile strength (Figure 8b) of composite resin was not significantly affected ($p > 0,05$) after inclusion of 2% in weight of ZnO NPs compared to the unmodified composite resin.

The Table 2 shows the degree of conversion (%) of unmodified and modified composite resin by 2% (weight) ZnO NPs. The DC% remains unchanged after inclusion of

the nanoparticles and no significant differences were found ($p > 0.05$) compared to unmodified composite resin.

The mean values of the surface roughness (SR) over time of the composite resin Filtek™ Z350 XT modified by ZnO and ZnO/Ag NPs are showed in the Table 3. The mixed-model repeated measures ANOVA analysis for SR showed that the sphericity assumption was not met (after Mauchly test) for the group in artificial saliva (Mauchly $W = 0,439$; $p < 0,001$). In this way, adjustments for degrees of freedom were performed, multiplying them by the Greenhouse-Geiser ϵ values. The general analysis showed a no significant effect of repeated measures interaction with the tested groups of modified composite resin ($p = 0.248$) on SR values over time (a within-subjects effect), indicating that the surface roughness of Filtek™ Z350 XT unmodified and modified by the ZnO and ZnO/Ag, NPs was not significantly affected by the inclusion of the nanoparticles. The pairwise comparison based on the estimated marginal means and adjustments for multiple comparisons by Bonferroni method indicated that the modified composite resin by ZnO NPs (Polymeric Precursor) provided significant SR changes compared to unmodified composite resin after 28 days (SR = 0.17/ baseline; SR = 0.51/ 28 days).

Discussion

Zinc oxide nanostructures are antibacterial metal oxides that probably presents the widest range of shapes in nanoscale, such as *nanowires*, *nanorods*, *nanobelts*, *nanopencils*, *nanosprings*, *nanocombs*, *nanoboxes* and *nanorings* (18,19). The shape of nanostructures is related with the physical-chemical factors, such as synthesis method, precursor agent, pH and temperature (28). In this current work, nanospheres and nanorods of ZnO have been successfully obtained by polymeric precursor method and microwave-assisted hydrothermal approach.

Zinc oxide nano and submicrostructures have been synthesized controllably by polymeric precursor method (Pechini) for a long time (29,30). Pechini method is an attractive sol-gel method for preparing nanometer size powders because of its easy control, low cost and low fabricating temperature. On the other hand, microwave heating obtained in microwave-assisted synthesis can provide the following advantages in comparison to conventional heating for chemical synthesis. For example, its provides high heating rates, excellent control of the reaction parameters, selective heating, if the reaction mixture contains compounds with different microwave absorbing properties, better selectivity due to

reduced side reactions, improvement of the reproducibility and automatization and high throughput synthesis (31).

Zinc oxide, silver and their hybrids nanoparticles have shown interesting antibacterial activities against both Gram-positive and Gram-negative bacteria such as spores (5,32). As demonstrated in this current research, metal oxides nanoparticles have been presented as a good choice to avoid the growth of bacteria over the dental restorative materials (6,23,33). According to the findings of this research, the first null hypothesis was rejected, since a modified composite resin blended with small amounts (2% in weight) of ZnO nanoparticles could successfully decrease the colony unit formation of a mature *S. mutans* biofilm over composite resin surface. Although the ZnO NPs by polymeric precursor method can slightly reduces *S. mutans* biofilm better than the others modified resin groups, including that modified with Ag decorated NPs, statistical differences were met only in comparison to unmodified composite resin group. The studies demonstrates that dissolved metal ions from metal oxide and ROS generation in ZnO NPs plays an important role in the ZnO antibacterial properties (32). Another reason could be related to the synergetic activity of Ag on ZnO heterostructures, which this effect could enhance photocatalytic and antibacterial activity of this nanomaterial (34). Ag decorated NPs have been synthesized in order to obtain antimicrobial agents and their morphology usually remain the same of the unmodified NPs (35). The morphology of the NPs synthesized in this current study reveals that shape could be, as well as the size, could play an important role in antibacterial activity. The nanospheres usually obtained by polymeric precursor method presents a high surface area, which could provide a better interact of NPs and cell membrane, enhancing the damage process. The diameter of the ZnO NPs by polymeric precursor of our study may not be consistent with the actual diameter, since the adsorption and desorption process of N₂ does not analyze isolated particles, and it can perform this process in particle agglomerates, typical of Pechini synthesis 25.

The rods and wires of ZnO NPs could penetrate into cell walls of bacteria more easily than spherical ZnO particles, leading to the shape-dependent concept regarding antibacterial materials that can assume different shapes depending on the physical-chemical parameters of the synthesis (16,17).

The results of the current study show that incorporation of ZnO NPs into the resin composites could significantly inhibit the *S. mutans* biofilm formation over the composite resin surface, without sacrificing compressive and diametral tensile strength of the

composite resin. Besides that, almost all NPs did not interfere on the surface roughness and degree of composite resin conversion.

Our results are in agreement with the findings of Hojati et al. (6), which demonstrated a great antibacterial activity of a composite resin without drastically changes on its mechanical and physical properties. As can be seen in Figure 9, the compressive and diametral tensile strength of the modified composite resin did not present an appreciable increase or decrease. Although statistical differences were not met for the experimental groups, the inclusion of all ZnO and Ag/ZnO NPs could slightly increase or at least maintain the tested mechanical properties compared to the unmodified resin. Previous studies have also reported the changes on mechanical properties of composite resins modified by ZnO and hybrids of ZnO NPs [14]. The maintenance of the compressive and diametral tensile strength could be attributed to the silanization of the NPs, which help the particles form a homogeneous surface along with the composite resin matrix (37). In the Figure 4 it is possible to confirm the success of silanization of NPs, with the appearance of modes of binding for the Si-O-C and Si-O-Si groups in the FTIR spectra. The silanization of NPs with organosilanes in order to enhance mechanical properties has already been described by Xia et al. (37), demonstrating that an organosilanes surface layer encourages further combination of the nanoparticles with the resin matrix.

Regarding physical properties, the findings of our research demonstrated in Table 2 a slightly decrease on degree of conversion of composite resin modified by NPs. Despite this, no statistical significant changes were met for DC% compared to control group. An improvement was desired, however the similar DC% of modified resin compared to unmodified group represent an important factor, since the NPs provided antibacterial activity of resin without sacrificing its physical properties. In agreement with our findings, Hojati et al. (6) reported the addition of up to 5% of ZnO NPs does not affect the DC% of flowable composites resins.

The data of surface roughness obtained for composite resin modified by NPs in this current work demonstrated that, except for um group (ZnO PREC POL after 28 days), the inclusion of ZnO and Ag/ZnO NPs did not increase the roughness of composite resin surface overtime, as demonstrated in the Table 3. The increase of roughness usually leads to higher biofilm accumulation over resin surface, which can comprise the resin-dentin interface contributing to the progression of secondary caries (4,35). Our results are in accordance with others studies, which demonstrated that have no influence of NPs inclusion on the roughness of the composite resin (8), but in contrary with others that finding a rougher

surface of an experimental composite adhesive containing silver nanoparticles compared to conventional adhesive (39).

The enhancement of dental resin performance associated to the antibacterial activity has been a challenge for dental materials science. It is clearly demonstrated that inclusion of NPs with different physical-chemical characteristics could provide benefits from the *S. mutans* biofilm formation control, strong mechanical properties and photoactivity. Further experiments are needed to achieve better performance of modified resin and to understanding the achieve the ideal nanostructured material to promote enhancement of the desired properties on resin based dental materials.

The inclusion of 2% (wt%) of ZnO and ZnO/Ag NPs from different synthesis provide *S. mutans* biofilm formation control without sacrificing of mechanical and physical properties of the composite resin. Based on these results, the use of these nanoparticles in the resin based dental materials development could be a good option to obtain a new restorative material with antibacterial properties.

Resumo

O objetivo deste estudo foi modificar uma resina composta com nanopartículas de óxido de zinco (ZnO) e nanopartículas de óxido de zinco decorado com prata (ZnO/Ag) e avaliar propriedades antibacterianas, mecânicas e físicas desta nova resina. As NPs foram sintetizadas pelos métodos de precursores poliméricos e hidrotérmal assistido por micro-ondas e tratadas com um agente organossilano. A resina composta Z350 XT foi modificada com 0,5, 1 e 2% (em peso) de NPs para realizar um *screening* antibacteriano por meio do teste de contato direto com biofilme de *Streptococcus mutans*. Os demais testes foram realizados com 2% de NPs. A resina modificada foi testada contra o biofilme de 7 dias de *S. mutans*, e a sua viabilidade foi testada por microscopia confocal a laser. A resistência à compressão e resistência à tração diametral da resina composta modificada (n=40), 8 espécimes por Grupo, foi testada utilizando uma máquina de ensaio universal (EMIC). O grau de conversão (n=25), 5 espécimes por Grupo, foi realizado por análise FTIR. A leitura da rugosidade superficial (n=50), 10 espécimes por Grupo, foi realizada utilizando um rugosímetro portátil. Os dados foram analisados usando o software IBM SPSS Statistics 20.0 (SPSS Inc. Chicago, EUA) por ANOVA um fator para a atividade antibacteriana sobre o biofilme e testes mecânicos; ANOVA dois fatores para o grau de conversão e teste de Tukey para comparação múltipla; ANOVA medidas repetidas e pós teste com ajuste de Bonferroni para estabilidade de cor e teste de rugosidade superficial, com nível de significância de 5%. A resina modificada com todas as nanopartículas testadas diminuiu significativamente a formação de biofilme ($p < 0,05$) nos testes antibacterianos, o que foi confirmado pelas imagens de microscopia confocal. As propriedades mecânicas, rugosidade superficial e grau de conversão não mudaram drasticamente por incorporação de NPs em comparação com a resina não modificada. Embora não tenham sido encontradas diferenças estatísticas para os testes mecânicos e físicos, a manutenção destas propriedades é importante para o desenvolvimento de uma nova resina composta antibacteriana sem alteração das outras propriedades originais.

Palavras-chave: óxido de zinco, prata, agentes antibacterianos, biofilmes, *Streptococcus mutans*.

Acknowledgments

The authors thank to the Amazon Research Foundation (FAPEAM) for the financial support for this investigation.

References

1. Ferracane JL. Resin composite—State of the art. *Dent Mater* 2011;27:29–38. doi:10.1016/j.dental.2010.10.020.
2. Ferracane JL. Current Trends in Dental Composites. *Crit Rev Oral Biol Med* 1995;6:302–18. doi:10.1177/10454411950060040301.
3. Chen L, Shen H, Suh BI. Antibacterial dental restorative materials: a state-of-the-art review. *Am J Dent* 2012;25:337–46.
4. Nedeljkovic I, Teughels W, De Munck J, Van Meerbeek B, Van Landuyt KL. Is secondary caries with composites a material-based problem? *Dent Mater* 2015;31:e247–77. doi:10.1016/j.dental.2015.09.001.
5. Wang Z, Shen Y, Haapasalo M. Dental materials with antibiofilm properties. *Dent Mater* 2014;30:e1–16. doi:10.1016/j.dental.2013.12.001.
6. Tavassoli Hojati S, Alaghemand H, Hamze F, Ahmadian Babaki F, Rajab-Nia R, Rezvani MB, et al. Antibacterial, physical and mechanical properties of flowable resin composites containing zinc oxide nanoparticles. *Dent Mater* 2013;29:495–505. doi:10.1016/j.dental.2013.03.011.
7. Kasraei S, Sami L, Hendi S, Alikhani M-Y, Rezaei-Soufi L, Khamverdi Z. Antibacterial properties of composite resins incorporating silver and zinc oxide nanoparticles on *Streptococcus mutans* and *Lactobacillus*. *Restor Dent Endod* 2014;39:109–14. doi:10.5395/rde.2014.39.2.109.
8. das Neves PBA, Agnelli JAM, Kurachi C, de Souza CWO. Addition of silver nanoparticles to composite resin: Effect on physical and bactericidal properties in vitro. *Braz Dent J* 2014;25:141–5. doi:10.1590/0103-6440201302398.
9. Melo MAS, Guedes SFF, Xu HHK, Rodrigues LKA. Nanotechnology-based restorative materials for dental caries management. *Trends Biotechnol* 2013;31:459–67. doi:10.1016/j.tibtech.2013.05.010.
10. Cheng L, Zhang K, Weir MD, Melo MAS, Zhou X, Xu HHK. Nanotechnology strategies for antibacterial and remineralizing composites and adhesives to tackle dental caries. *Nanomedicine (Lond)* 2015;10:627–41. doi:10.2217/nmm.14.191.

11. Fan C, Chu L, Rawls HR, Norling BK, Cardenas HL, Whang K. Development of an antimicrobial resin - A pilot study. *Dent Mater* 2011;27:322–8. doi:10.1016/j.dental.2010.11.008.
12. Jia H, Hou W, Wei L, Xu B, Liu X. The structures and antibacterial properties of nano-SiO₂ supported silver/zinc-silver materials. *Dent Mater* 2008;24:244–9. doi:10.1016/j.dental.2007.04.015.
13. Yamamoto K, Ohashi S, Aono M, Kokubo T, Yamada I, Yamauchi J. Antibacterial activity of silver ions implanted in SiO₂ filler on oral streptococci. *Dent Mater* 1996;12:227–229. doi:10.1016/S0109-5641(96)80027-3.
14. Niu LN, Fang M, Jiao K, Tang LH, Xiao YH, Shen LJ, et al. Tetrapod-like zinc oxide whisker enhancement of resin composite. *J Dent Res* 2010;89:746–50. doi:10.1177/0022034510366682.
15. Seil JT, Webster TJ. Antimicrobial applications of nanotechnology: Methods and literature. *Int J Nanomedicine* 2012;7:2767–81. doi:10.2147/IJN.S24805.
16. Sirelkhatim A, Hydrotud S, Seeni A, Kaus NHM, Ann LC, Bakhori SKM, et al. Review on zinc oxide nanoparticles: Antibacterial activity and toxicity mechanism. *Nano-Micro Lett* 2015;7:219–42. doi:10.1007/s40820-015-0040-x.
17. Yang H, Liu C, Yang D, Zhang H, Xi Z. Comparative study of cytotoxicity, oxidative stress and genotoxicity induced by four typical nanomaterials: The role of particle size, shape and composition. *J Appl Toxicol* 2009;29:69–78. doi:10.1002/jat.1385.
18. Sahu DR, Liu CP, Wang RC, Kuo CL, Huang JL. Growth and application of ZnO nanostructures. *Int J Appl Ceram Technol* 2013;10:814–38. doi:10.1111/j.1744-7402.2012.02795.x.
19. Raghupathi KR, Koodali RT, Manna AC. Size-dependent bacterial growth inhibition and mechanism of antibacterial activity of zinc oxide nanoparticles. *Langmuir* 2011;27:4020–8. doi:10.1021/la104825u.
20. Rago I, Chandraiahgari CR, Bracciale MP, De Bellis G, Zanni E, Cestelli Guidi M, et al. Zinc oxide microrods and nanorods: different antibacterial activity and their mode of action against Gram-positive bacteria. *RSC Adv* 2014;4:56031–40. doi:10.1039/C4RA08462D.

21. Wahab R, Kim YS, Mishra A, Yun S Il, Shin HS. Formation of ZnO Micro-Flowers Prepared via Solution Process and their Antibacterial Activity. *Nanoscale Res Lett* 2010;5:1675–81. doi:10.1007/s11671-010-9694-y.
22. Wahab R, Mishra A, Yun S Il, Hwang IH, Mussarat J, Al-Khedhairi AA, et al. Fabrication, growth mechanism and antibacterial activity of ZnO micro-spheres prepared via solution process. *Biomass and Bioenergy* 2012;39:227–36. doi:10.1016/j.biombioe.2012.01.005.
23. Sevinç BA, Hanley L. Antibacterial activity of dental composites containing zinc oxide nanoparticles. *J Biomed Mater ...* 2010;94:22–31. doi:10.1002/jbm.b.31620.Antibacterial.
24. Leite ER, Bernardi MIB, Longo E, Varela JA, Paskocimas CA. Enhanced electrical property of nanostructured Sb-doped SnO₂ thin film processed by soft chemical method. *Thin Solid Films* 2004;449:67–72. doi:10.1016/j.tsf.2003.10.101.
25. Walton RI. Subcritical solvothermal synthesis of condensed inorganic materials. *Chem Soc Rev* 2002;31:230–8. doi:10.1039/b105762f.
26. Zamperini CA, André RS, Longo VM, Mima EG, Vergani CE, Machado AL, et al. Antifungal applications of Ag-decorated hydroxyapatite nanoparticles. *J Nanomater* 2013;2013. doi:10.1155/2013/174398.
27. Ajdić D, McShan WM, McLaughlin RE, Savić G, Chang J, Carson MB, et al. Genome sequence of *Streptococcus mutans* UA159, a cariogenic dental pathogen. *Proc Natl Acad Sci U S A* 2002;99:14434–9. doi:10.1073/pnas.172501299.
28. Sirelkhatim A, Hydrotud S, Seeni A, Kaus NHM, Ann LC, Bakhori SKM, et al. Review on zinc oxide nanoparticles: Antibacterial activity and toxicity mechanism. *Nano-Micro Lett* 2015;7:219–42. doi:10.1007/s40820-015-0040-x.
29. Pechini MP, Adams N. Method of preparing lead and alkaline earth titanates and niobates and coating method using the same to form a capacitor. *United States Pat Off* 1967:01–7.
30. Razavi RS, Loghman-estarki MR, Farhadi-khouzani M. Synthesis and Characterization of ZnO Nanostructures by Polymeric Precursor Route 2012;121:98–100.

31. Bilecka I, Niederberger M. Microwave chemistry for inorganic nanomaterials synthesis. *Nanoscale* 2010;2:1358–74. doi:10.1039/b9nr00377k.
32. Jiang Y, Zhang L, Wen D, Ding Y. Role of physical and chemical interactions in the antibacterial behavior of ZnO nanoparticles against *E. coli*. *Mater Sci Eng C* 2016;69:1361–6. doi:10.1016/j.msec.2016.08.044.
33. Dias HB, Bernardi MIB, Ramos MA dos S, Trevisan TC, Bauab TM, Hernandez AC, et al. Zinc oxide 3D microstructures as an antimicrobial filler content for composite resins. *Microsc Res Tech* 2017:1–10. doi:10.1002/jemt.22840.
34. Zhang Y, Gao X, Zhi L, Liu X, Jiang W, Sun Y, et al. The synergetic antibacterial activity of Ag islands on ZnO (Ag/ZnO) heterostructure nanoparticles and its mode of action. *J Inorg Biochem* 2014;130:74–83. doi:10.1016/j.jinorgbio.2013.10.004.
35. Longo VM, Picon FC, Zamperini C, Albuquerque AR, Sambrano JR, Vergani CE, et al. Experimental and theoretical approach of nanocrystalline TiO₂ with antifungal activity. *Chem Phys Lett* 2013;577:114–20. doi:10.1016/j.cplett.2013.05.056.
36. Sing KSW, Everett DH, Haul R a. W, Moscou L, Pierotti R a., Rouquérol J, et al. REPORTING PHYSISORPTION DATA FOR GAS / SOLID SYSTEMS with Special Reference to the Determination of Surface Area and Porosity (Recommendations 1984). *Pure Appl Chem* 1985;57:603–19. doi:10.1351/pac198557040603.
37. Xia Y, Zhang F, Xie H, Gu N. Nanoparticle-reinforced resin-based dental composites. *J Dent* 2008;36:450–5. doi:10.1016/j.jdent.2008.03.001.
38. Bourbia M, Ma D, Cvitkovitch DG, Santerre JP, Finer Y. Cariogenic bacteria degrade dental resin composites and adhesives. *J Dent Res* 2013;92:989–94. doi:10.1177/0022034513504436.
39. Ahn SJ, Lee SJ, Kook JK, Lim BS. Experimental antimicrobial orthodontic adhesives using nanofillers and silver nanoparticles. *Dent Mater* 2009;25:206–13. doi:10.1016/j.dental.2008.06.002.

Tables

Table 1. Particle surface area and diameter calculated by BET data

Material	Surface area BET (m²/g)	Diameter by BET (nm)
ZnO PREC POL	2,18	490,06
ZnO/Ag PREC POL	8,60	124,58
ZnO Hidro	40,57	26,40
ZnO/Ag Hidro	40,72	26,31

Note: PREC POL = Polymeric precursor; Hidro = hydrothermal.

Table 2. Degree of conversion (%) of composite resin unmodified and modified by 2% (weight) ZnO NPs. *Different superscript letters indicates significant statistical differences

Material	Degree of conversion (%) and standard deviation (SD)
Z350 XT	59,2 ± 1,0 ^a
ZnO PREC POL 2% (wt.)	53,3 ± 2,7 ^a
ZnO Hidro 2% (wt.)	51,6 ± 2,8 ^a
ZnO/Ag PREC POL 2% (wt.)	56,0 ± 2,1 ^a
ZnO/Ag Hidro 2% (wt.)	53,8 ± 4,9 ^a

Note: PREC POL = Polymeric precursor; Hidro = hydrothermal.

Table 3. Surface roughness and standard deviation of unmodified and modified composite resin with ZnO NPs (2% in weight) over time. *Different superscript letters at the same line indicates significant statistical differences overtime

Group	Baseline	7 days	14 days	28 days
Unmodified Z350XT	0.18 ± 0.22^a	0.16 ± 0.08^a	0.35 ± 0.34^a	0.31 ± 0.21^a
ZnO Prec Pol	0.17 ± 0.13^a	0.24 ± 0.15^a	0.37 ± 0.35^{ab}	0.51 ± 0.26^b
ZnO/Ag Prec Pol	0.24 ± 0.18^a	0.45 ± 0.33^a	0.33 ± 0.21^a	0.54 ± 0.34^a
ZnO Hydrot	0.38 ± 0.14^a	0.27 ± 0.13^a	0.72 ± 0.45^a	0.59 ± 0.48^a
ZnO/Ag Hydrot	0.29 ± 0.16^a	0.35 ± 0.13^a	0.68 ± 0.46^a	0.60 ± 0.48^a

Note: Prec Pol = Polymeric precursor; Hydrot = hydrothermal.

Figures

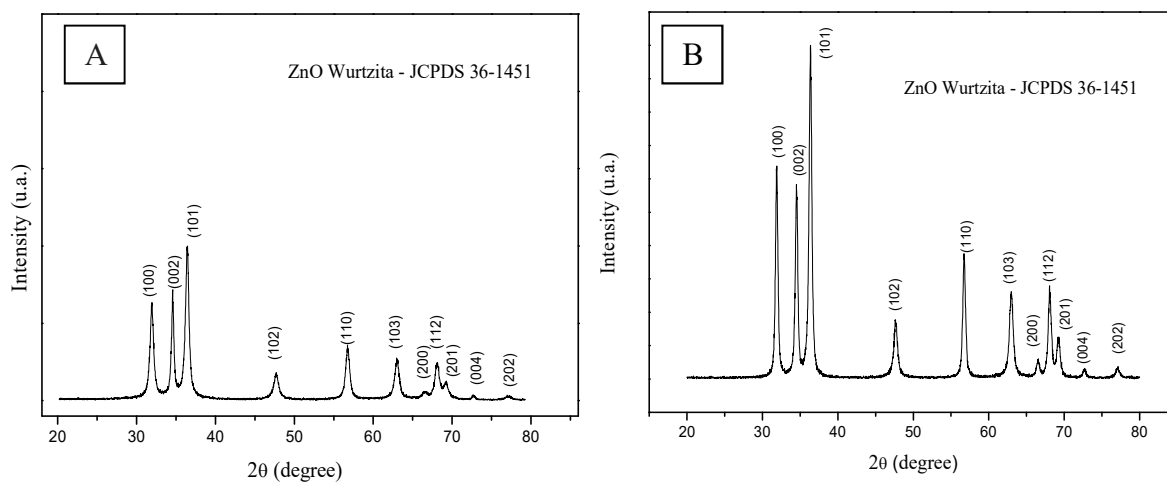


Figure 1. XRD pattern of ZnO synthesized by (a) polymeric precursor method and (b) hydrothermal approach.

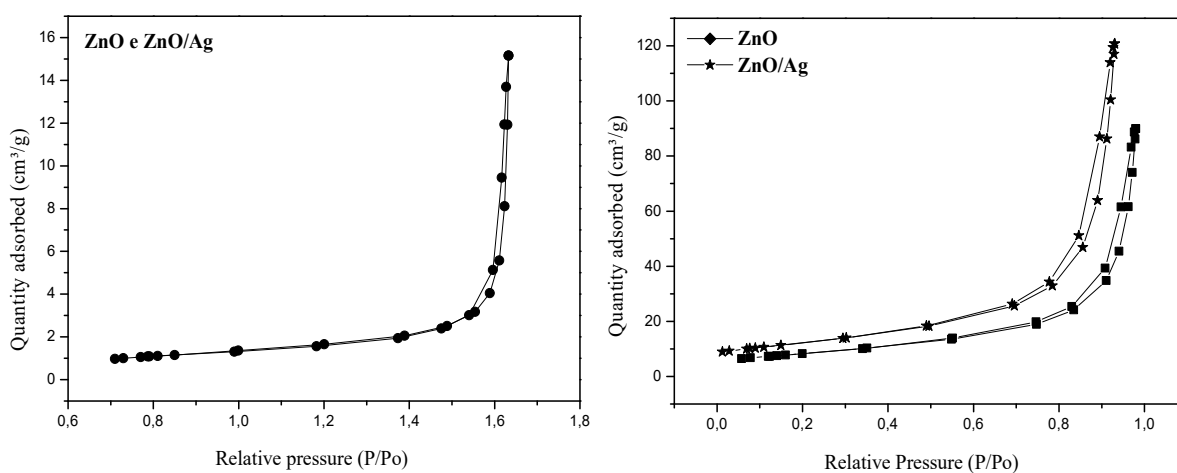


Figure 2. N_2 adsorption–desorption isotherms of ZnO powder synthesized by (a) polymeric precursor method and (b) hydrothermal approach.

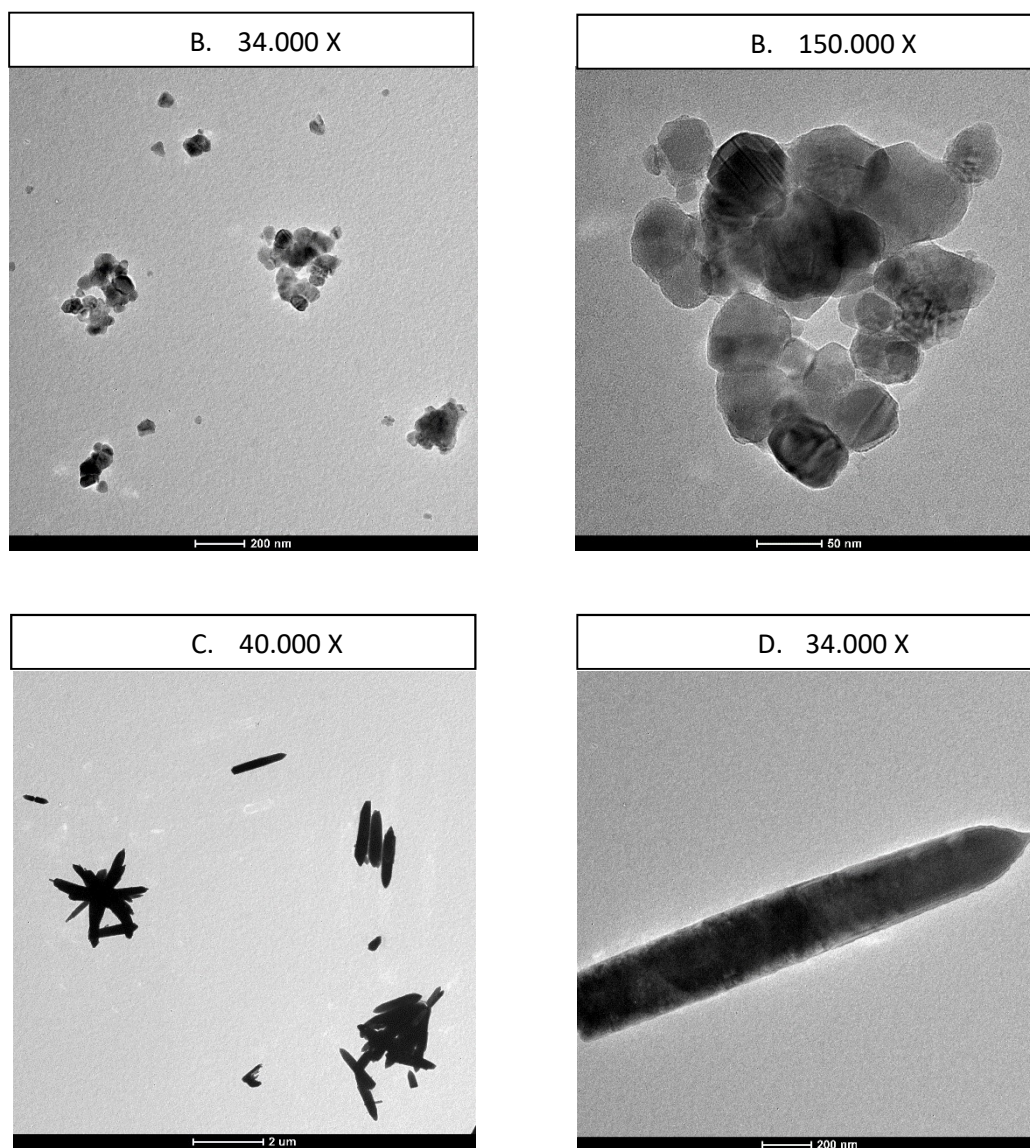


Figure 3. Transmission electron microscopy of Ag decorated ZnO (ZnO/Ag) synthesized by polymeric precursor (a-b) and hydrothermal approach (c-d).

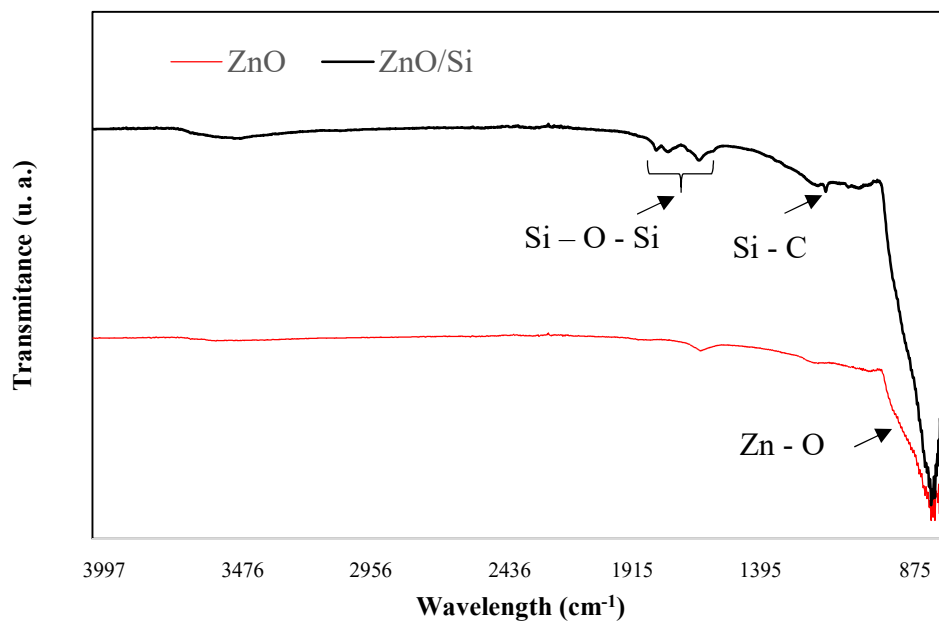


Figure 4 – The FTIR spectrum of the pure ZnO and modified ZnO by TEVS (Triethoxyvinylsilane) (ZnO/Si).

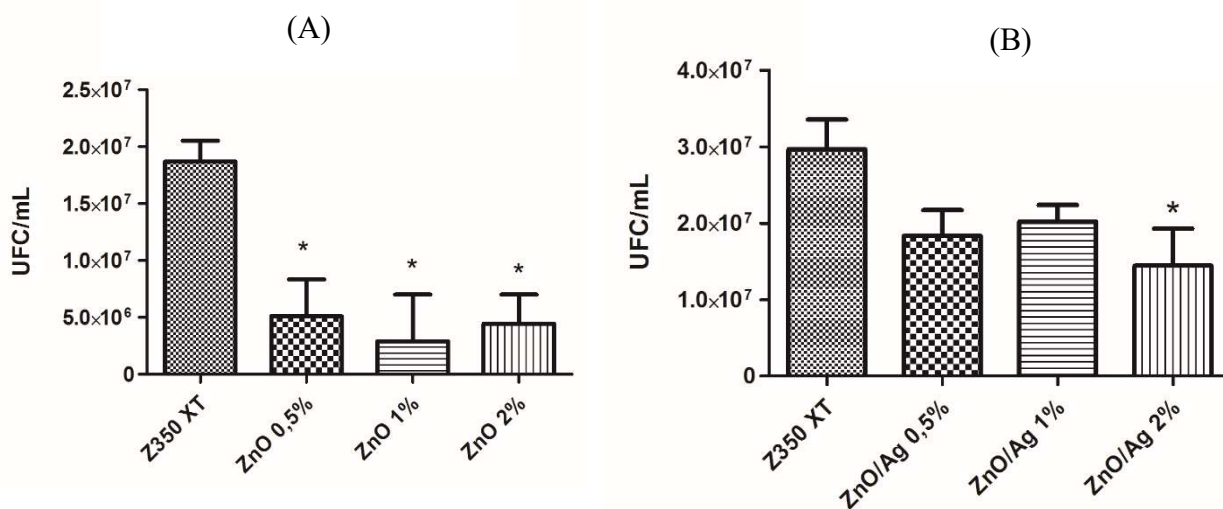


Figure 5. Colony forming unit per mL (CFU/mL) following direct contact between *S. mutans* biofilm and resin composite modified by ZnO and ZnO/Ag NPs (PREC POL) (% weight). *Indicate significant statistical differences in comparison to unmodified resin composite.

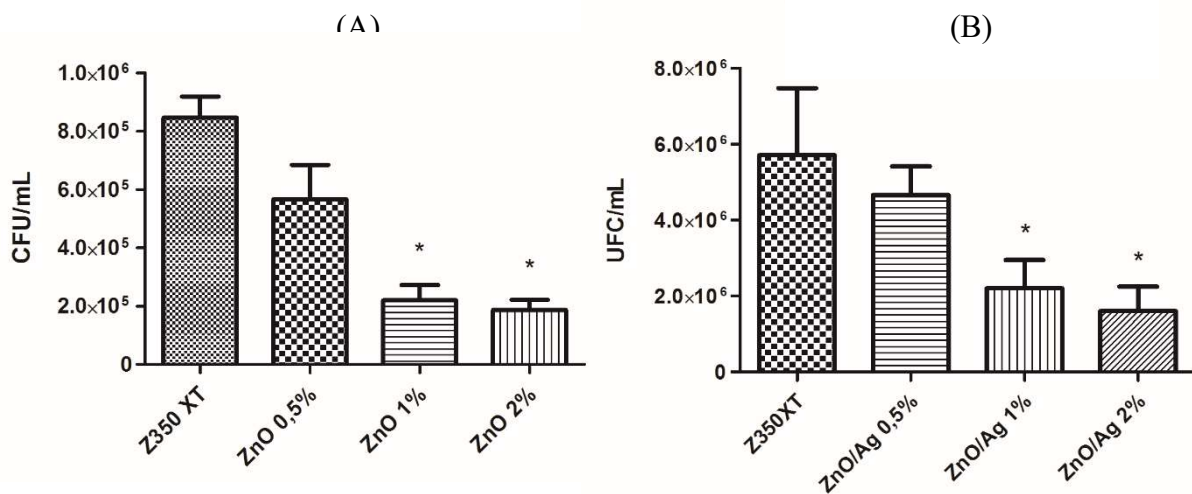


Figure 6. Colony forming unit per mL (CFU/mL) following direct contact between *S. mutans* biofilm and unmodified and modified composite resin by ZnO and ZnO/Ag NPs (HYDROT) (% weight). *Indicate significant statistical differences in comparison to unmodified resin composite.

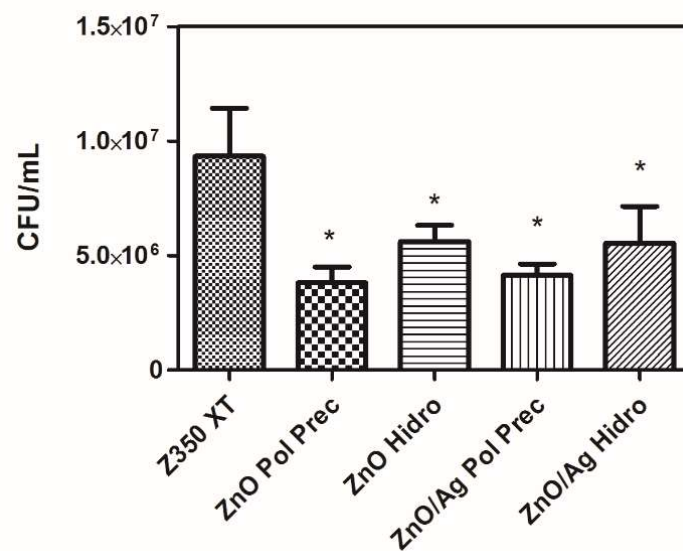


Figura 7. Colony forming unit per mL (CFU/mL) following 7-days *S. mutans* biofilm formation over unmodified and modified composite resin by ZnO and ZnO/Ag NPs (2% in weight). *Indicate significant statistical differences in comparison to unmodified composite resin.

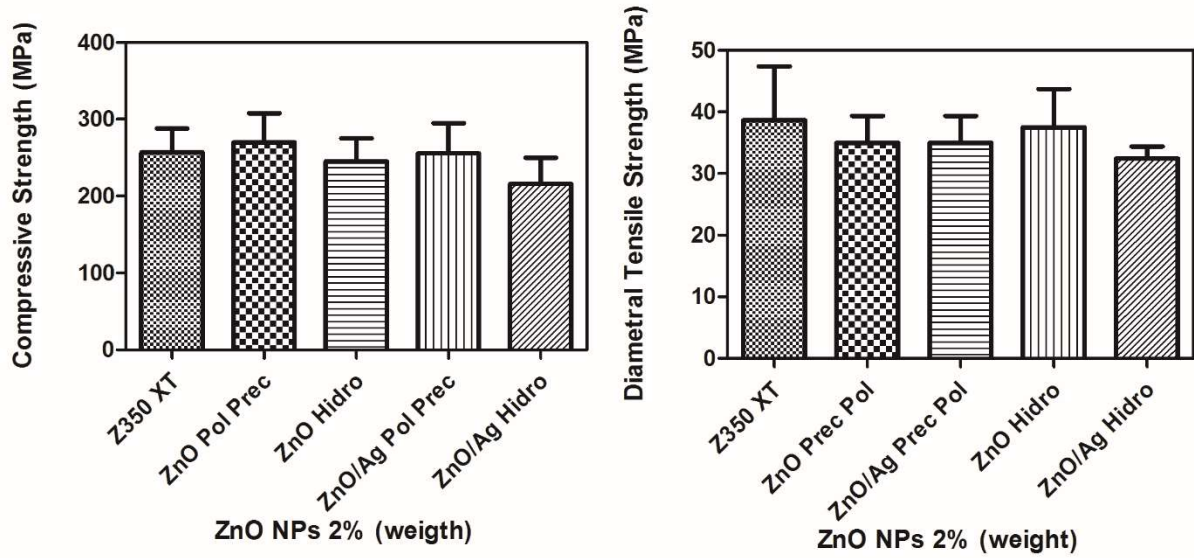


Figure 8. Compressive strength and diametral tensile strength of unmodified and modified composite resin by ZnO and ZnO/Ag nanoparticles (wt.%). Note: Prec Pol: polymeric precursor; Hidro: hydrothermal.

3.3 Artigo 3

Title page

Research area: Dental Materials; Restorative Dentistry.

Title: Color stability of a composite resin modified by metal oxides antibacterial nanoparticles.*

Authors: Hércules Bezerra Dias¹, Maria Inês Basso Bernardi², Antônio Carlos Hernandes², Alessandra Nara de Souza Rastelli^{1*}

¹Department of Restorative Dentistry, Araraquara School of Dentistry, Sao Paulo State University – UNESP, Araraquara, SP 14801-903, Brazil.

²Department of Physics and Materials Science, Physics Institute of São Carlos - IFSC, University of São Paulo - USP, São Carlos, São Paulo, 13566-590, Brazil.

*Corresponding author: Prof. Dr. Alessandra Nara de Souza Rastelli, São Paulo State University - UNESP, Araraquara School of Dentistry, Department of Restorative Dentistry, Araraquara, SP, Brazil. 1680 Humaita St., Araraquara, São Paulo, Brazil. MailBox: 331. ZipCode: 14.801-903. Telephone: +55 (016) 3301-6524 Fax: +55 (016) 3301-6393. e-mail address: alrastelli@foar.unesp.br

ABSTRACT

The aim of this study was to evaluate the color stability of a composite resin modified by ZnO and TiO₂ nanoparticles (pure and silver decorated), synthesized by different chemical routes. Zinc oxide (ZnO), titanium dioxide (TiO₂), and their Ag decorated forms (ZnO/Ag and TiO₂/Ag) nanoparticles (NPs) were previously synthesized by polymeric precursors and hydrothermal methods. The composite resin Filtek™ Z350 XT (3M do Brasil,) was modified with 2% (weight) of NPs. One hundred and eighty specimens (n=180), 10 specimens for each Group, were prepared using a metallic matrix (10 mm diameter and 2 mm thickness), covered by a polyester strip and a glass plate, and light cured for 40 s. The specimens were stored in two solutions: coffee (Pilão Tradicional – JDE Brasil) and artificial saliva (Arte & Ciência, Araraquara, SP, Brazil, pH 7.0). The color measurements were recorded using a spectrophotometer (Minolta, CM 2600d) and the data were converted to National Bureau of Standards (NBS) units to determine the color change by NBS scores. A mixed model repeated measurements ANOVA was used at 5% level of significance. The color stability of the resin unmodified and modified by the ZnO, ZnO/Ag, TiO₂ and TiO₂/Ag NPs was significantly affected by the storage time (p<0.001) and the tested solutions (p<0.001). The coffee solution provided the major color changes for unmodified composite resin ($\Delta E^* = 5.70/ 24h$; $\Delta E^* = 15.48/ 90$ days) over time. The addition of ZnO/Ag and TiO₂/Ag (hydrothermal) promoted similar drastic changes on color after 24h ($\Delta E^* = 8.34$ and $\Delta E^* = 4.78$ respectively) and 90 days ($\Delta E^* = 23.14$ and $\Delta E^* = 18.71$ respectively). The modified composite resin presented drastically changes on color stability when immersed in coffee solution, indicating that inclusion of NPs can interfere in the final esthetics of restorations.

Key-words: composite resins, pigmentation, coloring agents, zinc oxide, titanium.

INTRODUCTION

Composite resins are the main esthetic restorative material used in the clinical practice. The discoloration of composite resins can be caused by extrinsic and intrinsic factors. Extrinsic factors include biofilm accumulation over the composite resin surface, composite resin surface degradation and slight penetration of staining agents^{1,2}. Physicochemical reactions in the deeper portions of the restoration was described as the main cause of intrinsic stains^{2,3}. However, the color stability of these materials have a multifactorial nature, depending on the incomplete polymerization, water sorption, food intake, oral hygiene habits and surface smoothness of the restoration. The inorganic components of the composite resin also can affect the surface roughness of restorations and the susceptibility to staining².

The chemical compounds of composite resins does not present or at least present low antibacterial activity⁴, which could allow the accumulation of biofilm on the surface and leads even to secondary caries formation. In order to achieve antibacterial property, composite resins and dental adhesive systems have been modified with different materials, such as metal and metal oxides nanoparticles^{5,9}.

The use of metal oxide nanoparticles as filler content in composite resins was found to be a good option to fabricate an antibacterial restorative material, with enhancement of the mechanical properties^{10,12}. Zinc oxide (ZnO) NPs exhibits a variety of morphologies and show significant antibacterial activity over a wide spectrum of bacteria¹³. Titanium dioxide (TiO₂) is a nontoxic, low cost, and physical-chemical stable material with high oxidative power and antibacterial activity¹⁴. Silver is a well-known broad spectrum antibacterial metal and the NPs form are described to show enhanced antibacterial capacity⁹.

Although the composite resin restorations can reproduce the natural esthetic of tooth, the major disadvantage of this material is the susceptibility to discoloration^{1,15}.

Additionally, color changes of the restorative material are a frequent consequence of composite restorations over time¹⁶. Physical properties can be changed after modification of the composite resin composition, for example, the color of composite resin¹⁵.

The inclusion of metal oxides nanoparticles into the resin based restorative materials can provide antibacterial activity contributing to the inhibition of bacterial growth on the surface of dental restorations. Besides that, the hybrids of these nanoparticles containing silver presents enhanced antimicrobial capacity because of the synergetic effect between the components of the formed nanocomposite. Although the inclusion of these materials into the composite resin provides a desired antibacterial effect, they could not change the color stability of the material, especially when the silver is one of the components. In this way, the aim of this study was evaluate the color stability of a commercial composite resin modified by ZnO and TiO₂ nanoparticles (pure and silver decorated), synthesized by different chemical routes.

MATERIALS AND METHODS

Experimental Design

This research consists of an in vitro experimental study. The dependent variable was the color stability and the independent variables were immersion medium and the different nanoparticles.

Nanoparticles used in this study

The nanoparticles used in this study were synthesized at the Research Group of Ceramic Materials and Crystal Growth, Physics Institute of Sao Carlos - IFSC, University of Sao Paulo - USP, Sao Carlos, Brazil. The data regarding synthesis, size and surface area of ZnO, TiO₂, ZnO/Ag and TiO₂/Ag nanoparticles are summarized in Table 1.

Specimen's Preparation

The NPs were incorporated into the composite resin using manual mixing for 1 min, with a metal spatula and a glass plate. One hundred and eighty (n=180), 10 specimens for each Group, were prepared using Filtek™ Z350 XT (3M do Brasil,) nanofilled composite resin at color A₂ Body. The Table 2 summarizes the composition of the composite resin matrix and the inorganic fillers.

The specimens were prepared injecting a single increment of the composite resin into a metallic matrix (10 mm diameter and 2 mm thickness), covered by a colorless polyester strip and a glass plate. On the opposite side of matrix, another polyester strip and a glass plate were placed. A load of 1 kg was placed over the top surface of the composite resin during 30 seconds, to result in a standardized smooth surface. The composite resin was light-cured (light – curing unit LED Radii plus SDI, 440 nm – 480 nm of wavelength, 1500 mW/cm² of light intensity, SDI Limited Australia, Anvisa: 10282499002) for 40 seconds. Following, the specimens were removed from the matrix.

Color Measurements

The color measurements were recorded using a spectrophotometer (Minolta, CM 2600d). After calibration, the first measurement of color (baseline) was performed, before the specimens are placed in the immersion medium. After that, all specimens were immersed in the appropriate solution to each Group, so that in experimental times, measurements were performed. The solutions used were coffee (Pilão Tradicional – JDE Brasil) and artificial saliva (Arte & Ciência, Araraquara, SP, Brazil, pH 7.0). The coffee was prepared using 500 mL of water and 2 tablespoons of coffee.

In order to perform color measurements, the specimens were washed and cleaned with distilled water and a gauze, then the spectrophotometer was positioned to measurements according to CIEL*a*b* (Commission Internationale de l'Eclairage)¹. According to CIE L*a*b* system, L* is the measurement of the brightness, quantified with a scale ranging from zero (0) to one hundred (100), following from pure black to pure white, respectively. The measurements of a* and b* corresponded to chromaticity, in which a* is related to the axis green-red and b* to the axis blue-yellow. Therefore, the color data L (brightness), a (deviation in the green-red axis), and b (deviation in the blue-yellow axis) are automatically obtained¹.

In this way, the color difference was calculated using the following equation: $\Delta E = [(\Delta L^*)^2 + (\Delta a^*)^2 + (\Delta b^*)^2]^{1/2}$.

The data were converted to National Bureau of Standards units (NBS units) to relate ΔE^* values with the clinical environment, through the equation: NBS units = $\Delta E^* \times 0.92$, where critical remarks of color differences as expressed in terms of NBS units.²⁴

The NBS classify the color changes as follow: between 0 and 0.5 = trace, for extremely slight changes; 0.5 to 1.5 = slight, for slight changes; 1.5 to 3.0 = noticeable, for

perceivable changes; 3.0 to 6.0 = appreciable, for marked changes; 6.0 to 12.0 = much, for extremely marked changes; and 12.0 or more = very much, for change to another color.

Statistical Analysis

The data were analyzed using the software IBM SPSS Statistics 20.0 (SPSS Inc. Chicago, USA). A mixed model repeated measurements ANOVA was used in order to estimate the effects within-subjects (repeated measurements over time) and between-subjects (solutions) on ΔE^* parameters, considering 5% level of significance. Mauchly test was applied to verify the sphericity assumption (equality of variances in repeated measurements ANOVA) and pairwise comparisons and contrasts were verified using a post hoc test for repeated measures with adjusted of Bonferroni.

RESULTS

The data regarding NPs (synthesis, surface area and size) used to modify the composite resin is showed in Table 1. The mean values of color stability (ΔE^*) and 95% confidence interval (CI) of the composite resin Filtek™ Z350 XT modified by ZnO and ZnO/Ag NPs and immersed in artificial saliva and coffee are showed in the Tables 3 and 4, respectively. The mixed-model repeated measures ANOVA analysis for ΔE^* values showed that the sphericity assumption was not met (after Mauchly test) for the Group in artificial saliva (Mauchly $W=0.059$; $p<0.001$) as well as the Group immersed in coffee ($W=0.018$; $p<0.001$). In this way, adjustments for degrees of freedom were performed, multiplying them by the Greenhouse-Geiser ϵ values.

The mean values of color stability (ΔE^*) and 95% confidence interval (CI) of the composite resin Filtek™ Z350 XT modified by TiO₂ e TiO₂/Ag NPs and immersed in artificial saliva and coffee are showed in the Tables 5 and 6, respectively. For these Groups,

the statistical analysis for ΔE^* values also showed that the sphericity assumption was not met (after Mauchly test) for the Group in artificial saliva (Mauchly $W=0.051$; $p<0.001$) as well as the group immersed in coffee ($W=0.237$; $p<0.001$). The corrected Greenhouse-Geiser values were used to assumption of sphericity of data.

The general analysis showed a significant effect of repeated measures ($p<0.001$) and their interaction with the tested solutions ($p<0.001$) on ΔE^* values over time (a within-subjects effect), indicating that the color stability of unmodified and modified Filtek™ Z350 XT by the ZnO, ZnO/Ag, TiO₂ and TiO₂/Ag NPs was significantly affected by storage time and the tested solutions. The trend analysis showed that the most contrasts for ΔE^* values of all Groups had a linear trend for the both tested solutions, as showed in Figures 1, 2, 3 and 4.

The pairwise comparison based on the estimated marginal means and adjustments for multiple comparisons by Bonferroni method indicated the differences showed in Tables 3, 4, 5 and 6. The coffee solution provided significant color changes for unmodified composite resin ($\Delta E^* = 5.70/ 24h$; $\Delta E^* = 15.48/ 90$ days), while the artificial saliva did not provided significant changes ($\Delta E^* = 0.30/ 24h$; $\Delta E^* = 0.64/ 90$ days) over time. According to NBS parameters, the modified composite resin by ZnO/Ag e TiO₂ (hydrothermal synthesis) immersed in artificial saliva promoted an extremely slight change after 24h ($\Delta E^* = 0.34/ NBS = 0.31$ e $\Delta E^* = 0.23/ NBS = 0.21$, respectively), perceivable and slight changes after 90 days ($\Delta E^* = 2.51/ NBS = 2.31$ e $\Delta E^* = 1.51/ NBS = 1.39$, respectively). When immersed in coffee solution, the modified composite resin by ZnO/Ag and TiO₂/Ag (hydrothermal synthesis) promoted extremely marked changes on color after 24h ($\Delta E^* = 8.34/ NBS = 7.67$ e $\Delta E^* = 4.78/ NBS = 4.39$, respectively) and change to another color after 90 days ($\Delta E^* = 23.14/ NBS = 21.28$ and $\Delta E^* = 18.71/ NBS = 17.21$, respectively).

DISCUSSION

The new generation of composite resins are considered more hydrophobic than teeth, and it was demonstrated that hydrophobic materials are more susceptible to stain with hydrophobic substances, indicating the direct influence of chemical interaction on staining process¹⁷. In this current study, the color of composite resin was influenced by the addition of nanoparticles and also by the tested solutions. Although TiO₂ and ZnO are metal oxides, the nanoparticles powder based on these metal oxides presented a white color and the Ag decorated metal oxides presented a slight gray color. In this way, it was not noted drastic visible color changes after composite resin modification due to the small amounts used.

The nature of composite resin and teeth discoloration can be defined in terms of chemical interactions, such as electrostatic and van der Waals forces, short-range interactions such as hydration forces, hydrophobic interactions, dipole-dipole forces and hydrogen bonds¹⁸. In this cases, a chromogenic agent is responsible for discoloration by surface adhesion, for example the tannins, chemical compounds of the coffee¹⁸. Additionally, the structure of a composite resin including the types and physical chemical characteristic of the filler contents, and the finishing and polishing procedures have a direct influence on composite resin surface discoloration³.

Some studies have demonstrated the influence of different solutions on the color stability of composite resins^{16,19,20}, although these composite resins did not contain antimicrobial nanoparticles. Our results demonstrated significant effect of repeated measures and their interaction with the tested solutions on the color stability over time after the composite resin modification with the NPs. As previous studies reported^{16,21,22}, the coffee solution promoted highest changes on color of modified and unmodified composite resin even in the first 24h. Although the results after 24h demonstrated

significant color changes on composite resin, previous studies report that the average consumption time for one cup of coffee is 15 minutes, and among coffee drinkers the average consumption amount is 3.2 cups per day, which means that a 24-hour storage time simulates about one month of coffee consumption³.

The staining is caused by the chemical interaction between the composite resin surface and the colorant, wherein the chromogenic agents are taken up by the acquired pellicle, and the color imparted is determined by the natural color of the chromogen^{17,18}.

In order to explain the dental surface staining by chemical interactions, Nathoo proposed a system of classification based on the interaction between the tooth surface and chromogen, discoloration after this binding, and the capacity of prechromogens (colorless material) to undergo a chemical reaction after binding to the tooth or restoration¹⁸. Also, the chemical interaction between resin monomers and anthocyanins, present such as in red, purple and blue solutions, was described in terms of hydrophobic nature of this compounds²⁰. Although our results demonstrated, based on NBS standards, change to another color of composite resin in coffee after 90 days, the staining susceptibility of the tested composite resin and the continuous time of exposure on staining solution should be considered. Based on the previous information, after 90 days of exposure, our results simulated around 7.5 years of coffee consumption. Our findings are in agreement with a previous reported study², which evaluated the color stability of microfilled, microhybrid and nanocomposite resin in tea solution for 30 days and the microfilled was found to be more color stable, while the nanocomposite showed the highest discoloration in tea after 7 and 30 days.

The size of NPs used to modify the composite resin in the present study ranges from 3nm to agglomerates of 490 nm. Agglomerates particles, called nanoclusters, could increase the staining susceptibility of composite resin, due to the relatively high water

sorption. Even though ZnO and ZnO/Ag nanoparticles (polymeric precursor) were described as agglomerates, a higher color change was observed for the composite resin modified by ZnO and ZnO/Ag obtained by hydrothermal synthesis, with 26 nm of mean size. Actually, the BET technique used to determine the surface area is based only in adsorption and desorption process of N₂. This process does not take into account isolated particles, but can be performed for particle agglomerates.

A previous study¹⁵ determined the influence of TiO₂ nanoparticles addition on the opalescence, color, translucency and fluorescence of experimental composites resin, showing that color differences were on the range of 3.4–6.6 ΔE^* units. All the six combinations showed ΔE^* values higher than the threshold value after addition of 0, 0.1, 0.25 and 0.5 wt.% NPs.

The discoloration effects of the coffee in the oral cavity would very likely require a longer period of time because of the intermittent nature of the exposure. Besides that, the polishing of restorations by brushing overtime would also decrease the staining effect on composite resins.

CONCLUSION

Under the conditions for this in vitro study, it was possible to conclude that all nanoparticles used in the current study to modify the composite resin provided color changes, especially when stored in coffee solution after 90 days. The hydrophobic nature of new generation of nanofilled composite resin can be an important factor on staining susceptibility. The high surface area of the tested nanomaterials could be contributed to the stained effect. Further studies are necessary to achieve success for modification of composite resin without changes on physical properties such as color stability.

ACKNOWLEDGEMENTS

The authors would like to thank the Amazon State Research Foundation (FAPEAM) for the financial support for this investigation.

REFERENCES

1. A. Joiner, Tooth colour: A review of the literature, *J. Dent.* 32 (2004) 3–12. doi:10.1016/j.jdent.2003.10.013.
2. I. Nasim, P. Neelakantan, R. Sujeer, C. V. Subbarao, Color stability of microfilled, microhybrid and nanocomposite resins - An in vitro study, *J. Dent.* 38 (2010) e137–e142. doi:10.1016/j.jdent.2010.05.020.
3. E. Ertaş, A.U. Güler, A.C. Yücel, H. Köprülü, E. Güler, Color stability of resin composites after immersion in different drinks, *Dent. Mater. J.* 25 (2006) 371–376. doi:10.4012/dmj.25.371.
4. L. Chen, H. Shen, B.I. Suh, Antibacterial dental restorative materials: a state-of-the-art review, *Am. J. Dent.* 25 (2012) 337–346. <http://www.ncbi.nlm.nih.gov/pubmed/23409624>.
5. B.A. Sevinç, L. Hanley, Antibacterial activity of dental composites containing zinc oxide nanoparticles, *J. Biomed. Mater. Res. - Part B Appl. Biomater.* 94 (2010) 22–31. doi:10.1002/jbm.b.31620.
6. S. Tavassoli Hojati, H. Alaghemand, F. Hamze, F. Ahmadian Babaki, R. Rajab-Nia, M.B. Rezvani, M. Kaviani, M. Atai, Antibacterial, physical and mechanical properties of flowable resin composites containing zinc oxide nanoparticles, *Dent. Mater.* 29 (2013) 495–505. doi:10.1016/j.dental.2013.03.011.
7. C. Fan, L. Chu, H.R. Rawls, B.K. Norling, H.L. Cardenas, K. Whang, Development of an antimicrobial resin - A pilot study, *Dent. Mater.* 27 (2011) 322–328. doi:10.1016/j.dental.2010.11.008.
8. Y. Cai, M. Strømme, A. Melhus, H. Engqvist, K. Welch, Photocatalytic inactivation of biofilms on bioactive dental adhesives, *J. Biomed. Mater. Res. - Part B Appl. Biomater.* 102 (2014) 62–67. doi:10.1002/jbm.b.32980.

9. P.B.A. das Neves, J.A.M. Agnelli, C. Kurachi, C.W.O. de Souza, Addition of silver nanoparticles to composite resin: Effect on physical and bactericidal properties in vitro, *Braz. Dent. J.* 25 (2014) 141–145. doi:10.1590/0103-6440201302398.
10. J. Sun, A.M. Forster, P.M. Johnson, N. Eidelman, G. Quinn, G. Schumacher, X. Zhang, W.L. Wu, Improving performance of dental resins by adding titanium dioxide nanoparticles, *Dent. Mater.* 27 (2011) 972–982. doi:10.1016/j.dental.2011.06.003.
11. Y. Xia, F. Zhang, H. Xie, N. Gu, Nanoparticle-reinforced resin-based dental composites, *J. Dent.* 36 (2008) 450–455. doi:10.1016/j.jdent.2008.03.001.
12. J. Jin, G. Wei, A. Hao, W. Zhang, Y. Zhang, Q. Wang, Q. Chen, ZnO–AlBw-reinforced dental resin composites: the effect of pH level on mechanical properties, *RSC Adv.* 5 (2015) 26430–26437. doi:10.1039/C5RA01413A.
13. A. Sirelkhatim, S. Hydrotud, A. Seeni, N.H.M. Kaus, L.C. Ann, S.K.M. Bakhori, H. Hasan, D. Mohamad, Review on zinc oxide nanoparticles: Antibacterial activity and toxicity mechanism, *Nano-Micro Lett.* 7 (2015) 219–242. doi:10.1007/s40820-015-0040-x.
14. J. Bahadur, S. Agrawal, V. Panwar, A. Parveen, K. Pal, Antibacterial properties of silver doped TiO₂ nanoparticles synthesized via sol-gel technique, *Macromol. Res.* 24 (2016) 488–493. doi:10.1007/s13233-016-4066-9.
15. B. Yu, J.S. Ahn, J.I. Lim, Y.K. Lee, Influence of TiO₂ nanoparticles on the optical properties of resin composites, *Dent. Mater.* 25 (2009) 1142–1147. doi:10.1016/j.dental.2009.03.012.
16. K. Rajkumar, S. Mahalaxmi, P. Ragavi, T.A. Mageshwaran, Color stability of resin composites after immersing in coffee of different temperatures - an in vitro study, 2 (2011) 92–95.

17. M.N. Abdallah, N. Light, W.M. Amin, J.M. Retrouvey, M. Cerruti, F. Tamimi, Development of a composite resin disclosing agent based on the understanding of tooth staining mechanisms, *J. Dent.* 42 (2014) 697–708. doi:10.1016/j.jdent.2014.03.004.
18. S.A. Nathoo, The chemistry and mechanisms of extrinsic and intrinsic discoloration., *J. Am. Dent. Assoc.* 128 (1997) 6S–10S. doi:10.14219/jada.archive.1997.0428.
19. U. Erdemir, E. Yildiz, M.M. Eren, Effects of sports drinks on color stability of nanofilled and microhybrid composites after long-term immersion, *J. Dent.* 40 (2012) e55–e63. doi:10.1016/j.jdent.2012.06.002.
20. H.B. Dias, E.T. Carrera, A. Nara, D.S. Rastelli, The influence of pH and chemical composition of beverages on color stability of a nanofilled composite resin, (2016).
21. C. Poggio, M. Ceci, R. Beltrami, M. Mirando, J. Wassim, M. Colombo, Color stability of esthetic restorative materials: a spectrophotometric analysis, *Acta Biomater. Odontol. Scand.* 2 (2016) 95–101. doi:10.1080/23337931.2016.1217416.
22. S. Shamszadeh, S.M. Sheikh-Al-Eslamian, E. Hasani, A.N. Abrandabadi, N. Panahandeh, S. Shamszadeh, S.M. Sheikh-Al-Eslamian, E. Hasani, A.N. Abrandabadi, N. Panahandeh, Color Stability of the Bulk-Fill Composite Resins with Different Thickness in Response to Coffee/Water Immersion, *Int. J. Dent.* 2016 (2016) 1–5. doi:10.1155/2016/7186140.

Tables

Table 1. Characteristics of the nanoparticles used in this study

Material	Code	Surface area BET (m ² /g)	Diameter by BET (nm)
ZnO Polym Prec	ZP	2,18	490,06
ZnO/Ag Polym Prec	AZP	8,60	124,58
TiO ₂ Polym Prec	TP	58,02	24,44
TiO ₂ /Ag Polym Prec	ATP	56,26	25,21
ZnO Hydrot	ZH	40,57	26,40
ZnO/Ag Hydrot	AZH	40,72	26,31
TiO ₂ Hydrot	TH	322,58	4,40
TiO ₂ /Ag Hydrot	ATH	447,60	3,17

Note: Polym Prec = Polymeric precursors synthesis; Hydrot: Hydrothermal synthesis.

Table 2. Composite resin used in this study

Nanofilled RBC	Manufacturer	Resin matrix	Filler	Filler, weight/volume
Filtek™ Z350 XT	3M do Brasil	TEGDMA, UDMA, BIS-EMA	Combination of nonaggregated 20 nm silica, nonaggregated 4-11 nm zirconia, and aggregated zirconia/silica cluster filler	78.5/59.5

RBC – Resin based composite; UDMA – Urethane dimethacrylate; BIS-EMA – Bisphenol A ethoxylated dimethacrylate; TEGDMA – Triethylene glycoldimethacrylate

Table 3. Mean values (x) of color stability (ΔE^*) and 95% confidence interval (CI) of the Filtek™ Z350 XT composite resin modified with ZnO and ZnO / Ag NPs and immersed in coffee solution

ΔE^*	Z 350 XT		ZP 1%		AZP 2%		ZH 2%		AZH 2%	
	x	IC 95%	x	IC 95%	x	IC 95%	x	IC 95%	x	IC 95%
24h	5,70 ^a	4,68 - 6,71	4,20 ^a	3,54 - 4,87	4,90 ^a	3,71 - 6,10	6,88 ^a	6,06 - 7,69	8,34 ^a	7,38 - 9,30
48h	6,73 ^a	5,88 - 7,59	6,36 ^b	5,61 - 7,12	7,03 ^a	6,07 - 7,99	8,90 ^b	7,81 - 9,98	9,96 ^{a,b}	9,10 - 10,81
7 dias	8,64 ^b	7,49 - 9,80	8,79 ^c	7,76 - 9,83	10,08 ^b	9,02 - 11,13	11,47 ^c	10,49 - 12,45	12,55 ^b	11,35 - 13,76
14 dias	10,36 ^{b,c}	9,25 - 11,47	10,60 ^c	9,85 - 11,36	11,83 ^c	10,81 - 12,85	13,98 ^d	12,33 - 15,63	15,50 ^c	14,54 - 16,45
21 dias	11,08 ^c	9,74 - 12,43	12,17 ^d	11,40 - 12,94	13,74 ^d	12,69 - 14,80	15,47 ^c	14,18 - 16,76	18,45 ^d	17,60 - 19,31
28 dias	11,42 ^c	10,07 - 12,76	12,67 ^d	12,10 - 13,24	13,70 ^d	12,68 - 14,73	16,60 ^e	15,13 - 18,07	19,81 ^{d,e}	17,48 - 22,14
60 dias	12,20 ^c	11,05 - 13,35	13,93 ^e	13,35 - 14,51	15,22 ^c	14,26 - 16,18	17,85 ^f	16,48 - 19,32	20,98 ^{e,f}	18,75 - 23,20
90 dias	15,48 ^d	14,61 - 16,35	16,69 ^f	15,58 - 17,81	17,76 ^f	16,46 - 19,06	20,95 ^g	18,95 - 22,94	23,14 ^f	20,08 - 26,19

Note: Same superscript letters indicate statistically similarity of the mean values of ΔE^* along the columns for the unmodified resin (Filtek™ Z350XT) and modified with ZnO and ZnO/Ag NPs synthesized via Pechini (ZP and AZP) and Hydrothermal (ZH And AZH), respectively.

Table 4. Mean values (x) of color stability color stability (ΔE^*) and 95% confidence interval (CI) of the Filtek™ Z350 XT composite resin modified with ZnO and ZnO / Ag NPs and immersed in artificial saliva

ΔE^*	Z 350 XT		ZP 1%		AZP 2%		ZH 2%		AZH 2%	
	x	IC 95%	x	IC 95%	x	IC 95%	x	IC 95%	x	IC 95%
24h	0,301 ^a	0,18 - 0,42	0,40 ^a	0,28 - 0,526	0,23 ^a	0,10 - 0,35	0,26 ^a	0,14 - 0,38	0,46 ^a	0,34 - 0,58
48h	0,465 ^a	0,25 - 0,678	0,59 ^a	0,38 - 0,81	0,39 ^b	0,17 - 0,60	0,78 ^{b,c}	0,57 - 1,00	0,61 ^a	0,40 - 0,82
7 dias	0,548 ^a	0,32 - 0,76	0,63 ^a	0,41 - 0,85	0,60 ^c	0,38 - 0,82	0,95 ^c	0,73 - 1,17	0,83 ^b	0,61 - 1,05
14 dias	0,672 ^a	0,41 - 0,93	0,95 ^b	0,69 - 1,21	1,03 ^d	0,77 - 1,28	1,44 ^d	1,18 - 1,70	1,45 ^c	1,19 - 1,71
21 dias	0,742 ^a	0,48 - 1,00	1,29 ^{b,c}	1,03 - 1,55	1,69 ^e	1,43 - 1,95	1,94 ^e	1,68 - 2,20	1,62 ^{c,d}	1,37 - 1,88
28 dias	0,833 ^a	0,55 - 1,11	1,28 ^{b,c}	0,99 - 1,53	1,67 ^{e,f}	1,39 - 1,95	2,07 ^e	1,79 - 2,35	1,86 ^d	1,57 - 2,14
60 dias	0,687 ^a	0,42 - 0,95	1,50 ^c	1,24 - 1,77	2,16 ^f	1,90 - 2,43	2,35 ^f	2,09 - 2,62	2,23 ^e	1,97 - 2,50
90 dias	0,637 ^a	0,37 - 0,89	1,88 ^d	1,61 - 2,14	2,86 ^g	2,60 - 3,13	3,00 ^g	2,74 - 3,27	2,77 ^f	2,51 - 3,03

Note: Same superscript letters indicate statistically similarity of the mean values of ΔE^* along the columns for the unmodified resin (Filtek™ Z350XT) and modified with ZnO and ZnO/Ag NPs synthesized via Pechini (ZP and AZP) and Hydrothermal (ZH And AZH), respectively

Table 5. Mean values (x) of color stability color stability (ΔE^*) and 95% confidence interval (CI) of the Filtek™ Z350 XT composite resin modified with TiO₂ and TiO₂/Ag NPs and immersed in artificial saliva

ΔE^*	Z 350 XT		TP 2%		ATP 2%		TH 2%		ATH 2%	
	x	IC 95%	x	IC 95%	x	IC 95%	x	IC 95%	x	IC 95%
24h	0,301 ^a	0,18 - 0,42	0,23 ^a	0,11 - 0,36	0,30 ^a	0,18 - 0,42	0,26 ^a	0,14 - 0,38	0,34 ^a	0,22 - 0,46
48h	0,465 ^a	0,25 - 0,678	0,27 ^a	0,13 - 0,41	0,43 ^a	0,30 - 0,57	0,38 ^{ab}	0,24 - 0,51	0,48 ^a	0,35 - 0,62
7 dias	0,548 ^a	0,32 - 0,76	0,32 ^a	0,20 - 0,44	0,53 ^a	0,42 - 0,65	0,41 ^{ab}	0,29 - 0,52	0,71 ^b	0,60 - 0,83
14 dias	0,672 ^a	0,41 - 0,93	0,51 ^a	0,30 - 0,72	0,63 ^{ab}	0,42 - 0,84	0,53 ^b	0,32 - 0,74	0,97 ^c	0,76 - 1,18
21 dias	0,742 ^a	0,48 - 1,00	0,78 ^b	0,57 - 0,99	0,66 ^{ab}	0,45 - 0,87	0,76 ^c	0,55 - 0,97	0,95 ^{bc}	0,74 - 1,16
28 dias	0,833 ^a	0,55 - 1,11	0,71 ^{ab}	0,50 - 0,93	0,77 ^b	0,55 - 0,98	0,84 ^c	0,62 - 1,05	1,16 ^c	0,95 - 1,38
60 dias	0,687 ^a	0,42 - 0,95	1,02 ^c	0,73 - 1,30	1,03 ^b	0,75 - 1,32	1,04 ^c	0,76 - 1,33	0,96 ^c	0,68 - 1,25
90 dias	0,637 ^a	0,37 - 0,89	1,44 ^d	1,21 - 1,66	0,90 ^b	0,67 - 1,12	1,51 ^d	1,28 - 1,73	0,92 ^c	0,70 - 1,15

Note: Same superscript letters indicate statistically similarity of the mean values of ΔE^* along the columns for the unmodified resin (Filtek™ Z350XT) and modified with TiO₂ and TiO₂/Ag NPs synthesized via Pechini (TP and ATP) and Hydrothermal (TH and ATH), respectively.

Table 6. Mean values (x) of color stability (ΔE^*) and 95% confidence interval (CI) of the Filtek™ Z350 XT composite resin modified with TiO₂ and TiO₂/Ag NPs and immersed in coffee solution

ΔE^*	Z 350 XT		TP 2%		ATP 2%		TH 2%		ATH 2%	
	x	IC 95%	x	IC 95%	x	IC 95%	x	IC 95%	x	IC 95%
24h	5,70 ^a	4,68 - 6,71	4,57 ^a	3,82 - 5,32	5,25 ^a	4,50 - 6,00	4,51 ^a	3,76 - 5,26	4,78 ^a	3,99 - 5,49
48h	6,73 ^a	5,88 - 7,59	6,44 ^b	5,73 - 7,15	7,17 ^b	6,46 - 7,88	6,08 ^b	5,37 - 6,79	6,53 ^a	5,82 - 7,24
7 dias	8,64 ^b	7,49 - 9,80	9,75 ^c	8,81 - 10,68	10,22 ^c	9,29 - 11,16	8,01 ^c	7,08 - 8,95	9,42 ^b	8,49 - 10,36
14 dias	10,36 ^{b,c}	9,25 - 11,47	11,64 ^d	10,75 - 12,53	11,77 ^d	10,88 - 12,67	10,09 ^{d,e}	9,19 - 10,98	12,56 ^c	11,67 - 13,46
21 dias	11,08 ^c	9,74 - 12,43	12,80 ^{d,e}	11,91 - 13,68	14,53 ^e	13,65 - 15,42	11,26 ^c	10,38 - 12,1€	14,25 ^{c,d}	13,36 - 15,14
28 dias	11,42 ^c	10,07 - 12,76	13,79 ^{e,f}	12,88 - 14,69	14,83 ^e	13,92 - 15,73	12,56 ^f	11,66 - 13,4€	14,70 ^d	13,79 - 15,60
60 dias	12,20 ^c	11,05 - 13,35	15,15 ^f	14,28 - 16,01	16,42 ^f	15,55 - 17,28	13,11 ^f	12,25 - 13,98	15,86 ^c	14,99 - 16,72
90 dias	15,48 ^d	14,61 - 16,35	17,45 ^g	16,49 - 18,41	19,06 ^g	18,10 - 20,02	15,80 ^g	14,84 - 16,76	18,21 ^f	17,25 - 19,17

Note: Same superscript letters indicate statistically similarity of the mean values of ΔE^* along the columns for the unmodified resin (Filtek™ Z350XT) and modified with TiO₂ and TiO₂/Ag NPs synthesized via Pechini (TP and ATP) and Hydrothermal (TH and ATH), respectively.

Figures

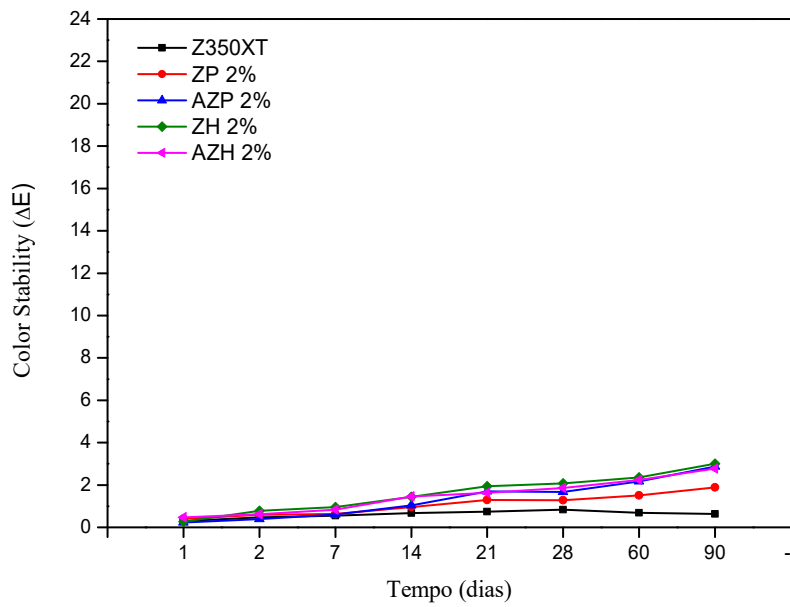


Figure 1. Linear trends for color change of one composite resin modified by ZnO and ZnO/Ag 2% (wt) stored in artificial saliva.

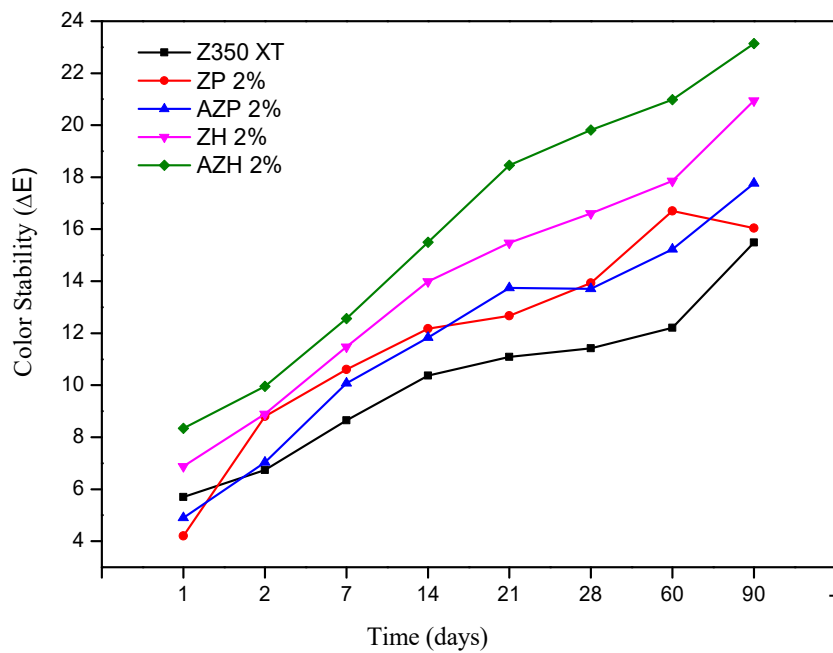


Figure 2. Linear trends for color change of one composite resin modified by ZnO and ZnO/Ag 2% (wt.) stored in coffee.

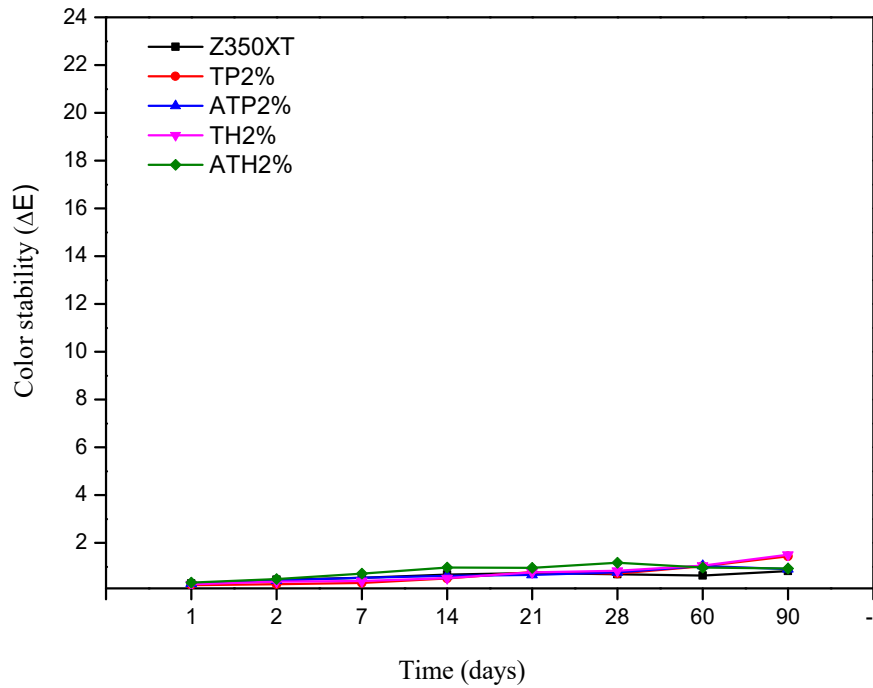


Figure 3. Linear trends for color change of one composite resin modified by TiO_2 e TiO_2/Ag 2% (wt.) stored in artificial saliva.

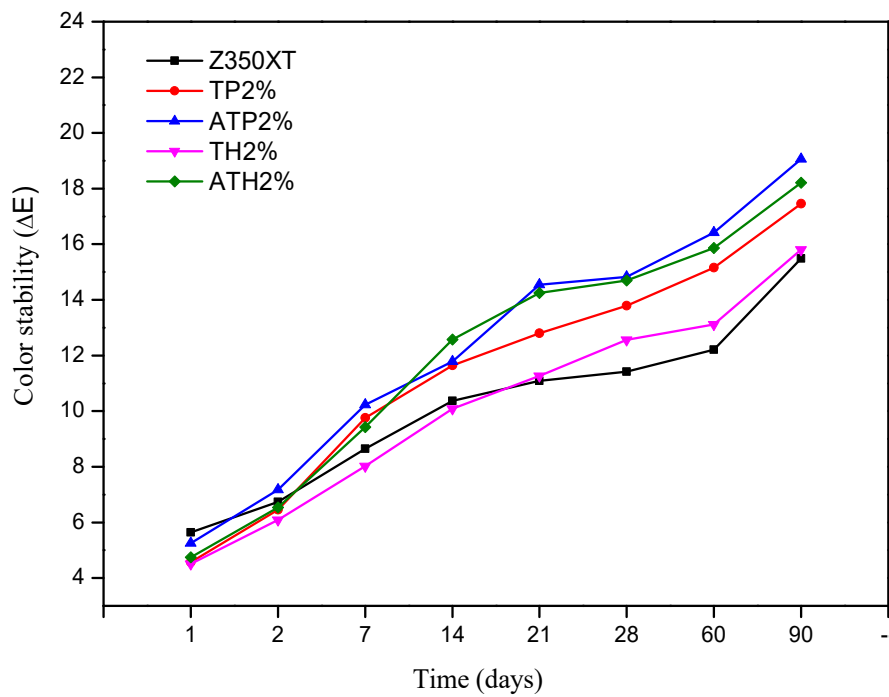


Figure 4. Linear trends for color change of one composite resin modified by TiO_2 e TiO_2/Ag 2% (wt.) stored in coffee.

Figure Legends

Figure 1 – Linear trends for color changes of one composite resin modified by ZnO and ZnO/Ag 2% (wt) stored in artificial saliva

Figure 2- Linear trends for color changes of one composite resin modified by ZnO and ZnO/Ag 2% (wt.) stored in coffee.

Figure 3 - Linear trends for color changes of one composite resin modified by TiO₂ e TiO₂/Ag 2% (wt.) stored in artificial saliva.

Figure 4 - Linear trends for color changes of one composite resin modified by TiO₂ e TiO₂/Ag 2% (wt.) stored in coffee.

4 CONCLUSÃO

O teste antibacteriano envolvendo biofilme maduro e contagem de unidades formadoras de colônia é o padrão ouro dentro das pesquisas, além disso biofilmes maduros podem ser até 500 vezes mais resistentes a produtos com ação antimicrobiana que células livres crescendo de forma planctônica, o que favorece os resultados obtidos nesse estudo. O uso de nanocompósitos tais como ZnO/Ag e TiO₂/Ag melhoraram o efeito antibacteriano do material provavelmente por meio do efeito sinérgico existente entre a prata e esses óxidos de metais. Esse efeito sinérgico, associado às propriedades físicas dessas nanopartículas, tais como área superficial e morfologia, permitiram ainda maior contato entre a superfície do nanomaterial e a célula bacteriana, além de aumentar sua capacidade de inibição celular. As alterações nas propriedades físicas e mecânicas são dependentes da concentração de nanopartículas utilizada e da presença ou não da prata. As drásticas alterações de cor, estão ainda, relacionadas ao fato do contato contínuo da resina composta com as soluções corantes. Ainda que significativamente afetadas pela inclusão das nanopartículas à resina composta, outras propriedades como a resistência à compressão foram melhoradas a partir do tratamento de superfície com um agente organossilano, e associando-se esses achados ao fator antibacteriano comprovado, sugere-se que o uso de nanopartículas de ZnO e TiO₂, decoradas ou não com Ag, podem ser boas opções de partículas de carga no desenvolvimento de resinas compostas restauradoras dentais, desde que bem definidas a concentração e composição ideal. Os achados desse estudo servirão como dados preliminares para a realização de uma série de pesquisas que podem levar à formulação de uma resina composta com propriedade antibacteriana.

REFERÊNCIAS*

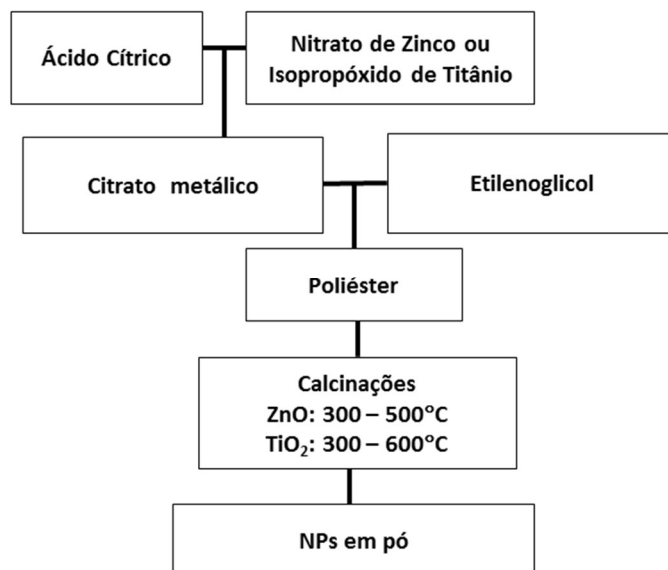
1. Allaker RP. The use of nanoparticles to control oral biofilm formation. *J Dent Res.* 2010; 89(11): 1175-86.
2. American National Standards Institute and American Dental Association. Standards n.27. for resin-based filling materials. Chicago: ADA; 1993.
3. Anusavice KJ. Phillip's science of dental materials. 12. ed. Rio de Janeiro: W.B. Saunders; 2013.
4. Cai Y, Strmme M, Melhus A, Engqvist H, Welch K. Photocatalytic inactivation of biofilms on bioactive dental adhesives. *J Biomed Mater Res-A.* 2014; 102B(1): 62-7.
5. Chen L, Shen H, Suh I. Antibacterial dental restorative materials: a state-of-the-art review. *Am J Dent.* 2012; 25(6): 337-46.
6. Conceição EN. Dentística: saúde e estética. 2.ed. Porto Alegre: Artmed; 2007.
7. Cui CX, Gao X, Qi YM, Liu SJ, Sun JB. Microstructure and antibacterial property of in situ TiO₂ nanotube layers/titanium biocomposites. *J Mech Behav Biomed.* 2012; (8): 178-83.
8. Fermanian J. Measure de l'accord entre deux juges: cas quantitatif. *Rev Epidemiol Sante Publique.* 1984; (32): 408-13.
9. Ferracane JL. Resin composite: state of the art. *Dent Mater.* 2011; 27(1): 29–38.
10. Fu G, Vary PS, Lin CT. Anatase TiO₂ nanocomposites for antimicrobial coatings. *J Phys Chem B.* 2005;109(18): 8889–98.
11. Hojati ST, Alaghemand H, Hamze F, Babaki FA, Rajab-Nia R, Rezvani MB, et al. Antibacterial, physical and mechanical properties of flowable resin composites containing zinc oxide nanoparticles. *Dent Mater.* 2013; 29(5): 495–505.
12. International Organization for Standardization. ISO 4049 – 2000: Dentistry-polymer based filling, restorative and luting materials. 3. ed. Geneva: ISO; 2000.
13. Klapdohr S, Moszner N. New inorganic components for dental filling composites. *Monatshefte fuer Chemie.* 2005; 136: 21-45.
14. Lepri CP, Palma-Dibb RG. Surface roughness and color change of a composite: Influence of beverages and brushing. *Dent Mat J.* 2012; 31(4): 689–96.
15. Liang C, Hong S, Suh, IB. Antibacterial dental restorative materials: a state-of-the-art review. *Am J Dent.* 2012; 25(6): 337-46.
16. Liu Y, Wang X, Yang F, Yang X. Excellent antimicrobial properties of mesoporous anatase TiO₂ and Ag/TiO₂ composite films. *Micropor Mesopor Mat.* 2008; (114): 431-9.

*De acordo com o Guia de Trabalhos Acadêmicos da FOAr, adaptado das Normas Vancouver. Disponível no site da Biblioteca: <http://www.foar.unesp.br/Home/Biblioteca/guia-de-normalizacao-marco-2015.pdf>

17. Lizenboim HKDK, Roth S, Zalsman B, McHale WA, Jaffe M, Griswold K. Performance enhancement of dental composites using electrospun nanofibers. *J Nanomater.* 2008; (2008): 1-6.
18. Melo MAS, Guedes SFF, Xu HHK, Rodrigues LKA. Nanotechnology-based restorative materials for dental caries management. *Trends Biotechnol.* 2013; 31(8): 459-67.
19. Pechini MP, inventor; Sprague Electric Co., cessionário. Method of preparing lead and alkaline earth-titanates and niobates and coatings method using the same to form a capacitor. United States patent US 3330697. 1967 Jul 11.
20. Raghupathi KR, Koodali RT, Manna AC. Size-dependent bacterial growth inhibition and mechanism of antibacterial activity of zinc oxide nanoparticles. *Langmuir.* 2011; 27(7): 4020–8.
21. Sahu, DR, Liu CP, Wang RC, Kuo CL, Huang JL. Growth and application of ZnO nanostructures. *Int J Appl Ceram Technol.* 2013; 10(5): 814–38.
22. Saunders SA. Current practicality of nanotechnology in dentistry. part 1: focus on nanocomposite restoratives and biomimetics. *Clin Cosm Investig Dent.* 2009; 1: 47–61.
23. Schneider LF, Consani S, Correr-Sobrinho L, Correr AB, Sinhoreti MA. Halogen and LED light curing of composite temperature increase and Knoop hardness. *Clin Oral Invest.* 2006; 10(1): 66–71.
24. Walton RI. Subcritical solvothermal synthesis of condensed inorganic materials. *Chem Soc Rev.* 2002; 31(4): 230-8.

APÊNDICE A - Esquemas dos experimentos realizados

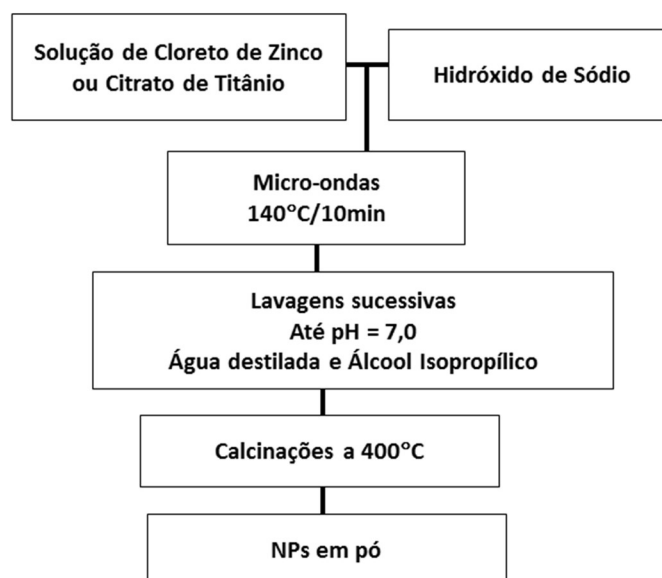
Síntese dos precursores polímeros



Esquema da Síntese dos Precursores Poliméricos

Fonte: Elaboração própria.

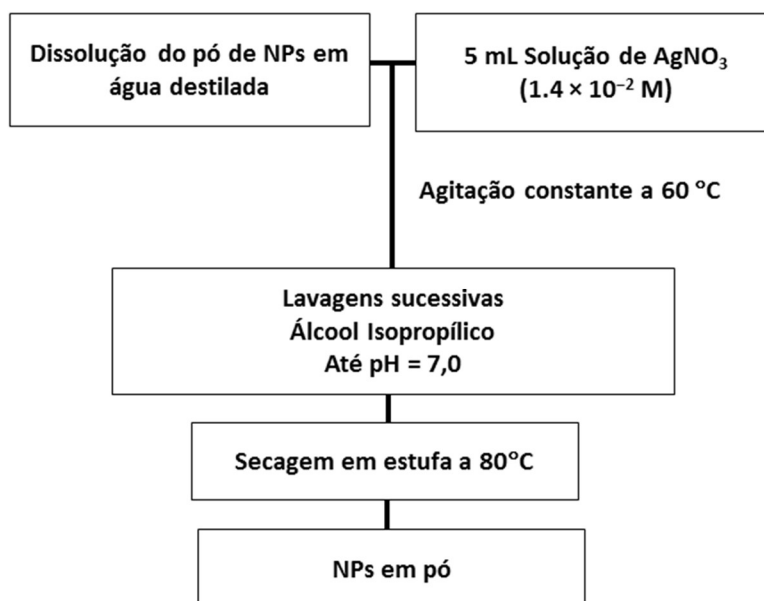
Síntese hidrotermal assistida por micro-ondas



Esquema da Síntese Hidrotermal assistida por micro-ondas

Fonte: Elaboração própria.

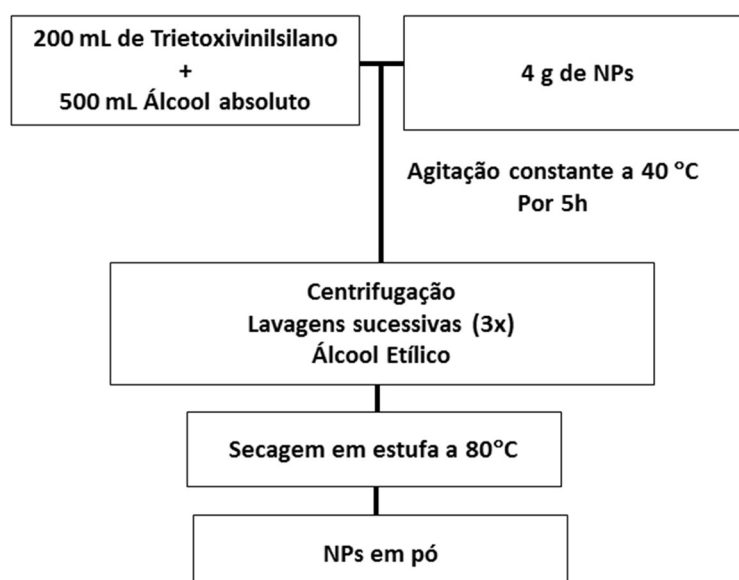
Decoração com Prata



Esquema da Decoração com Prata

Fonte: Elaboração própria.

Silanização das nanopartículas



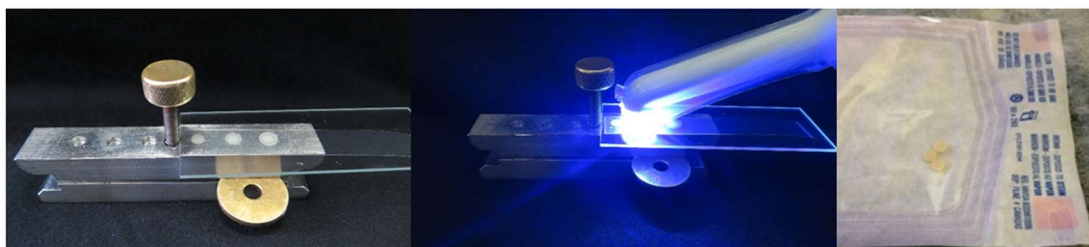
Esquema da Decoração com Prata

Fonte: Elaboração própria.

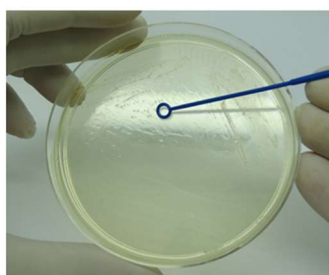
Análise da Atividade Antibacteriana

Teste antibacteriano por contato direto

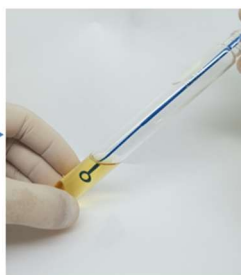
Confecção dos corpos de prova: 4 x 2 mm



Preparo dos corpos de prova de resina composta modificada com NPs para análise antibacteriana.



Coletar de 4 a 5 colônias
S. Mutans
ATCC 25177



BHI caldo



Após Incubação
a 37°C com 5% CO₂/ 24 h



Inóculo e tubos com
5 mL de BHI caldo

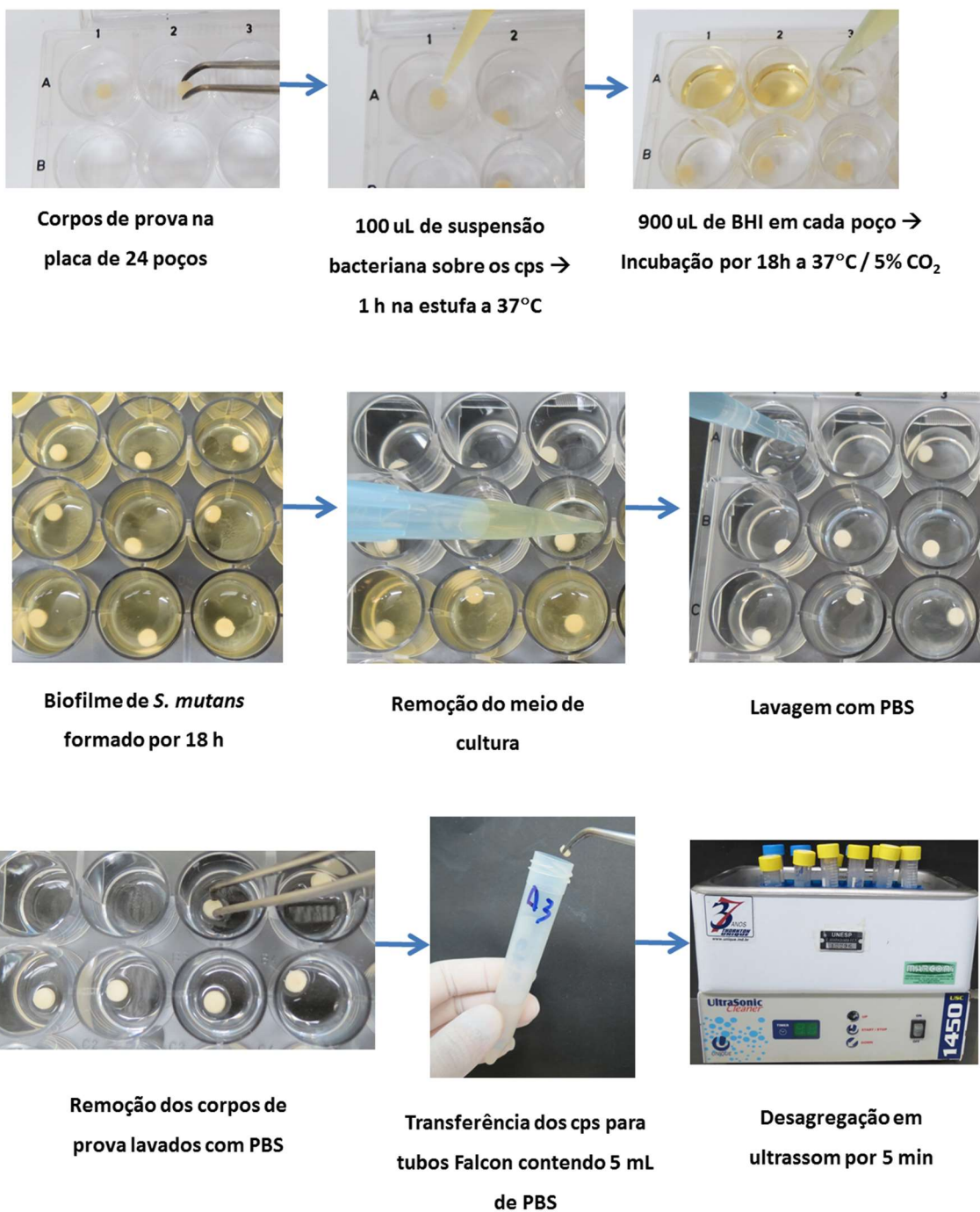


Padronização em Espectrofotômetro

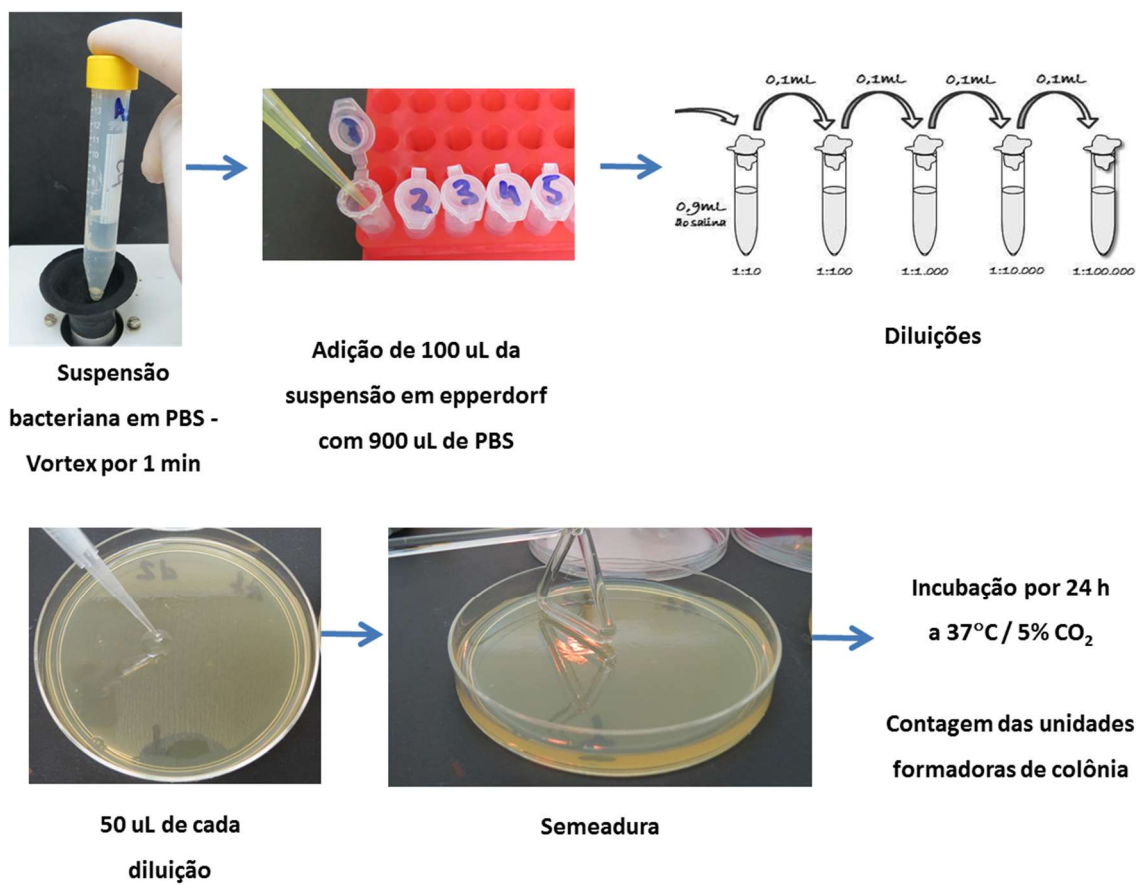
Escala 0,5 McFarland → D.O. 0,10 – 0,15 ($\lambda=620$ nm)

31

Fonte: Elaboração própria.



Fonte: Elaboração própria.



Fonte: Elaboração própria.

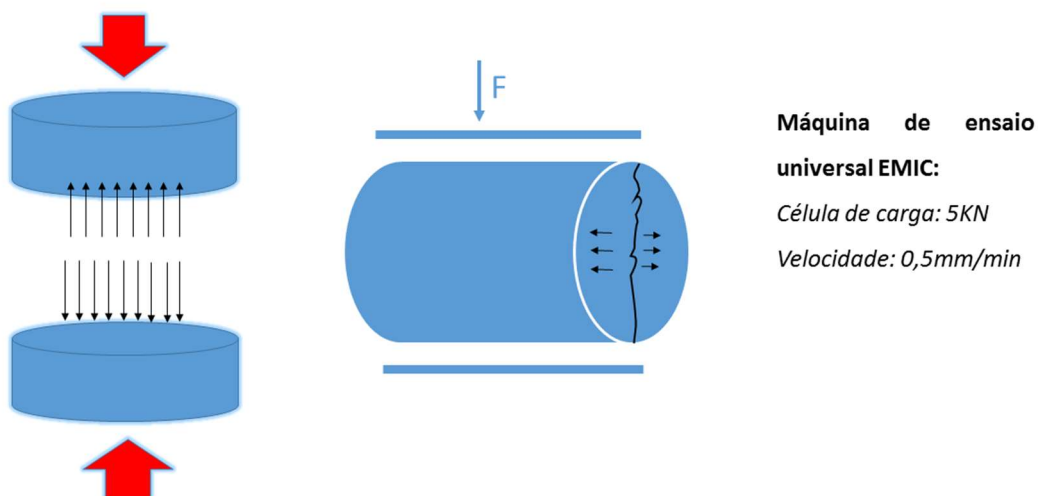
Resistência à compressão e à tração diametral

Confecção dos corpos de prova: 8 x 4 mm



Fonte: Elaboração própria.

Esquema do teste de resistência à compressão e à tensão diametral da resina composta.



Fonte: Elaboração própria.

Estabilidade de cor e Rugosidade Superficial

Confecção dos corpos de prova: $10 \times 2 \text{ mm}$



Estabilidade de cor

N= 180 CPs (10 CP por grupo)

Grupos: Resina não modificada; Resina + NPs de ZnO, ZnO/Ag, TiO₂ e TiO₂/Ag (Prec Pol e Hidrot). Soluções: Saliva Artificial e Café

Rugosidade Superficial

N= 100 CPs (10 CP por grupo)

Grupos: Resina não modificada; Resina + NPs de ZnO, ZnO/Ag, TiO₂ e TiO₂/Ag (Prec Pol e Hidrot).

Fonte: Elaboração própria.

Não autorizo a reprodução deste trabalho até 24/08/2019.

(Direitos de publicação reservado ao autor)

Araraquara, 24 de Agosto de 2017.

Hércules Bezerra Dias